

MONITORING BLUE-GREEN ALGAE IN THE IJSSELMEER USING REMOTE SENSING AND IN-SITU MEASUREMENTS

MARY CHAWIRA

February, 2012

SUPERVISORS:

Dr. Ir. Mhd. Suhyb Salama

Dr. Ir Rogier van der Velde



MONITORING BLUE-GREEN ALGAE IN THE IJSSELMEER USING REMOTE SENSING AND IN-SITU MEASUREMENTS

MARY CHAWIRA

Enschede, The Netherlands, February, 2012

Thesis submitted to the Faculty of Geo-Information Science and Earth Observation of the University of Twente in partial fulfilment of the requirements for the degree of Master of Science in Geo-information Science and Earth Observation.

Specialization: Water Resources and Environmental Management

SUPERVISORS:

Dr Ir. Mhd. Suhyb Salama

Dr. Ir Rogier van der Velde

THESIS ASSESSMENT BOARD:

Prof., Dr. Ir. W. Verhoef (Chair)

Dr. H. J. van der Woerd; Institute for Environmental Studies, University of Amsterdam, The Netherlands (External Examiner)

DISCLAIMER

This document describes work undertaken as part of a programme of study at the Faculty of Geo-Information Science and Earth Observation of the University of Twente. All views and opinions expressed therein remain the sole responsibility of the author, and do not necessarily represent those of the Faculty.

ABSTRACT

Remote sensing and in-situ measurements are of paramount importance for providing information on the state of water quality in turbid inland water bodies. The formation and growth of cyanobacteria is of serious concern to inland aquatic life forms and human life. The main cause of water quality deterioration stems from anthropogenic induced eutrophication. The goal of this study was to quantify and determine the spatial distribution of cyanobacteria concentrations in IJsselmeer in the Netherlands using remote sensing techniques. In this study we developed an algorithm to derive phycocyanin intensity index as a proxy for estimating cyanobacteria concentrations. The development of the index was based on the reflectance difference between MERIS band 620 nm and 665 nm. Semi-empirical band ratio model was applied in MEdium Resolution Imaging Spectrometer (MERIS) images for the derivation of phycocyanin pigment concentration and distribution maps. The semi-empirical band ratio model used on MERIS bands centered at 620, 665, 709, and 778.75 nm to derive the absorption coefficients of phycocyanin, chlorophyll_a and phycocyanin pigment concentrations. Atmospheric correction was performed first by removing adjacency effects with ICOL processor model followed by Case 2 water regional processor (C2R) model in BEAM VISAT software. In-situ Spectroradiometric reflectance was matched with MERIS reflectance and a stronger correlation was obtained for 28 September MERIS scene with $R^2 > 0.89$ for the six sampled locations. Two in-situ datasets were used to validate MERIS derived phycocyanin concentrations and these were WISP-3 Spectroradiometric, from a field campaign and averaged real-time phycocyanin fluorescence from two geographic locations in the lake. The first dataset gave a good correlation with $R^2 = 0.73$ and MAE 4.67 mg/m³ whilst fluorescence gave a much strong linear correlation with $R^2 = 0.92$ and 0.91 respectively for the two points. Phycocyanin absorption coefficient derived from the semi-empirical band ratio model correlated well with both predicted and measured phycocyanin concentrations with $R^2 = 0.983$ and 0.71 respectively. Generally, the index represented well the cyanobacteria populations. It correlated well with 28 September derived concentration with $R^2 = 0.903$. But a weaker relationship was observed for example image of 18 April R^2 was 0.48. Nevertheless, the combined 14 MERIS scenes from March to September provided a good correlation $R^2 = 0.55$ and RMSE= 7.61mg/m³ regardless the fact that in some images the index could not perform well as a result of chl_a concentrations that under estimated PC concentrations. The developed index was found to be a useful tool for monitoring cyanobacteria bloom. In addition, this study found that Lake IJsselmeer had cyanobacteria concentration above “high level” category set by WHOM for recreational water bodies. Daily, Monthly and seasonal variations cyanobacteria blooms investigations indicated that the PC pigment was dynamic in the lake. The spatial distribution seemed to be controlled by a number of factors which included wind, temperature and nutrient levels.

Key words: remote sensing, cyanobacteria blooms, phycocyanin intensity index, Chlorophyll_a and seasonal variability.

ACKNOWLEDGEMENTS

I am truly and deeply indebted to my supervisors who contributed to this dissertation in various ways.

First, my sincere appreciation goes to my primary supervisor Dr Suhyb Salama for his support and guidance he showed me throughout my dissertation writing. With his eagerness, his encouragement, and his great efforts to explain things clearly and simply, he helped to trouble shoot physics in remote sensing of water quality domain. Throughout my thesis-writing period, he provided support, sound advice, and lots of good ideas that framed my thesis. Honestly, would have been lost without him. It was a great pleasure to work with him.

Secondly, my deepest sincere and gratitude goes to my second supervisor Dr Rogier van der Velde for his motivation and encouragement. He granted me vast knowledge that shaped my work. Rogier is a warm hearted and awesome person to work with. He offered advice and insight throughout this challenging period.

I owe sincere and earnest thankfulness to Water Insight organization for making my research a success by providing WISP-3 spectrometer for field measurements. My special thanks go to Dr Steef Peters from Water Insight for his unwavering support in providing and developing my research skills, rich knowledge in optical water quality and advice throughout my thesis work. I would also want to thank you for enabling me to use your offices for two weeks, and providing me with MERIS images. It is an honor for me to express my gratitude to Dr Marnix Laannen from Water Insight for all the logistics he put in place arranging ferry boats for field measurements and transport to Lake IJsselmeer. Your support made this thesis a success, you did not restrict me in your offices during my time at Water Insight and I am heartily thankful. In my daily work at Water Insight I have been blessed with a friendly and cheerful Lady Semhar Ghebrehiwot Ghezehegn. Without your help and patience it was going to be difficult to complete this study. I appreciate the help you offered me on how to deploy WISP-3. Your assistance and support from the initial to the final period enabled me to develop an understanding of the subject.

I would like to show my gratitude to Rijks Waterstaat of the IJsselmeer for providing the Fluorescence data. The data added a lot of value to my work!

My deepest gratitude goes to European Space Agency (ESA) who provided MERIS images to make this research complete. The contribution you made to this research is greatly appreciated.

Many thanks go to ITC staff members from Water Resources and Environmental Management department for facilitating with best environment and knowledge to successfully complete my studies. I know that this research would not have been possible without the financial assistance from Netherlands Fellowship programme (NUFFIC). I greatly appreciate for granting me the opportunity. I would also like to thank my family members for the support they provided me through my entire period at University of Twente (ITC) in The Netherlands and most importantly, I must acknowledge my dad, mom, my sister Fungai and children Karen and Apollonia for their encouragement. Your prayers were thunderous otherwise I would have fallen especially after the loss of my husband Joe, you stood by my side.

Lastly, I offer my honors and blessings to Zimbabwe Environmental Law Association Staff for all the support they offered which contributed to further my education at ITC and all of those who supported me in any respect during the entire period.

TABLE OF CONTENTS

1.	INTRODUCTION.....	1
1.1.	Background.....	1
1.2.	Research Problem.....	3
1.3.	Research Objectives.....	4
1.3.1.	Specific Objectives.....	4
1.3.2.	Tasks.....	4
1.3.3.	Research Questions.....	4
1.4.	Research outline.....	4
2.	LITERATURE REVIEW.....	5
2.1.	Eutrophication In Lake IJsselmeer.....	5
2.2.	Cyanobacteria Adaptations.....	5
2.3.	Cyanobacteria Seasonal Variability.....	6
2.4.	Temporal and Spatial variability of Cyanobacteria.....	6
2.5.	Recreational Water Quality indices.....	7
2.6.	Remote Sensing of Cyanobacteria blooms.....	7
2.6.1.	Relationship between Spectral Reflectance and Inherent Optical Properties.....	8
2.7.	MERIS Sensor Characteristics and Water Quality Applications.....	9
3.	STUDY AREA AND MATERIAL USED.....	10
3.1.	The Geography of the Study Area.....	10
3.2.	Climate.....	11
3.2.1.	Soils.....	11
3.2.2.	Economic significance of Lake IJsselmeer.....	11
3.3.	Field Measurements.....	11
3.3.1.	Datasets.....	11
3.3.2.	Field Sampling and Data Collection.....	11
3.3.3.	General Description.....	12
3.4.	In-situ Measurements.....	12
3.4.1.	Measurements Performed within this Study.....	12
3.4.2.	Real –time Measurements Data Collected by the Rijkswaterstaat in the IJsselmeer.....	14
3.4.3.	Data Processing.....	15
3.5.	Satellite Data.....	15
3.4.	In-situ and MERIS Data Match-up.....	15
4.	METHODOLOGY.....	17
4.1.	Proposed Approach.....	17
4.2.	Computation of Above and Subsurface Irradiance Reflectance.....	18
4.3.	Case II Water Atmospheric Correction Algorithms.....	18
4.3.1.	Adjacency Effects.....	19
4.3.2.	Case 2 Regional Processor.....	19
4.3.3.	Water Processor (WeW).....	20
4.4.	Semi-empirical Band Ratio Model.....	20
4.5.	Statistical Error Analysis.....	22
4.5.1.	Root Mean Square Error.....	22
4.5.2.	Mean Absolute error.....	23
4.6.	Phycocyanin Intensity Index.....	23

4.7	Phycocyanin fluorescence	24
5	RESULTS AND DISCUSSION	25
5.1	Spectral Signature of Lake IJsselmeer.....	25
5.1.1	MERIS Reflectance versus in- situ Reflectance.....	26
5.2	Atmospheric Correction Evaluation	26
5.2.1	Case 2 Regional Processor.....	26
5.2.2	Improve Contrast over Ocean and Land for Adjacency Effects and C2R.....	27
5.2.3	Water Processor WeW	27
5.3	Atmospheric Correction and Validation	29
5.4	Phycocyanin Concentration from MERIS image	33
5.4.1	Phycocyanin Absorption	34
5.5	Phycocyanin Intensity Index	35
5.5.1	Cyanobacteria Distribution	39
5.5.2	Three-tier Alert System.....	40
5.6	Phycocyanin Fluorescence	41
5.6.1	Diurnal and Monthly Variations of Cyanobacteria	41
5.6.2	Seasonal Variability of Cyanobacteria blooms	43
5.6.3	Comparisons of PC Concentrations and Chl_a from MERIS and Real-time Measurements ...	43
5.7	Seasonal Succession of Cyanobacteria and chl_a	45
5.8	Limitations	46
6	CONCLUSIONS AND RECOMMENDATIONS.....	47
6.1	Conclusions	47
6.2	Recommendations.....	48
	LIST OF REFERENCES	49
	APPENDICES.....	54

LIST OF FIGURES

Figure 2.1: Structure of Guidelines for Recreational Waters; adopted from (Ibelings, 2005).....	7
Figure 2.2: The concept of remote sensing of water; Adopted from Sampsa Koponen (2009)	8
Figure 3.1: Location Map of Lake IJsselmeer showing sampled sites during the field campaign.	10
Figure 3.2: Wisp-3 optical spectrometer sensors	13
Figure 3.3: Spectroradiometric measurements in Lake IJsselmeer.	14
Figure 4.1: The schematic procedures taken for Atmospheric correction, derivation of PC concentrations and PC intensity Index	17
Figure: 5.1: a, b and c: Subsurface Irradiance reflectance spectra for day 23, 25 and 28 September	25
Figure 5.2: MERIS predicted and WISP-3 measured reflectance spectra typical of Lake IJsselmeer	26
Figure 5.3: Comparison between C2R MERIS Reflectance and In-situ Reflectance.....	27
Figure 5.4: Comparisons between ICOL- C2R MERIS reflectance and In-situ reflectance.	27
Figure 5.5: Comparisons between ICOL-WeW Reflectance and In-situ measured Reflectance.....	28
Figure 5.6: a, b: Comparison between ICOL-WeW and ICOL-C2R spectra with In-situ reflectance	28
Figure 5.7: Accuracy assessment of Atmospheric Correction for the 6 sampled geographical locations in Lake IJsselmeer. The left panel indicates C2R without ICOL and the right panel indicates C2R with ICOL. MERIS centered bands are displayed	30
Figure 5.8: Correlation of Atmospheric matchup points of In-situ and MERIS before and after implementation of ICOL. Plots on the left panel indicates C2R without ICOL whilst the right panel indicates C2R with ICOL.....	31
Figure 5.9: Correlation of the Spectral match-ups of WeW – ICOL and In-situ Reflectance Spectra	32
Figure 5.10: Correlation between WISP-3 measured and MERIS predicted PC concentrations.	34
Figure 5.11: a, b: Scatter plots showing relationship between predicted PC concentration versus PC absorption and (b) Observed PC concentration versus PC absorption.	35
Figure 5.12: a, b, c: Relationship between PC.I.I and PC concentration for 28 September 2011, 10 May and 18 April. The PC.I.I plotted values were log transformed before they were plotted.	36
Figure 5.13: Scatter plot of PC.I.I versus PC concentrations for 14 maps. The PC.I.I plotted values are log transformed.....	37
Figure 5.14: Scatter plot of PC.I.I versus chl_a concentrations for 14 maps	37
Figure 5.15: A and B: Distribution maps of PC concentration and PC Intensity Index.....	39
Figure 5.16 a, b: Daily averages of PC Fluorescence variation between 8:00 am and 15:00 pm for 6 July and 28 September. PC Fluorescence values were log transformed before they were plotted.	42
Figure 5.17: Monthly Variations of Oxygen, Temperature, Turbidity, chl_a and PC.....	42
Figure 5.18: Seasonal variations of turbidity, temperature, Oxygen, PC fluorescence and chl_a. Log transformed PC fluorescence and Oxygen are displayed on secondary axis.	43
Figure 5.19: Scatter plots of PC fluorescence and MERIS PC concentrations. PC Fluoresce is given in (RFU) units	44
Figure 5.20: Comparisons between PC fluorescence and MERIS chl_a concentrations.....	44
Figure 5.21a, b: Time series of PC and chl_a from in-situ measurements and MERIS image for pole 46 and 47. PC fluorescence is displayed on the secondary axis and its values were log transformed before they were plotted.	45
Figure 5.22: Mean and Standard deviation (vertical bar) of chl_a and PC concentration.....	46

LIST OF TABLES

Table 2-1 MERIS Spectral Bands and Applications.....	9
Table 2-2 MERIS sensor characteristics	9
Table 3-1: MERIS Full Resolution Level 1b Metadata	15
Table 3-2: MERIS Match-up Sites in Lake IJsselmeer. Coordinates are in Decimal Degrees (DD)	16
Table 4-1 Constants for Semi -empirical Band Ratio Model	22
Table 5-1 Summary Statistics of atmospheric correction: n = 6.	32
Table 5-2 Retrieved PC Concentrations and absorption coefficients from MERIS and measured PC concentrations	34
Table 5-3: PC Intensity Index Guidance levels for Lake IJsselmeer	40

LIST OF ACRONYMS

Term	Description
AC	Atmospheric Correction
AOPs	Apparent Optical Properties
BGA	Blue Green Algae
CDOM	Colored Dissolved Organic Matter
C-PC	Cyanophyceae Phycocyanin
C2R	Case 2 Regional
DD	Decimal Degree
ENVI	Environment for Visualizing Images
ENVISAT	Environment Satellite
EOLISA	Earth Observation Link-Stand Alone
ESA	European Space Agency
FOV	Field of View
FR	Full Resolution
GPS	Global Positioning System
ICOL	Improve Contrast over Ocean and Land
IOPs	Inherent Optical Properties
NIR	near Infra-Red
NN	Neutral Network
PC	Phycocyanin
PC.SI	Phycocyanin Severity Index
MAE	Mean Absolute Error
MERIS	Medium Resolution Imaging Spectrometer
MOMO	Matrix Operator Method
RMSE	Root Mean Square Error
R-PC	Rhodophyceae Phycocyanin
RR	Reduced Resolution
SIOPs	Specific inherent optical properties
TOA	Top of Atmosphere
TSM	Total Suspended Matter
WHO	World Health Organization
WISP-3	Water Insight SPectrometer

LIST OF SYMBOLS

Symbol	Description	Unit
a_{ph}	Absorption coefficient of phytoplankton	m^{-1}
a_{pc}	Absorption coefficient of phycocyanin	m^{-1}
a_{pc}^*	Specific absorption coefficient of phycocyanin	m^2/mg
a_w	Absorption of water molecules	m^{-1}
b_b	Back scattering coefficient	m^{-1}
Chl_a	Chlorophyll <i>a</i> pigment	mg/m^3
Chl_b	Chlorophyll <i>b</i> pigment	mg/m^3
E_d	Downwelling irradiance reflectance	$Wm^{-2}nm^{-1}$
E_u	Upwelling irradiance reflectance	$Wm^{-2}nm^{-1}$
L_{wu}	Upwelling radiance reflectance	$Wm^{-2}nm^{-1}sr^{-1}$
L_{sky}	Water leaving Radiance	$Wm^{-2}nm^{-1}sr^{-1}$
K_d	Diffuse attenuation coefficient	m^{-1}
Rrs	Remote sensing reflectance	sr^{-1}
R(0-)	Subsurface irradiance reflectance	Dimensionless
R(0+)	Above surface irradiance reflectance	Dimensionless
R_{Lw}	Water leaving radiance Reflectance	$Wm^{-2}nm^{-1}sr^{-1}$
λ	Wavelength	nm

1. INTRODUCTION

1.1. Background

Water quality monitoring of blue- green algae (BGA) is a global growing concern and Lake IJsselmeer is among inland fresh water facing this problem. Lake IJsselmeer is recognized by the Dutch government for its socio- economic and ecological importance yet it is vulnerable to eutrophication resulting from human related activities. Lake IJsselmeer is a very important conservation area and supports a diversity of aquatic bird species, fish, and mussels among other aquatic organisms. In drought periods the water is used for drinking purposes mostly in the Northern provinces of Netherlands. It stands as the largest fresh water lake in Western Europe and offers recreational activities to both local and regional visitors. Unfortunately, it faces a challenging problem of pollutants from a number of countries which include; Switzerland, Germany, Austria, Belgium, Italy, France, Luxembourg, Lichtenstein and Netherlands. The pollutants are transported through river Rhine into a tributary IJssel river which then discharges 15% into Ketemeer and then IJsselmeer (Raat, 2001). The main sources of pollutants include; industrial effluent, agricultural fertilizers (phosphates, nitrates and animal manure) as well as municipal waste water from the countries mentioned above. This situation subjects Lake IJsselmeer to serious eutrophication problems which in turn triggers BGA formation and consequently adversely affecting aquatic ecosystems and human health from toxins produced by this algae (Rijkswaterstaat, 2011). Water management authorities have been confronted with the problems of efficiently quantifying the intensity of blue green algae. Traditional in-situ methods lack high spatial and temporal coverage needed for regular and timely warnings in case of intense blooms. One way to overcome this information gap is to integrate remote sensing techniques with conventional methods in management tools so as to improve water quality monitoring. Therefore, the aim of this study to derive indicators of blue green algae and develop a proxy to measure the intensity of blue-green algae using remote sensing techniques coupled with in- situ measurements.

We use term blue green algae interchangeably with cyanobacteria and these are photosynthetic bacteria that have similar properties with algae and are inhabitants of inland water bodies as described in (Chorus et al., 1999). They are a common feature in highly eutrophic water bodies. Owing to nutritional enrichment of Lake IJsselmeer, occurrences of cyanobacteria blooms in surface waters are becoming a growing problem. Their adaptations to changing environment make them more ubiquitous than any other phytoplankton species of algae and exposes humans and ecosystems at risk. A bloom in the context of this study means the accumulation of blue green algae biomass at the surface of the water. Like many lakes in the Netherlands, IJsselmeer is highly eutrophic and supports dense cyanobacterial blooms (Ibelings, 2005).

Blue green algae hereafter referred to as cyanobacteria constitute some of the most hazardous toxins of water borne biological substances in IJsselmeer. They have a tendency of proliferating during spring and summer seasons notably around May and between July and September as noted by (Simis et al., 2005b). During this period, temperature, and light increases and rains are more intense resulting enormous nutrient loads in the lake particularly phosphates as aforementioned. Besides, anthropogenic related activities attributed to eutrophication in IJsselmeer, it is believed that natural phenomenon such as global warming is alleged to accelerate cyanobacteria dominance over phytoplankton population as also posited by (Kanoshina et al., 2003; Paerl et al., 2011).

Cyanobacteria are widely discredited for their undesirable effects in water bodies especially when they form surface scums. In given situations like this, recreational activities which range from, fishing boating, diving, and yachting become hampered (Hunter et al., 2010; Simis et al., 2005b). Natural ecosystems are disrupted and in worse cases they dwindle and vulnerable species go extinct for example Otter in the IJsselmeer (Laane et al., 1993). This leads to loss of economic and aesthetic value of the water body. Cyanobacteria are well known to produce toxins which include neurotoxins, hepatoxins and cytotoxins Ibelings et al (2007). Hepatoxins are associated with ill functioning of the liver, kidney and other gastrointestinal illness if accidentally ingested or swallowed by humans and animals as (Backer, 2002). Cytotoxins are associated with dermal diseases such as skin irritations and blistering whilst neurotoxins affect the nervous system of animals. Fatal cases have been reported in inland waters and coastal areas in which large populations of shell fish have been killed (Hunter et al., 2010; Hunter et al., 2008; Kutser et al., 2006; Mishra et al., 2009; Romay et al., 1998). A more recent and pathetic issue reported in the IJsselmeer is of the two dogs which died from cyanobacteria ingestion after drinking the water from this lake (Hoyer, 2010). Given a situation like this, it really demands very effective monitoring methods to be put in place like remote sensing techniques we have proposed.

In this study we assess the presence of cyanobacteria using a pigment called phycocyanin and the assumption is that, pigment concentration increases with increasing cyanobacteria biomass. Phycocyanin is defined in (Dingjian. et al., 2006; Duan et al., 2010) as a functional protein found in cyanobacteria, with characteristic absorption peak around wavelength 620 nm. Two phycocyanin pigments Cyanophyceae (C-PC) and Rhodophyceae (R-PC) exist, and these can be optically and biologically distinguished from each other. The pigment C-PC has a distinct spectral absorption at 620 nm whilst R-PC peak absorption is measured at 550 nm (Jiang et al., 2001) thus, we are able to detect it using satellites from space.. Biologically C-PC falls in the blue-green cyanobacteria group whilst R-PC pigment belongs to a family of red harmful algae and these are more common in Florida coastal area in the United States of America.

Phycocyanin (C-PC) hereafter re -abbreviated (PC) forms the central core subject of this study. Previous researchers employed known optical properties of PC and evaluated the usefulness of field collected spectral response patterns for determining concentrations of PC pigments and ultimately blue-green algal abundance (Randolph et al., 2008). Light absorption properties of PC pigment makes it a good candidate for optical detection methods, such as remote sensing. Thus this study utilized the spectral properties of this pigment to quantify cyanobacteria in the lake.

Monitoring cyanobacteria blooms is critical in the IJsselmeer as we have already highlighted earlier on. This study realized that, one of the most effective ways to communicate information on water quality is with indices. Therefore, this study's main objective is to develop a PC Intensity Index (PC.I.I) of cyanobacteria concentrations from MERIS imagery. Bartram et al. (1999) concurred that, health impairments from cyanobacteria in recreational waters has to be distinguished from mild symptoms to severe hazardous exposure to high concentrations. This can be achieved through development of guidance levels with set thresholds according to international standards such as the European and World Health Organization (WHO) for recreational water according to incremental severity of the cyanobacteria. The probability of the adverse effects of cyanobacteria were classified in three levels in which each category will have a threshold set according to the concentration of cyanobacteria stipulated by the WHO recreational water standards Bartram and Ballance (1999).

We explore Seasonal variability of PC concentration and distribution using relationships between phycocyanin and turbidity, dissolved oxygen, temperature, and chl_a concentrations as did Vincent et al.

(2004) in Lake Eire. Investigation on the dynamics and spatial variability of cyanobacteria blooms taking into consideration variables such as wind, temperature, turbidity and oxygen is of paramount importance in order to determine peak seasons of the blooms. However in this study wind data was not available for analysis therefore, we rely on information from literature.

The existing conventional monitoring programs provide a more general assessment of the ecological quality of Lake IJsselmeer yet human health is at high risk and many aquatic animals succumb in the waters. Traditional in-situ monitoring methods cannot provide complete information on the state of the water body since these techniques provide very low temporal and spatial coverage. Furthermore, recreational water users are more vulnerable especially during the summer time when the demand for recreational facilities increases, a time that coincides with high cyanobacteria blooms. To circumvent these problems, remote sensing based methods are proposed to be used for the detection of cyanobacteria blooms. Maps showing the distribution and concentrations of the blooms are also going to be produced.

MEdium Resolution Imaging Spectrometer (MERIS) was chosen for this research because its spectral band at 620 nm facilitates the discriminate phycocyanin from other photosynthetic pigments. Algorithm developed by Simis (2005b) semi-empirical band ratio model for the Dutch lakes make it possible to map and detect PC pigment concentrations. This model has been used for purpose of this research. In-situ Spectroradiometric measurements shall be conducted for checking atmospheric correction accuracy and validating remotely sensed derived PC concentrations. Furthermore, PC fluorescence data from real time measurements will be used to validate different MERIS scenes acquired from March to September 2011.

1.2. Research Problem

Lake IJsselmeer is of significant and intrinsic economic value for the Netherlands yet it is vulnerable to eutrophication which in turn has led to cyanobacteria blooms. Cyanobacteria blooms perpetuate due to eutrophication induced by anthropogenic related activities. The situation is further exacerbated by the climate change which has seen a rise in temperature in recent years. As a result recreational activities have been hampered and many populations of aquatic organisms are under threat. Additionally, people who visit the lake for recreational activities are susceptible to health risks. Ibelings (2005) postulated that monitoring cyanobacteria in Netherlands is problematic and potentially exposes the public health to risks.

Whilst cyanobacteria bloom in IJsselmeer has been investigated using various point in-situ measurements coupled with remote sensing methods, water resources authorities lack a comprehensive and quick monitoring tool capable of providing information on the severity of cyanobacteria blooms in the entire lake at once. Traditional approaches which are largely applied for example, phycocyanin pigment cell counting are laborious and time consuming considering that cyanobacteria blooms are very dynamic in both time and space. Furthermore, cell counts can differ significantly depending entirely upon the proficiency and subjective decision of an individual. Cell counting and other in-situ methods based on point sampling do not represent the entire lake. Thus the realization of the necessity to develop methods that complement the existing monitoring approaches. To circumvent these shortcomings, this study developed from remote sensing techniques a phycocyanin intensity index (P.C.I.I) and concentration PC maps from MERIS images as fast a monitoring tool. Seasonal variability was assed using 14 MERIS images from March to September 2011 in order to see which months of the year pose the greatest risk to human life and aquatic ecosystems.

1.3. Research Objectives

The main objective of this study is to derive indicators of cyanobacteria (blue-green algae) and develop an index to measure the intensity of cyanobacteria blooms.

1.3.1. Specific Objectives

- To derive absorption coefficient of phycocyanin pigment and using MERIS data.
- To derive phycocyanin pigment distribution and concentration maps of Lake IJsselmeer from MERIS data
- To investigate seasonal variation of cyanobacteria blooms.

1.3.2. Tasks

- To carry out in situ radiometric measurements.
- To perform atmospheric correction for MERIS images.
- To validate MERIS derived PC concentrations with Wisp-3 in-situ measurements and real-time PC fluorescence.

1.3.3. Research Questions

- Can we develop Intensity index of phycocyanin pigment concentration from remote sensing techniques?
- Is it possible to derive absorption coefficient of phycocyanin from the image?
- Can phycocyanin concentration maps provide information useful for monitoring cyanobacterial blooms?
- Can PC absorption coefficient be related to model derived PC concentrations and in-situ measured PC concentrations?
- Is there any seasonal variability of cyanobacteria blooms in IJsselmeer?

1.4. Research outline

This document is structured in the following manner; first, we provide background on blue green algae and remote sensing. We also provide the research problem, objectives, tasks and research questions. Chapter two provides literature on cyanobacteria; its formation, variability and usefulness of remote sensing techniques for mapping it. Chapter 3 provides a description of the study area and data sets used in this study while chapter 4 describes the methodologies applied to achieve the objectives of this study. In chapter 5 we provide results and discussion on atmospheric correction methods used, phycocyanin retrieval and validation with in-situ measurements. We also discuss the phycocyanin intensity index with respect to PC concentration. In chapter 5 we provide results and discussion. Chapter 6 provides conclusions and recommendation on the findings of this study. Finally, chapter 7 provides list of references used in this study followed by appendices.

2. LITERATURE REVIEW

2.1. Eutrophication In Lake IJsselmeer

Eutrophication is a phenomenon caused by high nutrient concentration, notably phosphates, nitrates resulting from anthropogenic related activities. The exterior input to the lakes of phosphorus and nitrogen and of polluted waters from waterways as rivers have been the major cause of eutrophication as noted in (Gulati et al., 2002). In addition to this, climate change, habitat division and biotic exploitation of many of waters bodies have probably led to loss of resilience and thus have speeded up eutrophication Gulati et al. (2002). Eutrophication is associated with number of adverse effects such as bloom of cyanobacteria, which in turn depletes available oxygen in water leading to the death of aquatic organisms. Gulati and van Donk (2002) argued that, lake eutrophication is manifested mainly in the low under-water light climate with high turbidity for example a Secchi-disc depth of between 20 and 40 cm caused usually by phytoplankton algal blooms. There exist very challenging problems in the Netherlands with intensive agriculture and animal husbandry which has led to Lake Eutrophication despite the fact that the source of pollutants originates from a number of other nations as already mentioned.

2.2. Cyanobacteria Adaptations

Cyanobacteria are natural and cosmopolitan inhabitants of inland fresh, brackish and turbid coastal waters. They are known to contain phycocyanin, one of the phycobiliproteins as important accessory pigments in photosynthesis of Rhodophyceae, Cyanophyceae and Cryptophyceae (B. W. Ibelings et al., 2008; Otsuki et al., 1994). They are particularly well adapted for growth in nutrient-enriched inland lakes as well as slow flowing inland waters. They often form mass populations (as blooms, scums or biofilms) during summer and autumn in temperate latitudes Hunter et al. (2010). Similarly, (Newcombe et al., 2010) established that cyanobacteria are adapted to turbulent mixing by enlarged gas vesicles and it takes a few days to decrease their buoyancy in order to adapt to more calm conditions. Furthermore, literature points out that cyanobacteria possess a unique character of energy balance. They need small amount of energy to sustain cell function and structure and, they are able to survive well under low nutrient conditions Chorus and Bartram (1999).

Like many species of algae, cyanobacteria contain phycocyanin as a major pigment for gathering light and performing photosynthesis. In actual fact they contain three pigments with phycobiliproteins which include allophycocyanin (blue), phycocyanin (blue) and phycoerythrin (red) as envisaged by (Chorus and Bartram, 1999; Lüring et al., 2011). These pigments of cyanobacteria gather light in the green, yellow and between green and red (orange) part of the spectrum (500 nm - 650 nm) which is rarely exploited by other phytoplankton species. The accessory pigments of phycocyanin are able to efficiently use a region of the light spectrum between the absorption crests of Chl_a and the carotenoids for photosynthetic metabolism.

Adaptations such as gas-filled cytoplasmic inclusions enable buoyancy regulation and the vesicles optimize their upright position in the water column to find a proper place for survival and growth as Codd et al (2005) and Chorus and Bartram (1999) highlighted thus, they are more dominant in inland waters than other photosynthetic phytoplankton species. Owing to their extensive spectrum of life strategies, “cyanobacteria represent a significant component of virtually all photosynthetic assemblages, colonizing

different types of lakes over the whole trophic range” (Salmaso, 2000). These complex forms of adaptations expose human life and ecosystems at risk. Thus there is need for constant and frequent monitoring with remote sensing techniques so people can be timely alerted in case of a fatal bloom.

Chorus and Bartram (1999) maintained that, in suitable environmental conditions, cyanobacteria experiences high growth rate resulting in formation of large blooms. In environments where they are exposed intermittently to high light intensity for example, an intensity roughly less than half of what would be at the surface of a lake, they promulgate at a maximum rate. Cyanobacteria at higher surfaces are tolerant of high light intensities do not require it for bloom formation Chorus and Bartram (1999).

2.3. Cyanobacteria Seasonal Variability

In this study we attempt to explore the changes in cyanobacteria intensity with respect to different seasons. Seasonal patterns in cyanobacterial abundance have been observed to be affected substantially by, solar irradiance, nutrient supply and temperature. A study by Mihaljević et al. (2011) in temperate climatic environments indicated that cyanobacteria form during all seasons of the year. This is expected to be the same situation in the IJsselmeer as it lies in the temperate climatic zone. However, (Graham et al., 2008) observed in their study in USA that cyanobacterial populations tend to peak in spring and summer months. One interesting feature to note is that in light limiting conditions cyanobacterial growth rates are greater than that of other phytoplankton species, and this coupled with their buoyancy allows them to out-compete other algae in highly turbid waters (Vincent et al., 2004). Other research has indicated that high water temperature leads to an increase in cyanobacteria density (Lehman et al., 2008) with a significant growth for temperature above 15°C. Nevertheless, maximum growth rates attained at temperatures above 25°C Newcombe et al. (2010). Mass blooms of cyanobacteria are generally associated with high nutrient concentrations, particularly phosphorus but their growth and biomass is unlimited by phosphate availability for they can store sufficient phosphorus to make two to four cell divisions corresponding to a four to thirty -two folds increase in biomass Newcombe et al. (2010). A recent study by Xie et al. (2011) in USA has shown that cyanobacteria maintain a viable population and are correlated with turbidity in Muskegon Lake. Based on these dynamism characteristics of cyanobacteria, point based quantification methods are not adequate enough and need to be replaced by high spatial and temporal remote sensing methods.

Topçu et al. (2004) and Simis et al. (2007) maintained that, seasonal changes of nutrients are strongest during spring, leading to phytoplankton spring bloom spring blooms a situation which has been observed in the Dutch lakes particularly in IJsselmeer. Oxygen is saturated in winter seasons a season when most organisms are in a torpor state and proliferation of cyanobacteria coupled with other phytoplankton species leads to its depletion. Weather changes from stormy to fine conditions result in excessive colonies accumulating at the surface.

2.4. Temporal and Spatial variability of Cyanobacteria

Cyanobacteria vary on short time scales as in hours or days and their vertical migration, entrainment in temporary circulation cells, or wind movement of surface accumulations may changes quickly in a water column but not its overall abundance (Graham et al., 2008). Under light wind conditions cyanobacteria is moved towards the shoreline of area lakes and bays, where they form thick scums (Graham et al., 2008; P. W. Lehman et al., 2005). In extreme cases, such clusters may become very thick and even acquire a sticky consistency (Nöges et al., 2010). Cyanobacteria changes rapidly with changing hydrological conditions for example ‘circulation patterns or inflow events’ Graham et al. (2008). Under calm weather conditions

cyanobacteria has been observed to spread evenly throughout reservoirs however, currents and prevailing winds may lead to irregular distribution.

2.5. Recreational Water Quality indices

A water quality index forms a basis of a framework for monitoring potentially toxic cyanobacterial blooms for monitoring. WHO and European Water framework established alert guidance levels framework for recreational waters which have been universally adopted by many nations, Bartram and Ballance (1999) and these were essentially developed for monitoring cyanobacteria. These are developed based on cell counting methods from water samples taken from certain points not representative of the whole water body. Development of methods to detect potentially toxic cyanobacterial blooms in water bodies are crucial (Vardaka et al., 2005). Figure 2.1 illustrates structural development of standard recreational water guidelines thresholds (Ibelings, 2005).

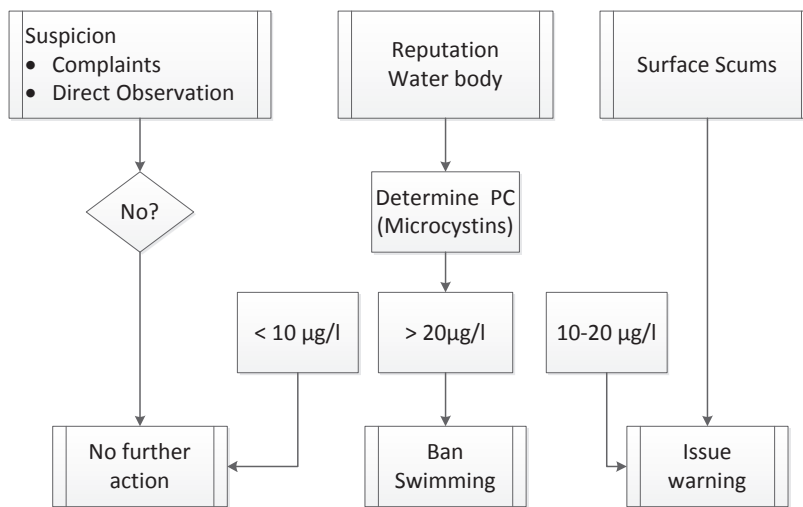


Figure 2.1: Structure of Guidelines for Recreational Waters; adopted from (Ibelings, 2005)

2.6. Remote Sensing of Cyanobacteria blooms

Point based methods are insufficient for monitoring cyanobacteria distribution and concentrations as these are known to change rapidly in space and time for example, with wind speed and direction. Observations from fixed stations or along established divides could be unrepresentative of cyanobacteria distribution and abundance. Remote sensing based techniques bridge this gap by offering rapid detection of cyanobacteria distribution and concentrations in the whole lake. It is macroscopic remote observation ability which makes remote sensing a more superior platform. Furthermore these advances have led to the development of algorithms specifically for mapping phytoplankton pigments and in case of this study PC.

The concentrations of phytoplankton pigments are retrieved from the column of the water using mathematical algorithms that estimate the concentrations based on the spectral amount of light emerging from the water as maintained by (Gons et al., 2005a; Hunter et al., 2010). Simis et al. (2007) demonstrated this prospect by developing a model which they termed semi-empirical band ratio model based on the absorption feature of at 620 nm and it was tested in this study for the derivation of PC concentrations in Lake IJsselmeer. It is important to note that inherent optical properties of a water body differs notably case 1 waters (largely ocean) and case 2 (turbid coastal and inland waters). Case 2 waters have optical properties strongly influenced by high concentrations of mineral particles as well as CDOM and these do

not co-vary with phytoplankton biomass (Hunter et al., 2010). The following are some of the algorithms that have been specifically developed for the quantification PC based on its absorption feature at 620 nm; single band ratio algorithm by (Schalles et al., 2000) and semi-empirical algorithm by Dekker(1993). These algorithms quantify PC from remote sensing reflectance (R_{rs}) and employ different wavelengths in the NIR.

2.6.1. Relationship between Spectral Reflectance and Inherent Optical Properties

The above mentioned algorithms makes use of the relationship that exists between the IOPs that is absorption and back scattering coefficients of water constituents and subsurface irradiance reflectance $R(0-)$ (Gordon et al., 1975). Subsurface irradiance reflectance as described in Dekker et al (2002) is the ratio of upwelling to downwelling light. These relationship have been found to be valid as argued by (Rijkeboer et al., 1997) because $R(0-)$ is relatively stable under varying solar angles, as well as nature of the water surface and the condition of the atmosphere. Figure 2.2 illustrates an overview of how water quality parameters are retrieved from a water column using remote sensing techniques.

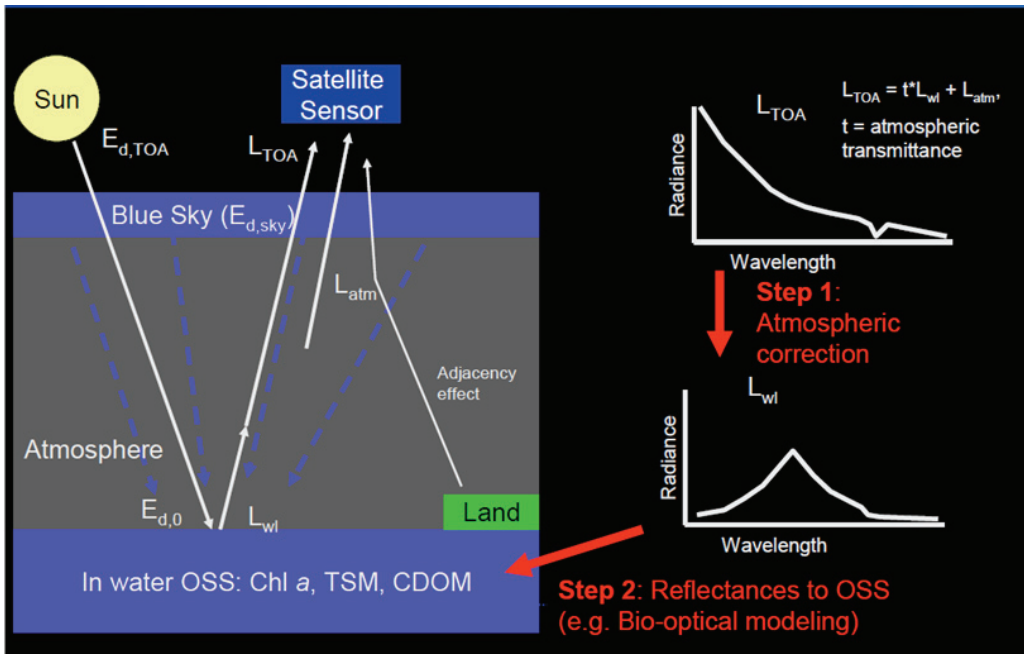


Figure 2.2: The concept of remote sensing of water; Adopted from Sampsa Koponen (2009)

The semi-empirical band ratio algorithm developed by (Simis et al., 2005b), was adopted for estimating cyanobacteria concentration in this study. The model uses a band ratio 709 nm to 620 nm to estimate PC pigment. It was selected based on the fact that it considers the influence of Chl_a absorption at 620 nm and it includes the impact of variable PC: Chl_a ratio. The semi-empirical band ratio was specifically developed for MERIS band configurations and relates PC to the absorption coefficient at band positioned at 620 nm, Ruiz-Verdu (2008), which is retrieved from the ratio of the 620 nm band and a near infra-red band, centered at 709 nm, as reference. Medium Resolution Imaging Spectrometer (MERIS) sensor which is on board the European Space Agency's ENVISAT, has good temporal and spectral resolution needed acquire imagery for cyanobacteria blooms in many inland waters (Gómez et al., 2011). That's we found it imperative for our study.

2.7. MERIS Sensor Characteristics and Water Quality Applications

MERIS has a 68.5° field-of-view push-broom imaging spectrometer which measures the solar energy or radiation that is reflected by the Earth, at a spatial resolution of 300 m on the ground, in 15 spectral bands. The bands are programmable in width and position, in the visible and near infrared wavelengths (ESA, 2006). It was the first sensor to offer the combination of several narrow spectral wavebands targeting both Chl_a and other accessory pigments absorption in the red and NIR, at a spatial resolution of 260 m across track sufficient for medium-sized water bodies. The sensor’s signal-to-noise ratio is acceptable as posited by (Simis et al., 2007). MERIS allows global coverage of the Earth in 3 days (ESA, 2006) thus it was found to be crucial for this study in providing high temporal resolution data.

Table 2-1 MERIS Spectral Bands and Applications

Band number	Band center (nm)	Band width (nm)	Application
1	412.5	10	Yellow substance and detrital pigments
2	442.5	10	Chlorophyll absorption maximum
3	490	10	Chlorophyll and other pigments
4	510	10	Suspended sediment, red tides
5	560	10	Chlorophyll absorption minimum
6	620	10	Suspended sediment
7	665	10	Chlorophyll absorption & fluorescence reference
8	681.25	7.5	Chlorophyll fluorescence peak
9	708.75	10	Fluorescence peak reference, atmosphere corrections
10	753.75	7.5	Vegetation, cloud
11	760.625	3.75	O ₂ R- branch absorption band
12	778.75	15	Atmosphere corrections
13	865	20	Vegetation, water vapor reference
14	885	10	Atmosphere corrections
15	900	10	Water vapor, land

Source: MERIS User Guide Version 2 http://earth.esa.int/pub/ESA_DOC/ENVISAT/MERIS/meris

Table 2-2 MERIS sensor characteristics

Sensor characteristics	Spectral	Spatial	Orbital
MERIS	-Vis-NIR bands -Across range 390nm to 1040nm	15 -Ocean reduced resolution -Coastal, 260- 300m Full resolution	1040-1200m -Polar orbital-Sun synchronous -FOV 68.5o -Swath width 1150km

3. STUDY AREA AND MATERIAL USED

3.1. The Geography of the Study Area

Lake IJsselmeer is the largest inland water body in Netherlands covering an area of 1190 km² and it is about 8 meters above the sea level. It is situated at 52° 49' N latitude and 5° 15' E longitude. It can be described as a shallow eutrophic freshwater lake, which was reclaimed from the Wadden Sea in 1932 by a dike and with an average depth of 4.4 meters Dekker (2004). Previously the lake had a total area of 3,440 km² and the area was reduced by reclamation projects that were aimed at increasing the land area of Netherlands Dekker (2004) through constructing enclosing dikes and pumping the water out. The lake area is surrounded with about 600 km of shore and it is nearly 30 km long. The surrounding land is largely used for agricultural purposes notably large scale market gardening and cattle ranching.

Lake IJsselmeer has favorable conditions for the occurrence of floating layers of blue-green algae. The river IJssel (a branch of the river Rhine) supplies continuously enormous amounts of nutrients mostly phosphates nitrates and animal waste products into the lake. Simis et al. (2005a) noted that lake is shallow and as a result the water temperature rises quickly. Thus, during summer sunny season, cyanobacteria blooms are expected to be high and more frequent. The figure 3.1 illustrates map of the study area.

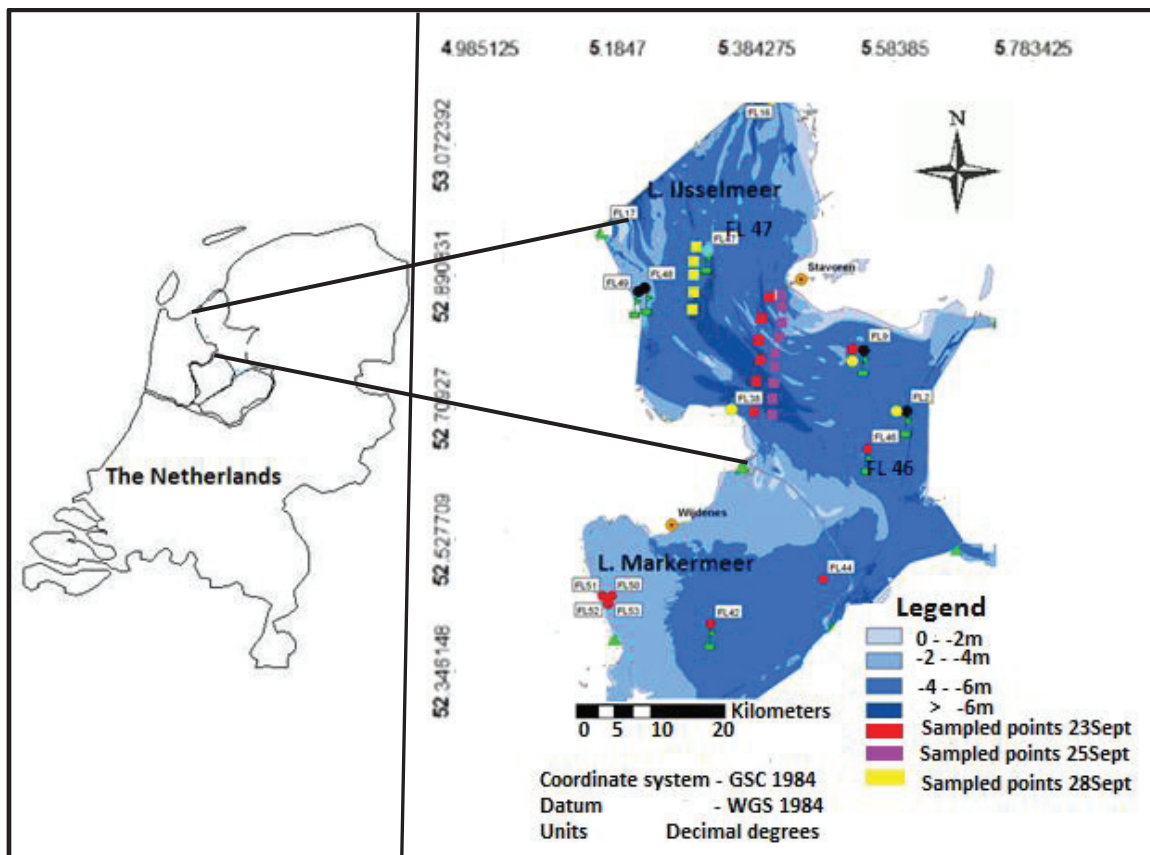


Figure 3.1: Location Map of Lake IJsselmeer showing sampled sites during the field campaign.

Source of plain map: <http://geography.about.com/library/blank>

Besides the adverse ecological impacts, buoyant layers of blooms also impacts greatly on economic uses of the water in particular recreational activities such as boating, yachting, swimming and boat skiing among others.

3.2. Climate

The predominant wind in the Netherlands is mostly from South-west direction and it results in moderate maritime climate. Precipitation is experienced throughout the year and it is relatively equally shared in each month. However summer and autumn season tend to gather a bit more precipitation than other months mainly due to the intensity of the rainfall rather than frequency of the rain days (Wikipedia, 2012). The following climate data which are long-term averages between 1981 to 2010 recorded at De Bilt weather station a forecasting substation for Lake IJsselmeer was obtained from (StatLine, 2011). The average temperature for the whole period of 30 years was 7.7°C and average summer temperature for same period was 17°C. Precipitation for the same period was 997.5mm.

3.2.1. Soils

The soil profile is made up of a layer of mainly fine to very soft Holocene sediments (mineral) and peat overlying sandy Pleistocene subsoil Gloppe (IJsselmeer polders Development Authority, Scientific Department) unpublished work.

3.2.2. Economic significance of Lake IJsselmeer

IJsselmeer has a severe problem of cyanobacteria yet it plays a significant role in the economy of Netherlands Gulati and van Donk (2002). The water is mostly used for irrigation and drinking purposes during drought seasons (Huiteima, 2002). It also attracts a wide range of recreational activities yet it poses danger to human health and aquatic life forms.

3.3. Field Measurements

3.3.1. Datasets

The in-situ datasets mainly consisted of WISP-3 Spectroradiometric measurements and real-time PC fluorescence, temperature, oxygen chl_a and turbidity measurements. Satellite data consisted of MERIS images and these are explained in detail in the sections below.

3.3.2 Field Sampling and Data Collection

In-situ measurements were carried out during a field campaign on the 23rd, 25th and 28th of September 2011 in Lake IJsselmeer. Radiometric measurements were recorded using Water Insight SPectrometer (WISP-3) issued by Water Insight. The first and second field campaign for collecting spectra of water leaving reflectance was carried between Enkhuizen and Stavoren on 23 and 25 September 2011 with total number of 15 samples. On 28 September the spectral reflectance measurements were taken on the other side of the Lake from Enkhuizen to Den Oever with 6 sampled sites. The spatial coordinates of each site from the lake were recorded using a Garmin etrex global positioning system (GPS). The measurements were taken concurrently with MERIS satellite overpass for 28 September. For 23 and 25 September measurements were taken an hour before and after the satellite overpass.

WISP-3 spectroradiometer instrument was used to collect downwelling sky and upwelling radiances from water as well as sky irradiance. The flexible hand held instrument provided instant preliminary water quality parameters which included; chl-a, PC concentration, CDOM, and Total suspended particulate matter (TSM diffuse attenuation coefficient (K_d) from embedded formulas. However, for the purpose of

this study chl-a and PC concentrations were considered. Ancillary data were also collected on water temperature, wind speed, secchi depth and sea level pressure on 28 September 2011. See appendix A table 4. The sample sites were selected based on factors listed below;

- The distance of about 2 km away from the lake shore line to avoid land adjacency effects.
- The Lake bathymetry was considered to avoid bottom effects.
- Measurements were taken at 5 minutes intervals however, clouds inhibited consistency.
- The distance chosen between the measuring points was based on the spatial resolution of MERIS sensor of 300m to avoid repeated measurements on one pixel.

3.3.3 General Description

Day 23 and 25 September was characterized by partly cloudy conditions. As a result, most of the measurements were taken when clouds had dispersed. Fine weather conditions persisted on 28 September and reflectance spectra collected on this day were considered for matchup with MERIS image reflectances. The sampled points/sites where measurements were taken on the 23rd, 25th and 28th of September 2011 respectively are illustrated on figure 3.1. The total number of sampled points for all 3 days with defined geographic coordinates were 22, (n = 22). The information is provided in table 3.2.

3.4 In-situ Measurements

3.4.1 Measurements Performed within this Study

The field campaign followed the protocols described in the WISP-3 manual (Peters et al., 2005). The wavelength of the instrument ranges of 380 to 780 nm, with a spectral resolution of 4 nm and 3° field of view (FOV) aperture. The 0.3 nm spectral intervals were interpolated to 1 nm interval in a database created in excel so that we could match MERIS center bands. The signal to noise ratio of the spectrometers is 250:1. The hand held optical device has three channels which measures three optical properties simultaneously. At each site the spectrometer on the top measured downwelling sky irradiance (E_d), the other two spectrometers sensors pointing at angles of 42° measured downwelling sky radiance (L_{sky}) and upwelling radiance (L_{wu}) from the water. In order to avoid sun glint, the instrument was held about 135° away from the sun. Figure 3.2 illustrates the Wisp-3 spectrometer sensors positions. To ensure proper measurements the instrument was calibrated at Water Insight before the field campaign.

Spectroradiometric measurements were made concurrent to MERIS satellite overpass for the purpose of checking accuracy atmospheric correction for remote sensed data according to Simis et al. (2005b). Ground truth samples and field reflectance spectra with total of 5, 10 and 6 were collected on 23, 25 and 28 September 2011 respectively. The first two were measured between Ekhuizen and Stavoren and on 28 September the field spectra were collected between Ekhuizen and Den Over.



Figure 3.2: Wisp-3 optical spectrometer sensors

We measured subsurface irradiance reflectance because it provides characteristics of the true features of the water color as claimed by (Morel, 2006). Field-based Spectroradiometric instruments are mostly used for remote sensing projects as suggested by Schalles and Yakobi (2000) because they offer high spectral resolution suitable for water quality monitoring needs in this case, phytoplankton pigments. WISP-3 was desired as it computes instant preliminary data for chl_a and PC concentrations. The formulas for deriving these parameters including subsurface irradiance reflectance are all embedded in the instrument.

As aforementioned, the measurements were taken from the side of the boat as illustrated on middle field photographs on figure 3.3, to mimic the satellite which observes from above the water surface. Figure 3.4 shows the activities involved during field measurements. The general water color was green an indication that the lake is eutrophic and these observation were also made by (Gons et al., 2005a). Green algal colonies were visually observed floating near the surface.

The photographs on (fig 3.4) shows the water colour and measurements setups. The middle and bottom shows Wisp-3 deployment and data collection including recording of geographic points and aerosol optical thickness data from Sunphotometer.



Figure 3.3: Spectroradiometric measurements in Lake IJsselmeer.

3.4.2 Real-time Measurements Data Collected by the Rijkswaterstaat in the IJsselmeer

A second independent dataset was acquired from lake IJsselmeer from two geographic points (longitude 5.492902; latitude 52.70991 and longitude 5.223987; latitude 52.91201) that is, pole 46 and 47 respectively and they are illustrated on (fig 2.1). The data was issued by Rijkswaterstaat an arm of the Dutch Ministry of Transportation and Water Management. These points which are fixed poles/stations were chosen by the Rijkswaterstaat to represent the whole lake and the data was made available for this study by Water Insight. The data collected included, turbidity, water temperature, oxygen chl_a and PC fluorescence. Phycocyanin pigment was measured using fluorimeter probe called YSI 6131 Phycocyanin Blue-green Algae Sensor. Turbidity was measured using YSI 6136 fouling-resistant sensor. Oxygen was measured using a ROX optical sensor. Chlorophyll was measured using YSI 6025 sensor and lastly temperature was measured using 130 EcoSense Temperature Sensor.

The MERIS 14 scenes for 22, 27, 29 March, 10, 18, 20, 21, 23, 25 April, 01 May, 03, 27 June, 06 July and 28 September 2011 PC concentrations were validated using Chl_a and PC fluorescence measured on days that coincided with the satellite overpass for the respective days. The images were also made available for this study by Water Insight. These data were crucial for investigating seasonal variability of cyanobacteria blooms and chl_a concentrations. The images were all atmospherically corrected prior to model implementation. PC fluorescence has a characteristic absorption peak and fluorescence emission peak, is often used as the indicator for cyanobacteria detection, Becker et al. (2009). Thus, PC fluorescence was

found imperative in this research for validating MERIS derived PC concentrations. Besides PC fluorescence data, we also collected other data which included turbidity, dissolved oxygen, water temperature and chl_a. We considered diurnal measurements recorded between 8:00 am and 15:00 hours for analysis purposes based on the fact that more recreational activities are conducted during day time. For five variables, averages were taken per day between 8:00 and 15:00 hours and likewise per month. The PC fluorescence and chl_a monthly averaged and standard deviation values are provided in Appendix (A) in tables 2 and 3.

3.4.3 Data Processing

Data collected from the field had some outliers and these were filtered out from the used dataset. At certain occasions, two or three measurements were taken on a single pixel and these extra recordings were discarded so that only one measurement could be retained for matching with MERIS. Furthermore, the data was filtered based on weather conditions (clear skies) and images for 23 and 25 September were not considered for atmospheric correction as the days were cloudy.

3.5 Satellite Data

MERIS was used to derive the final maps of PC concentrations and PC intensity index. MERIS has high spectral resolution and has a revisit period of 2–3 days (latitude dependent). It has a dual spatial resolution of 300 m full resolution (FR) and 1200 m reduced resolution (RR). However, FR level 1b top of atmosphere radiance (TOA) are used and presented in this study. The FR images were obtained from ESA through Water insight. The satellite data were useful in this study for interpreting PC concentrations from in situ measurements by providing large spatio-temporal coverage images that in situ data cannot (CEARAC, 2007). Phycocyanin pigment has a distinct spectral signature at 620 nm, picked up by MERIS sensor. Owing to these features, MERIS was chosen for mapping cyanobacteria distributions (Gons et al., 2005a; Mittenzwey et al., 1992).

The three images metadata is provided on table 3.1. The image of 28 September had the clearest atmosphere as such it was considered for match-up purposes with in situ measurements and it is highlighted on table 3.1.

Table 3-1: MERIS Full Resolution Level 1b Metadata

Date	Metadata of available images	Sensing start time	Track	Orbit
23/09/2011	MER_FRS_1PNPDE20110923_101942	12:36:40	80	50094
25/09/2011	MER_FRS_1PNPDE20110925_104627	12:46:31	37	50051
28/09/2011	MER_FRS_1PNPDE20110928_103627	12:20:07	8	50022

3.4. In-situ and MERIS Data Match-up

A match-up is a time related sampled location in the field and image pixel with same geographic coordinates. The match-up is crucial for validating developed models and in this case, the semi empirical band ratio model for deriving water quality parameters such as PC and chl_a concentrations from remotely sensed satellite data (Campbell et al., 2011). Table 3.2 provides in-situ measured sites, time and geographic locations that were matched with MERIS data.

Table 3-2: MERIS Match-up Sites in Lake IJsselmeer. Coordinates are in Decimal Degrees (DD)

Date	Sampled points/ sites	Sensing start time	Latitude (DD)	Longitude (DD)	Time (GMT)
23/09/2011	P1	12:20:07	52.78606	5.31159	11:10
	P2		52.79768	5.31225	11:18
	P3		52.81106	5.31506	11:22
	P4		52.82641	5.31992	11:29
	P5		52.84235	5.32773	11:34
25/09/2011	P1	12:46:31	52.71158	5.31003	12:49
	P2		52.72663	5.31195	12:53
	P3		52.75067	5.31291	12:59
	P4		52.76459	5.31124	13:04
	P5		52.77754	5.31075	13:09
	P6		52.79201	5.31117	13:14
	P7		52.80566	5.30754	13:19
	P8		52.83618	5.3093	13:31
	P9		52.84887	5.31581	13:36
	P10		52.86170	5.32726	13:42
28/09/2011	P1	12:36:40	52.86424	5.14974	11:38
	P2		52.88106	5.13437	12:38
	P3		52.88112	5.13433	12:40
	P4		52.88037	5.13397	12:54
	P5		52.87196	5.14295	13:24
	P6		52.86682	5.14799	13:44

4 METHODOLOGY

4.1 Proposed Approach

This study aimed at deriving indicators of cyanobacteria as a proxy to measure the intensity of cyanobacteria blooms from remote sensing data. First, field spectra were used to validate the atmospheric correction. A semi empirical nested band ratio model by Simis et al. (2005a) was then applied to the corrected images for deriving PC concentrations. Furthermore, the MERIS derived PC concentrations were validated with in-situ real-time fluorescence measurements. Figure 4.1 illustrates a summary of the procedures that was followed to achieve the objectives of this research.

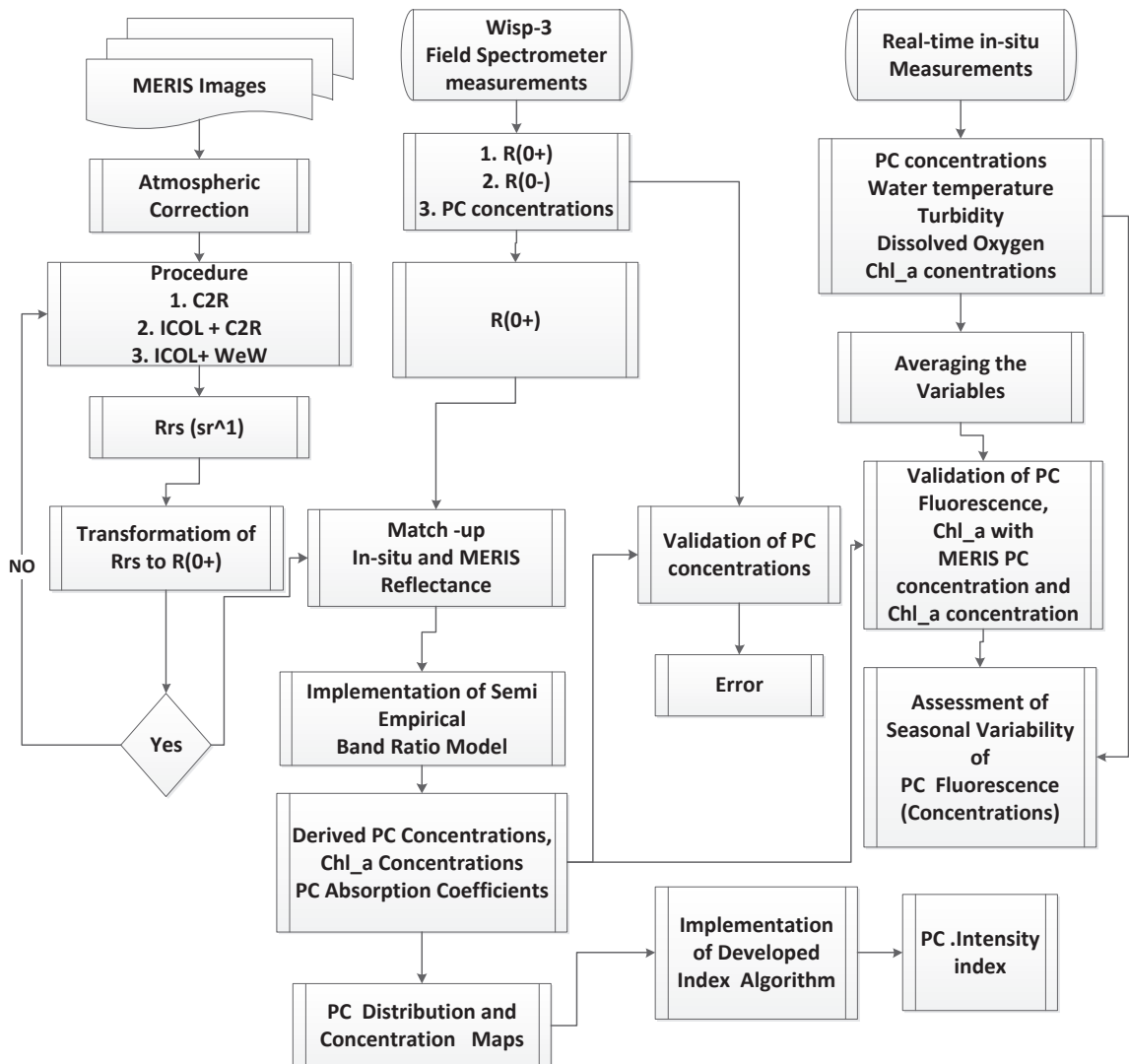


Figure 4.1: The schematic procedures taken for Atmospheric correction, derivation of PC concentrations and PC intensity Index

4.2 Computation of Above and Subsurface Irradiance Reflectance

At each sampled point, three optical properties, upwelling radiance from water, L_{wu} , and the downwelling radiance, L_{sky} , and downwelling sky irradiance (E_d), were measured simultaneously above the water. Two other spectrometers L_{sky} and L_{wu} were pointed at angles of 42° to measure radiance from respectively the sky and the water respectively (Gons et al., 2005b). The zenith angle of 42° was maintained to avoid instrument from boat shadow and self-shading. An azimuth angle of 135° to minimize sun glint effects maintained in order to adhere to NASA ocean optics protocols (Mueller et al., 2003). Angles of $90^\circ - 180^\circ$ were avoided. WISP-3's embedded formula computed above irradiance reflectance as follows;

$$R(0+) = \left(\frac{L_{wu} - \sigma * L_{sky}}{E_d} \right) * n_w^2 * Q \quad \text{Equation (1)}$$

Where; L_{sky} = downwelling sky radiance ($Wm^{-2} nm^{-1} sr^{-1}$)

L_{wu} = upwelling water radiance from water ($Wm^{-2} nm^{-1} sr^{-1}$)

E_d = downwelling sky irradiance ($Wm^2 nm^{-1}$)

σ = direct surface reflectance with value taken 0.022

n_w = index of refraction at water/ air interface and (value taken = 1.33)

Q = conversion coefficient for L_{wu} to E_u in (equation 2) and is taken as pi (π) isotropic light field.

The Subsurface irradiance reflectance is approximated from equation 1 as follows;

Upwelling subsurface irradiance

$$E_u(0+) = n_w^2 * Q * [L_{wu}(0+) - \sigma * L_{sky}(0+)] * (1 - \sigma - w) \quad \text{Equation (2)}$$

$$E_d(0-) = E_d(0+) + 0.5 * E_u(0-) \quad \text{Equation (3)}$$

Finally, subsurface irradiance was computed simply as follows;

$$R(0-) = \frac{E_u(0-)}{E_d(0-)} \quad \text{Equation (4)}$$

Where; $E_u(0-)$ = Upwelling subsurface irradiance.

4.3 Case II Water Atmospheric Correction Algorithms

MERIS satellites observe the water body from an altitude of almost 800 km. The water leaving radiance thus is expected to travel very long distances through interactions with the atmosphere before it gets recorded by the sensor (Kirk 1994). A bigger fraction (0.8) of the signal recorded by the satellite originates from the atmosphere. About 0.1 interacts with the water surface and the remaining 0.1 with the water column (Marnix, 2007). Consequently, some corrections had to be applied on attenuation of the upwelling radiance between the surface and the sensor by the atmosphere to remove the radiance path. Guanter et al. (2010) postulated that AC is a pre-requisite for quantitative remote sensing method requiring images to be calibrated to surface reflectance. Unwanted signal from atmospheric scattering is dominant causing drastic change in the spectral composition light received by the remote sensor sensor (Guanter et al., 2010) and as such need to be removed. First adjacent effects were removed using Improve contrast over land and ocean (ICOL) then case2 regional processor (C2R) and water processor (WeW) were applied to remove

the influence of the atmosphere. C2R and WeW were applied to MERIS images FR level 1b to compare the performance of the two and determine one which simulates PC absorption trough at 620 nm.

4.3.1 Adjacency Effects

Improve Contrast over Ocean and Land (ICOL) is a processing tool developed by (Sante, 2007). It was implemented in BEAM VISAT command line routine (D. Odermatt et al., 2008) to correct for adjacency effects. The images retrieved from spectrometers such as MERIS, are prone to an increase in the radiances, (Gao et al., 2009; Kratzer et al., 2010) mainly in the near infrared bands. Based on the fact that land areas that border lakes have typically higher reflectance than water in the NIR such that some photons reflected by the land surface are scattered in the atmosphere and these get recorded by the satellite sensor which is acquiring data over land pixels (Guanter et al., 2010). If not considered, the effect can lead to an overestimation of atmospheric radiance and subsequent underestimation of the water leaving radiance, Kratzer and Vinterhav (2010); Ruiz-VerdúKoponen et al. (2008). In this study ICOL was implemented as a pre-processing step and C2R and WeW were later applied. The reason for implementing the tool was to see if there would be possible improvements in lake surface reflectance. The inputs to the algorithm were 14 MERIS level 1b images. The output products are 8 water leaving reflectance bands and these include; 412.5, 442.5, 490, 510, 560, 620, 665 and 708.75 nm bands. Band 761 nm and 900 nm remained unchanged after the correction. Adjacency effects correction is applied only up to 30 km from the land (Sante, 2007). Lake IJsselmeer is less than 30 kilometers across and because of this was necessary to implement ICOL.

The processor calculates adjacency effects for surface reflectance, (ρ) as follows;

$$\rho = \rho^u + \frac{t \uparrow_{dif}}{t \uparrow_{dir}} [\rho^u - \bar{\rho}] \quad \text{Equation (5)}$$

Where, ρ^u = target reflectance before adjacency correction,

$\bar{\rho}$ = the background reflectance calculated as distance- weighted average reflectance of neighboring pixels and

$t \uparrow_{dir}$, $t \uparrow_{dif}$ = atmospheric transmittance functions between the surface and sensor for direct and diffuse radiation Guanter et al. (2010) and Doron et al. (2011).

4.3.2 Case 2 Regional Processor

Case 2 Regional Processor (C2R) is a processor for BEAM software and it executes batch processing type of routine. This tool was developed by Doerffer et al. (2007). In this study the tool was applied prior to ICOL as well as after ICOL. We used this processor because it was developed for coastal and Case 2 inland turbid waters and it describes the inherent properties of these waters as asserted by (Giardino et al., 2010). It is a two-step algorithm, which include neural-network based atmospheric correction process and retrieval of water constituents. The two are performed as separate tasks as claimed by (Koponen, 2006; D. Odermatt et al., 2008). The processing steps are shown on figure 2 under appendix B.

MERIS L1b was used in C2R, to compute path radiances and transmittances of bands 412 nm -708 nm derived from the TOA directional radiance reflectance of 4 MERIS bands in the NIR spectral range band 708 -870 nm by using neural network (NN) algorithm (Guanter et al., 2010). The processor has a number of output products and the one necessary for the study were water leaving reflectance and water quality parameters for example, chl_a concentrations. The water leaving reflectance from the first 12 bands of MERIS were transformed to above surface irradiance reflectance in order to check for the accuracy of atmospheric correction.

4.3.3 Water Processor (WeW)

WeW like C2R is a processor and stand-alone module for the BEAM VISAT software developed by Freie Univesitat Berlin (FUB) Kratzer et al. (2008). The atmospheric correction algorithm is based on two large databases generated by a radiative transfer code based on the Matrix Operator Method (MOMO) code (Harff et al., 2011; Kratzer et al., 2008). It was important for the retrieval water quality parameters such as chl_a but more significant for this study was water-leaving reflectance. Within the processor itself, MERIS data were first masked for glint risk, land, bright and invalid pixels. The output water leaving radiance reflectances were produced from the image. We transformed water leaving radiance reflectances to above surface irradiance reflectance for atmospheric correction accuracy checking. The retrieval process followed the steps listed and summarized in (fig 3) appendix B. This task was only performed on image of 28 September. Based on these characteristics, semi empirical band ratio model was applied on MERIS image for derivation of absorption coefficients of PC and Chl_a as well as back scattering coefficient.

4.4 Semi-empirical Band Ratio Model

The semi empirical band ratio model was developed by (Simis et al., 2007) and the model assumes that phycocyanin and chl_a pigments are major light absorbers in a water column in red and NIR bands. The model is based on the relationship between subsurface irradiance reflectance and the absorption as well as backscattering coefficients of the optically active water constituents in the water column (Gordon et al., 1975). These IOPs are physically related to the subsurface irradiance reflectance an apparent optical property (AOP) which are a key parameter linking optical properties to the remotely sensed radiance data (Hunter et al., 2010; Mishra et al., 2009). The algorithm was developed for the band configuration of MERIS channel 6, 7, 9 and 12 centered at 620, 665, 709 and 778.75 nm respectively. It is assumed that absorption at 620 and 665 nm is dominated by phytoplankton pigments PC and chl_a Hunter et al. (2008) and Dekker (1993). Band 620 nm is dominated by both PC and chl_a, and 665nm by chl_a alone whilst 709nm and 778.75 are dominated by water alone Ruiz-Verdu et al (2008). Back scattering was retrieved at 778.75 nm, a wide 15 nm band and it is assumed to be spectrally neutral thus λ was ignored. Simis (2005b) model will be used as described hereafter.

The IOPs and AOPs are related to each other in given water column as defined by Gordon et al (1975). The spectral reflectance just beneath the surface of water, $R(0^-, \lambda)$, is thus related to IOPs which are, absorption $a(\lambda)$ and $b_b(\lambda)$ through a factor (f) a coefficient that is dependent on the geographic latitude and longitude and light field according to (Morel, 2006).

The relation was derived as follows;

$$R(0^-, \lambda) = f \cdot \frac{b_b(\lambda)}{a(\lambda) + b_b(\lambda)} \quad \text{Equation (5)}$$

Where, f is an empirically determined scale factor dependent on the ambient light field and $a(\lambda)$ and $b_b(\lambda)$ are the coefficients for total absorption and backscattering respectively. As aforementioned, f and b_b are assumed to be spectrally neutral thus λ can be ignored

Two ratios were used to derive absorption of PC (a_{pc}) and these are reflectance (R) at 709 nm (λ_2) and 665 nm (λ_1) for retrieval of chl_a absorption so that the derived value can be used to infer its absorption at 620 nm. The second ratio, R at 709 nm (λ_2) and 620 nm (λ_1) was used to retrieve a_{pc} Mittenzwey et al. (1992) and Anold G. Dekker (1993). The application of the ratios $R(\lambda_2): R(\lambda_1)$ gave the following relation;

$$\frac{R(\lambda_2)}{R(\lambda_1)} = \frac{a(\lambda_1) + b_b}{a(\lambda_2) + b_b} \quad \text{Equation (6)}$$

Absorption by water and its constituents at (λ_1) [$a(\lambda_1)$] was solved from equation 6 as given below;

$$a(\lambda_1) = \frac{R(\lambda_2) \times (a(\lambda_2) + b_b)}{R(\lambda_1)} - b_b \quad \text{Equation (7)}$$

The supposition that pigment absorption is insignificant and can be neglected at 709 nm, may lead to an underestimation of $a(\lambda_1)$, which increases with pigment concentration. Furthermore, the absorption by CDOM and SPM is considered negligible, which may result also in an overestimation of $a(\lambda_1)$ that is not necessarily correlated with pigment concentration Gons et al. (2005b) and Simis et al. (2007). Thus, PC concentrations derived from MERIS images are expected to be higher than those measured in the field.

In order to retrieve a_{pc} and a_{chl} , b_b was first estimated. Back scattering by particulate matter was retrieved from 778.75 nm by first solving for absorption of water equation 5 where $a(778.75) = a_w(778.75)$ and the value f was taken from Andre et al. (1991). The value is realistic for turbid waters and it is used by many researchers today.

$$R(778.75) = f \frac{b_b}{a_w(778.75) + b_b} \quad \text{Equation (8)}$$

Having known the reflectance value and absorption by pure water at 778.75 nm as well as scale factor f , b_b was solved as follows;

$$b_b = \frac{R(778.75) * a_w(778.75)}{f - R(778.75)} \quad \text{Equation (9)}$$

The simplifications are corrected for by the introduction of factor γ that reflects the ratio of retrieved absorption against the measured absorption by phytoplankton pigments at wavelength λ_1 (Simis et al., 2005b). Chl_a absorption at 665 nm was derived using ratio 1 (λ_2) = 709 nm: (λ_1) = 665 nm as follows;

$$a_{chl}(665) = \left[\frac{R(709) \times (a_w(709) + b_b)}{R(665)} - b_b - a_w(665) \right] \times \gamma^{-1} \quad \text{Equation (10)}$$

As highlighted earlier on, pigments PC and Chl_a have an absorption overlap around 620 nm that is apparent from reflectance spectra of cyanobacteria dominated waters (Simis et al., 2005b). This reflectance feature is captured within the 620-nm band. Thus, equation 10 will be re-written for reflectance band ratio 2 and the factor δ was introduced for the correction of absorption at 620 nm like γ for the rectification at 665 nm as given below;

$$a_{chl(620)} + a_{pc(620)} = \left[\frac{R(709) \times (a_w(709) + b_b)}{R(620)} - b_b - a_w(620) \right] \times \delta^{-1} \quad \text{Equation (11)}$$

To separate the absorption by chl_a and PC at 620 nm, absorption of chl_a will be obtained from absorption of chl_a at 665 nm retrieved from equation 10 In order to relate the absorption by chl_a at 665 nm to its absorption at 620 nm a conversion factor ε will be introduced. Absorption by PC at 620 nm was solved as follows;

$$a_{pc}(620) = \left[\frac{R(709) \times (a_w(709) + b_b)}{R(620)} - b_b - a_w(620) \right] \times \delta^{-1} - [\varepsilon \times a_{chl(665)}] \quad \text{Equation (12)}$$

Finally, PC concentration were obtained by dividing $a_{pc}(620)$ by specific absorption coefficient of PC [$a^*_{pc}(620)$] as follows;

$$PC = \frac{a_{pc}(620)}{a^*_{pc}(620)} \quad \text{Equation (13)}$$

The following correction factors and constants presented here for the derivation PC concentrations were obtained from (Simis et al., 2005b) on their experiments in Dutch lakes.

$\gamma = 0.68$, (a constant derived from linear least squares fit for estimating chl_a absorption measured at 665 nm)

$\delta = 0.84$, (a correction factor derived from linear least squares fit for estimating a_{pc} measured at 620 nm)

$\varepsilon = 0.24$; Proportion of absorption at 620 nm attributed to chl_a (Randolph et al., 2008). The values of absorption by pure water molecules (a_w) were obtained from Buiteveld (1995). This information is provided in table 4.1.

Table 4-1 Constants for Semi-empirical Band Ratio Model

Constant/Coefficient	Unit	
$a_w(620)$ -	0.281	m^{-1}
$a_w(665)$ -	0.0401	m^{-1}
$a_w(709)$ -	0.727	m^{-1}
$a_w(778.75)$ -	2.71	m^{-1}
γ	0.68	unitless
δ	0.84	unitless
ε	0.24	unitless
a^*_{pc}	0.007	$m^2/mg (PC^{-1})$
f	0.34	unitless

The semi-empirical band ratio model utilizes NIR to derive abundance of the suspended matter. This part of the electromagnetic spectrum, back scattering from suspended particulate matter (SPM) is the most dominant factor defining the observed spectrum including water molecules for atmospherically corrected images. Thus, absorption by colored dissolved organic matter (CDOM) and SPM are ignored to decrease the number of optically active constituents that are taken into account (Randolph et al., 2008; Simis et al., 2005a).

4.5 Statistical Error Analysis

The mean, standard deviation, mean absolute error (MAE) and root mean square error (RMSE) were computed between measured and derived concentrations and also between measured and MERIS observed reflectance.

4.5.1 Root Mean Square Error

The root mean square error (RMSE) of a prediction can be defined as the average of the error between the actual and predicted values of a model. This error is caused because of the inadequacy of the model to account for all of the variability of the data. The RMSE was calculated as follows;

$$RMSE = \sqrt{\frac{1}{n} \sum_{i=1}^n (L_1 - L_2)^2} \quad \text{Equation (14)}$$

Where, L_1 is the value of observed/measured, L_2 is the predicted observation and “ n ” is the number of observations in the data set (Duan et al., 2010).

4.5.2 Mean Absolute error

Mean absolute error (MAE) defines the mean or average absolute value of the error. Its drawback is that, it is less sensitive to errors as compared to RMSE. Nonetheless it is a good measure of error in dataset that are not huge. It is given here by the following formula;

$$MAE = \sum_{n=1}^n |Y_1 - Y_2| \quad \text{Equation (15)}$$

Where, n represents the number of samples, Y_1 represents the observed value and Y_2 the predicted value. It was chosen to assess the error between MERIS and measured reflectance because it gives the actual error between the measured and predicted. Willmott and Matsuura (2005) also agreed that MAE is the most natural measure of average error magnitude. In this study we applied it to verify differences in error between WISP-3 in-situ and MERIS reflectances.

4.6 Phycocyanin Intensity Index

The main objective of this study was to derive from remote sensing a phycocyanin intensity index (P.C.I.I) as a proxy for estimating cyanobacteria distribution and concentrations in the IJsselmeer. The numerical index was developed to derive cyanobacteria concentrations based on the reflectance difference between MERIS band 620 nm and 665 nm as defined in equation 16. The negative log was used to render the negative values positive from the derived index although it is correct to make it easier for interpretation and derive the linear correlation between the index and concentrations. A general assumption was made in the development of the algorithm; that band 620 and 665 nm are dominated by PC and chl_a pigment respectively. However, there is an influence of chl_a absorption at 620 nm. It is expected that as PC pigment increases at 620 the value of the index will rise and vice versa. However, potential influence of TSM variability on the index can be expected decrease index.

In this method, it is expected that if atmospheric correction was poor and chl_a absorption at 620 is high, the intensity of the index will decrease. Wynne et al. (2010) carried a more related study although the method was a bit different and asserted that “a positive PC index is indicative of elevated densities of cyanobacteria”. In their study, they calculated cyanobacteria Index from the spectral shape (curvature) around 681nm of MERIS satellite RR level 2. In this research, the index was developed as a convenient means for summarizing variable PC pigment concentrations. It is hoped to facilitate communication on the state of water quality with water authorities and the general public, Herrera-Silveira et al. (2009).

The P.C.I.I is defined as by the following equation;

$$P.C.I.I = -\log \left[\frac{R(620) - R(665)}{R(620) + R(665)} \right] \quad \text{Equation (16)}$$

4.7 Phycocyanin fluorescence

Real-time PC fluorescence measurements were obtained from two geographic points given as pole 46 and 47 and the geographic coordinates of the two poles are given under section 3.6. The 10 minutes interval data was averaged for each day between 08:00 am and 15:00 pm that coincided with MERIS satellite over pass. Parameters which were taken into consideration to assess the daily, monthly and seasonal variability of cyanobacteria and chl_a concentrations included turbidity, temperature and oxygen. Furthermore, a time series analysis was done to investigate how the five aforementioned parameters vary and influence PC between March and September 2011. Chlorophyll and PC from MERIS were compared with log transformed PC fluorescence. Finally, PC fluorescence data from the two locations, pole 46 and 47 were validated with 14 MERIS derived PC and chl_a concentrations. In this set of data we calculated the average and standard deviation values for time period between 8:00 am and 15:00 pm for all the parameters. We derived daily averages and from daily mean we derived monthly averages.

5 RESULTS AND DISCUSSION

5.1 Spectral Signature of Lake IJsselmeer

Subsurface irradiance reflectance was obtained from above water measurements using WISP-3 and figure 5.1 illustrates reflectance spectra which were obtained on 23, 25, and 28 September 2011 in Lake IJsselmeer.

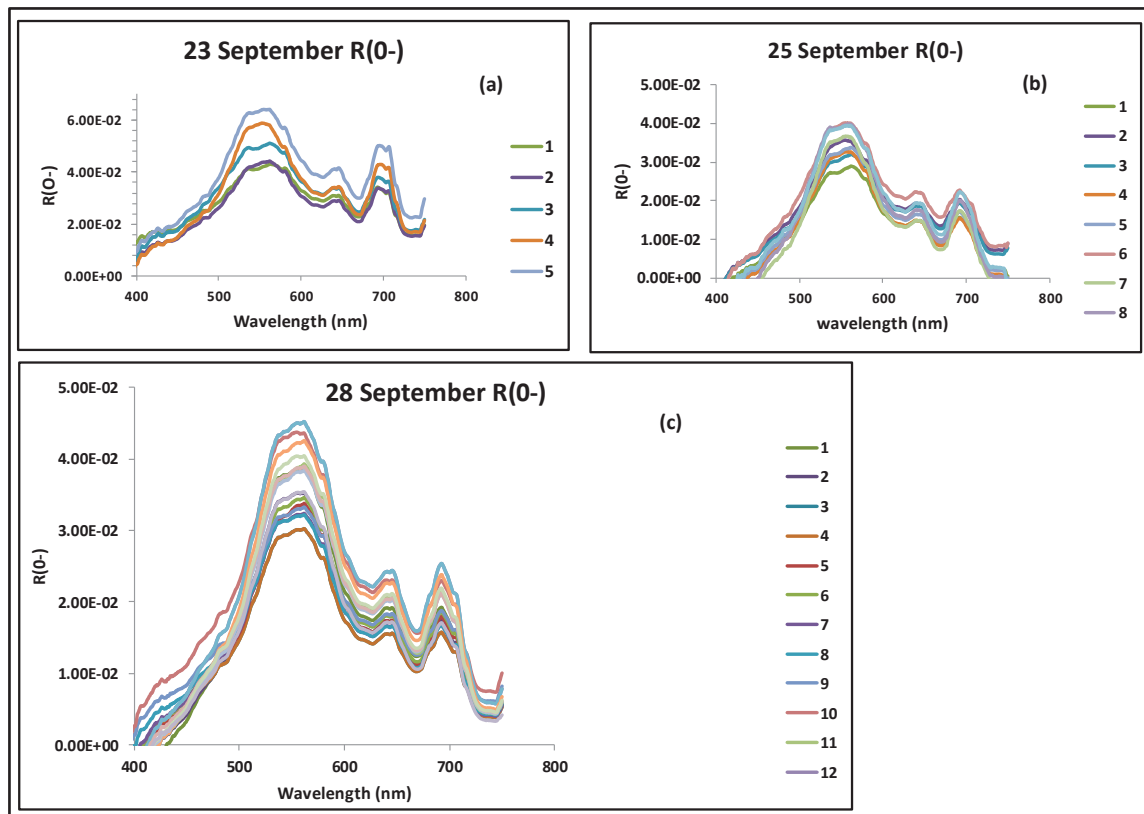


Figure: 5.1: a, b and c: Subsurface Irradiance reflectance spectra for day 23, 25 and 28 September

Generally, reflectance spectra for all the days show a similar pattern and shape as is expected of a particular water body. The conspicuous absorption trough at 620 nm and 665 nm is attributed to high absorption by PC and chl_a pigments respectively. The two absorption valleys clearly indicate that Lake IJsselmeer is dominated cyanobacteria and chl_a biomass. This spectral characteristic agrees with that obtained by (Dingjian et al., 2006) in Lake Taihu China with respect to absorption peaks of the two pigments. In their research they used a different instrument called hyperspectral ASD to measure PC absorption peak and found the peak was centred at 620 nm and compared it to laboratory phosphorus buffer measurements. The spectrum with highest reflectance (6%) was acquired on 23 September. The reflectance peaks on 28 and 25 September, recorded 4.5%, 4% respectively. These troughs are flanked by the local reflectance peaks between 570-600 nm and about 704 to 710 nm respectively. This reflectance spectra suggest that cyanobacteria were close to the water surface as claimed by (Kutser et al., 2006) in a study which they carried out in Estonia. Lower reflectances recorded on these respective days were approximately 0.23%; a clear indication that higher PC concentrations were retrieved at these measured points. However, the reflectances were expected to vary as PC concentration spatial distribution not homogeneous in nature.

5.1.1 MERIS Reflectance versus in- situ Reflectance

The results of atmospheric correction were all based on MERIS image of 28 September 2011. In figure 5.2, we compared WISP-3 measured reflectance to MERIS observed reflectance. At all six sampled points, MERIS gave analogous reflectance values at each wave length as if these were from one pixel. As can be seen the reflectance peak around 550 nm from MERIS was much lower, about 2.5% compared to 4% from WISP-3. MERIS spectra are low an indication that some influence from the atmosphere played part even after C2R was implemented. Furthermore, the error properties that exist in the NIR can possibly be attributed to adjacency effects as also noted by (Hunter et al., 2010) in their study.

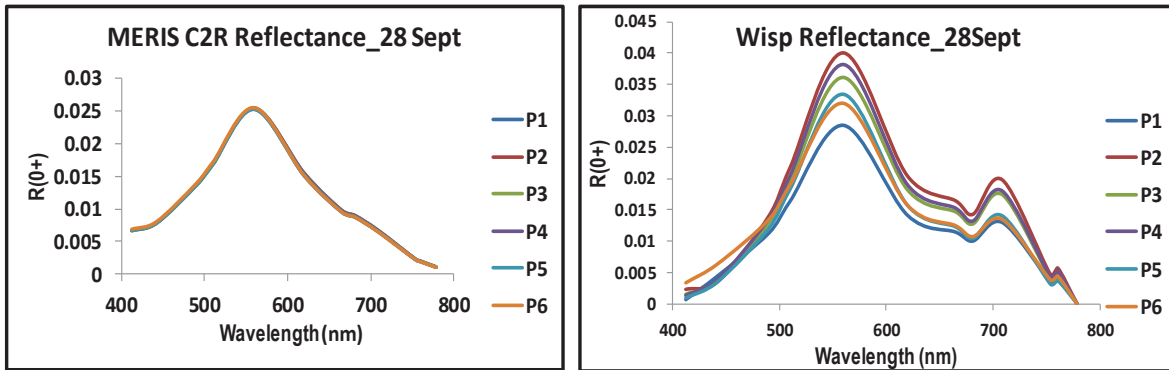


Figure 5.2: MERIS predicted and WISP-3 measured reflectance spectra typical of Lake IJsselmeer

5.2 Atmospheric Correction Evaluation

5.2.1 Case 2 Regional Processor

Atmospheric correction was performed based on the method explained on section 4.3.2; and MERIS image level 1b was transformed from Top of Atmosphere radiances (TOA) to remote sensing reflectance R_{rs} (sr^{-1}). The water leaving radiance reflectance was further converted to above surface irradiance reflectance to render it unit less and enable comparisons between in-situ derived reflectance. Water leaving radiance reflectance for the twelve bands; 412.5, 442.5, 490, 510, 560, 620, 665, 681.25, 708.75, 753.75, 760.63 and 778.75 nm were obtained. Band 11, 14 and 15 were excluded to avoid the over-correction of bands in the visible part of the electromagnetic spectrum. However, the results of this study indicate that C2R yielded lower reflectance as compared WISP-3 measured reflectance and this is shown on figure 5.3. Generally the observed reflectance from MERIS was smaller than that measured. MERIS reflectance spectra were higher between 412.5 nm and 480 nm than WISP-3 whist between 665 and 778.75 it was lower than that of WISP-3. Furthermore, a wide difference was noted at 560 nm where WISP-3 recorded 4% reflectance and MERIS recorded 2.5% reflectance at the same wavelength. In light of this; a consideration to improve reflectance was made.

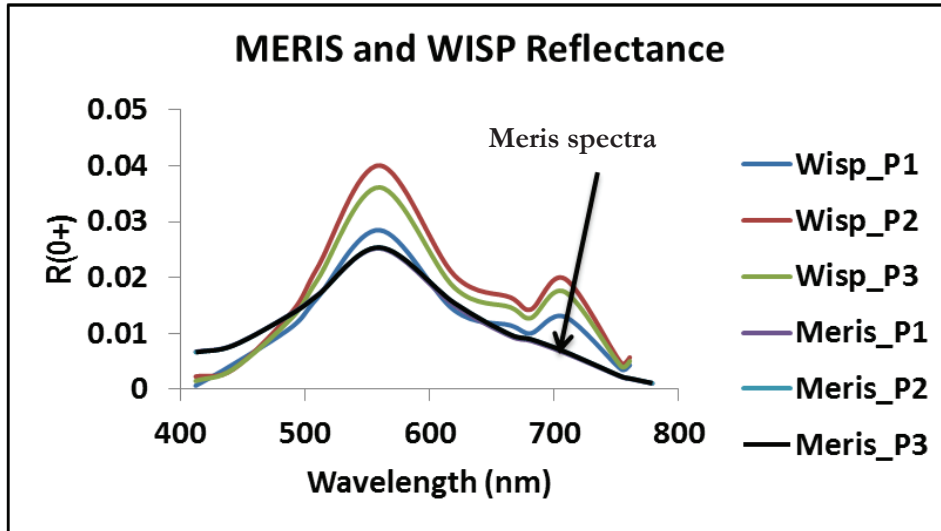


Figure 5.3: Comparison between C2R MERIS Reflectance and In-situ Reflectance.

5.2.2 Improve Contrast over Ocean and Land for Adjacency Effects and C2R

The observations over water bodies near to land surfaces are affected because of the large contrast in the red and infrared part of the spectrum, where water is nearly black and vegetated areas are very bright Odermatt et al. (2010). The results presented on figure 5.4 indicate a significant improvement reflectance particularly in the NIR bands. Interestingly, MERIS spectrum got amplitude nearly equivalent to that of field data! ICOL significantly improved the retrieved reflectance spectrum as noted by Odermatt et al. (2010) and this is depicted at band 665 nm where the dip became more conspicuous and gave an expected spectra shape. We found that the small valley at 620 nm from PC absorption could not be picked even after the application of ICOL and C2R.

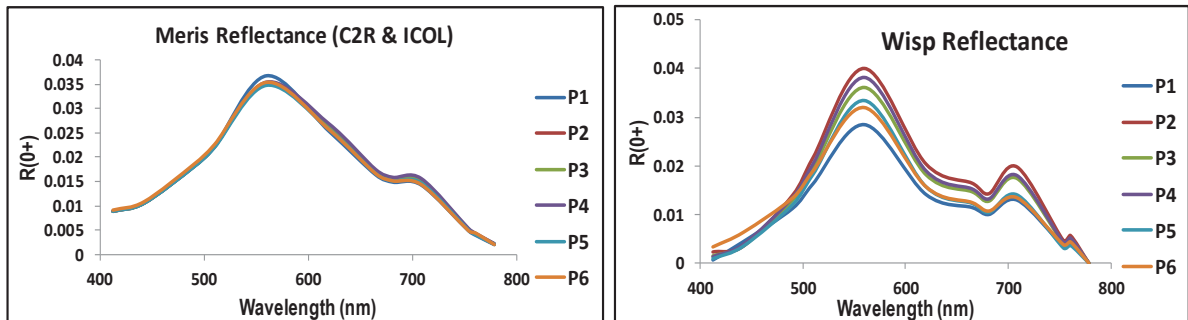


Figure 5.4: Comparisons between ICOL- C2R MERIS reflectance and In-situ reflectance.

The results of Odermatt et al. (2010) agrees with the findings of this research on the performance of ICOL and C2R. They further argued that; “the role of the ICOL on adjacency effects correction in the processing of MERIS data is consistently positive as far as the retrieval of accurate R_{rs} by C2R is concerned”. The only disadvantage of ICOL and C2R we noticed was the failure of the algorithms to pick the absorption dip of PC at 620 nm and this prompted another method. We found that it was imperative to test WeW processor as it was also specifically developed for Case 2 waters.

5.2.3 Water Processor WeW

The results WeW with ICOL on figure 5.5 gave good match especially in the visible range. The following reflectance bands were processed; 412.5, 442.5, 490, 510, 560, 620, 665 and 708.75 nm out of 15 bands.

This is shown on figure 5.5, in which the spectra span from 412.5 to 708.75 nm. Although it showed high precision in the visible portion of the electromagnetic wavelength, the desired spectral shape that is, valleys at 620 and 665 nm did not show and as a result ICOL and C2R was considered a better candidate for the processing of PC concentrations, back scattering by SPM 778.75, a_{pc} and a_{chl} . Figure 5.6 (a) and (b) presents the inadequacy of WeW in the NIR bands for this study. Point based plots measured during the field campaign for ICOL-WeW are indicated on figure 1 appendix B.

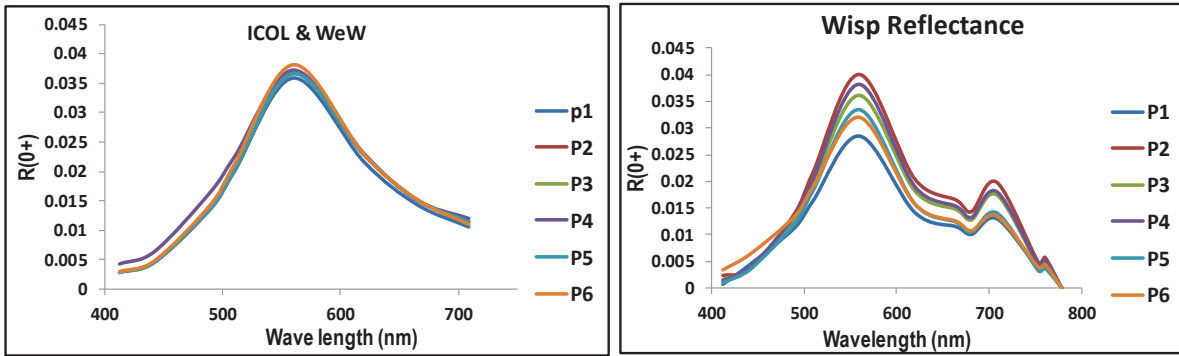


Figure 5.5: Comparisons between ICOL-WeW Reflectance and In-situ measured Reflectance

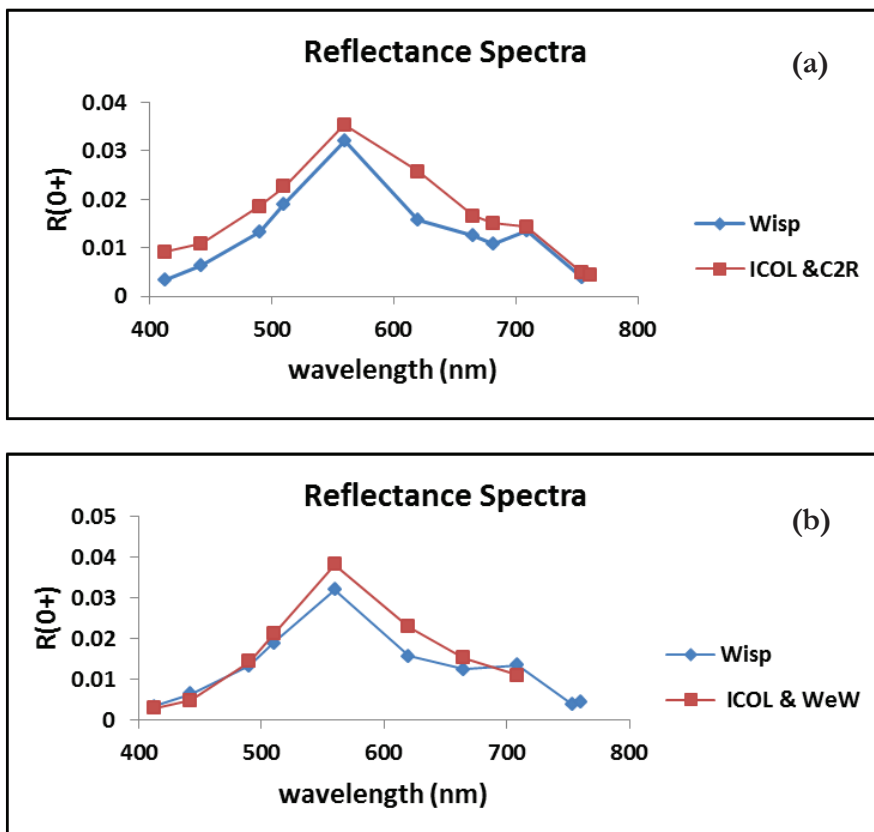


Figure 5.6: a, b: Comparison between ICOL-WeW and ICOL-C2R spectra with In-situ reflectance

A qualitative evaluation of 28 September case from one selected match up point 6 indicated that ICOL - C2R had a better matchup than ICOL - WeW at 665 nm as shown on figure 5.6 a and b. Odermatt et al.

(2010) in their study compared Spectroradiometric reflectance to C2R without ICOL and with ICOL and the findings of their investigation showed that ICOL - C2R are well automatable algorithms.

5.3 Atmospheric Correction and Validation

The results of C2R processor alone could not simulate the absorption peak by PC at 620 nm. As such, the expected trough could not show regardless of the fact that adjacency effects were corrected for before AC was applied. Ruiz-Verdu et al. (2008) argued that this usually leads to over estimation of the atmospheric radiance and a subsequent under estimation of the water leaving radiance. On the other side ICOL and WeW failed match well the reflectance of Spectroradiometric measurements in the desired part of the spectrum as mentioned in the discussion above on section 5.2.3.

There was an over estimation in the reflectance in the visible portion of electromagnetic spectrum between 400 nm and 550nm with increase from between 0.2% - 0.8% to 0.9% - 3.5%. This suggested that the image was over corrected in these wavelengths. There was also a considerable increase in reflectance on band 620 nm which was important for the derivation of PC concentrations. The reflectance was approximately 0.35% before the removal of adjacent effects and after the implementation of ICOL - C2R there was a significant improvement with an increase of up to 1.6%. This scenario is indicated on figure 5.3 and 5.4 respectively. This was expected to yield better PC concentrations.

In a different case, ICOL - C2R was tested in the Italian lakes in Maggiore and Garda lakes in 2006 and 2008 respectively (ESA, 2008) and there was good agreement in reflectance for the ICOL corrected images with an overestimation in the blue regions. Thus, as shown of figure 5.4 the R(0+) spectra of MERIS was in agreement with in-situ measured reflectance in the red region. It is evident that, Lake IJsselmeer is dominated by Cyanobacteria, while the specific inherent optical properties (SIOPs) of Cyanobacteria were not trained for use in the processor's NN.

The reflectances from 6 sampled points were matched with MERIS image 'without ICOL' and 'with ICOL' and the results are shown on paired plots on figure 5.7. The first 11 bands of MERIS without ICOL gave a correlation which ranged between R^2 of 0.7978 and 0.8893. After the implementation of ICOL- C2R there was a significant improvement in R^2 and ranged between 0.8854 and 0.937. After ICOL -C2R were implemented, reflectance increased considerably at all 6 sampled points and it got more pronounced between 600 and 780 nm. Thus a conclusion can be drawn that land pixels affected the initial results of C2R method. The magnitudes of errors were assessed based on Mean Absolute Error (MAE) and the range was between 0.003361 and 0.005364. It is imperative to note that the C2R alone gave a smaller error than ICOL-C2R and is the reverse was expected. However the fact that the MAE was marginal almost close to zero on both cases we can rule out bias. A summary of these statistics is provided in table 5.1 and figure 5.8 shows the scatter plots reflectances as a function of wavelength for the six sampled sites.

C2R alone proved to be insufficient for it underestimated reflectances in the NIR. Performance of ICOL plus C2R gave a positive effect on the spectral shape despite weaker absolute reflectance values with respect to the in situ measurements. Therefore, considerations for adjacency effects should be put into consideration for future studies in Lake IJsselmeer. Figure 5.4 illustrates this improvement in reflectance after pre-processing with ICOL and implementation of C2R. Table 5.1 shows the summary of statistical analysis, MAE and R^2 for the 6 sampled sites.

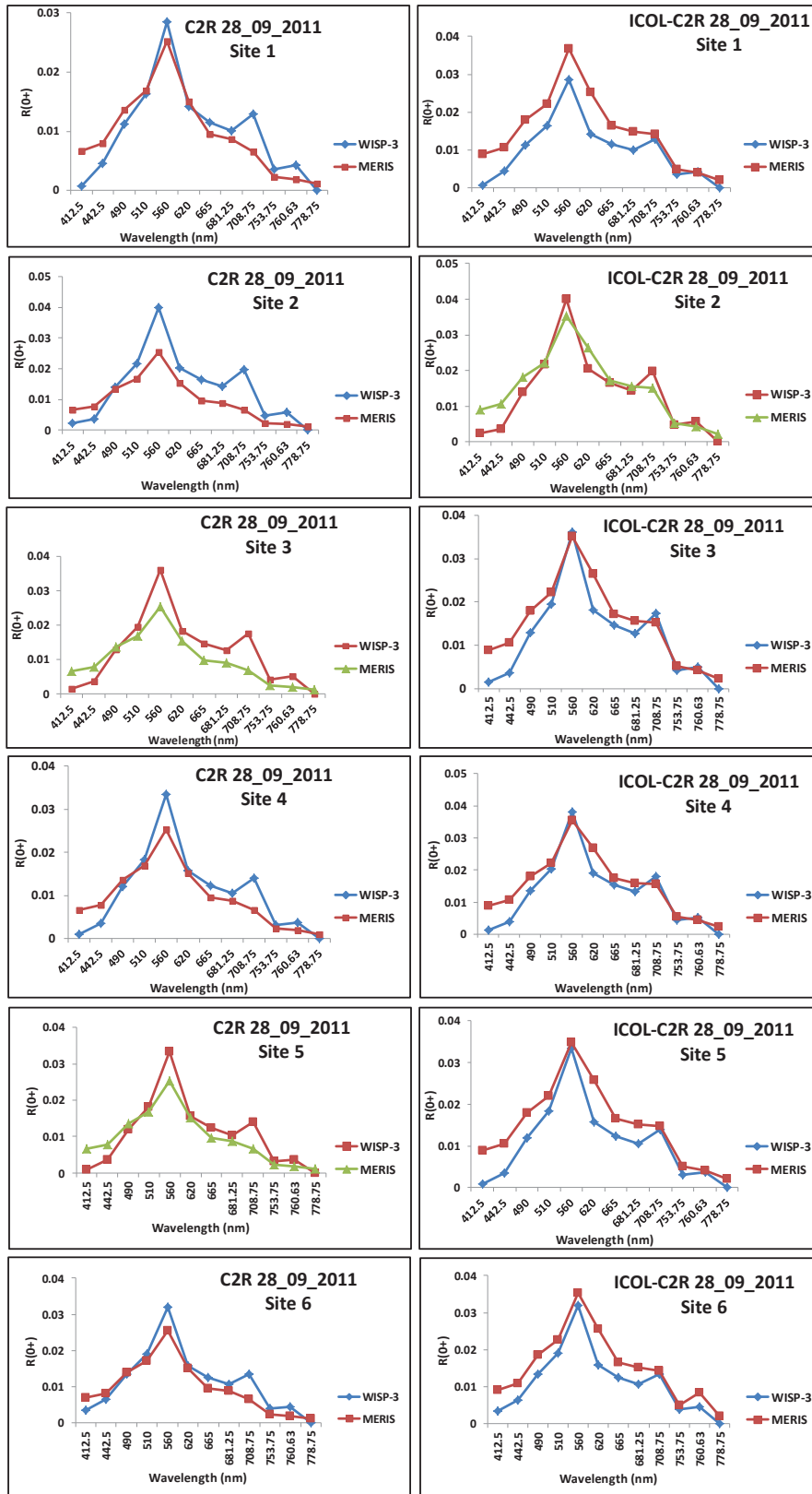


Figure 5.7: Accuracy assessment of Atmospheric Correction for the 6 sampled geographical locations in Lake IJsselmeer. The left panel indicates C2R without ICOL and the right panel indicates C2R with ICOL. MERIS centered bands are displayed

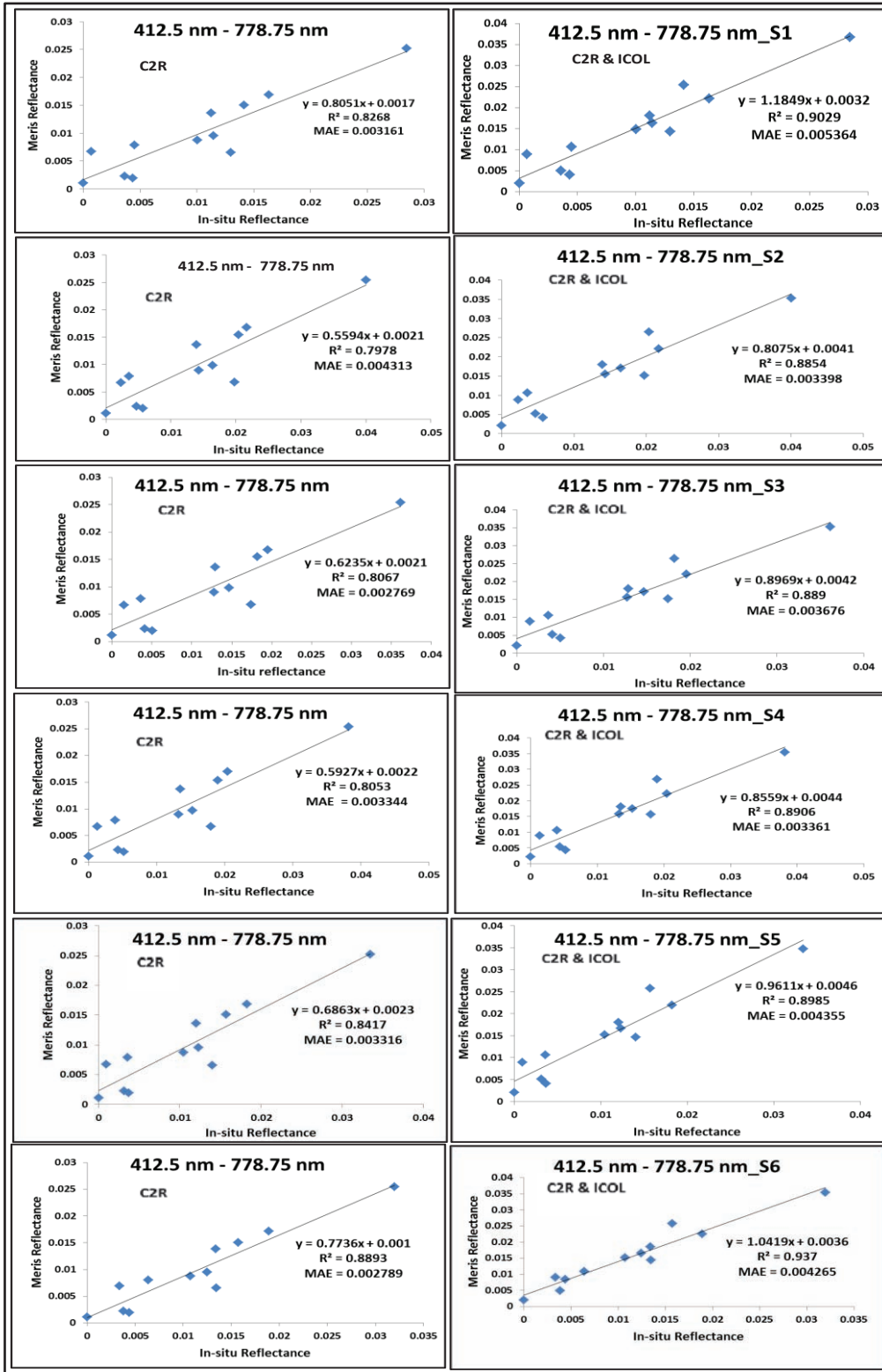


Figure 5.8: Correlation of Atmospheric matchup points of In-situ and MERIS before and after implementation of ICOL. Plots on the left panel indicates C2R without ICOL whilst the right panel indicates C2R with ICOL

Table 5-1 Summary Statistics of atmospheric correction: n = 6.

Date- 28/09/2011	C2R		ICOL +C2R	
Sampled sites	MAE	R ²	MAE	R ²
1	0.0032	0.8268	0.0054	0.9029
2	0.0043	0.7978	0.0034	0.8854
3	0.0028	0.8067	0.0037	0.8890
4	0.0033	0.8053	0.0034	0.8906
5	0.0033	0.8417	0.0044	0.8985
6	0.0028	0.8893	0.0043	0.9370

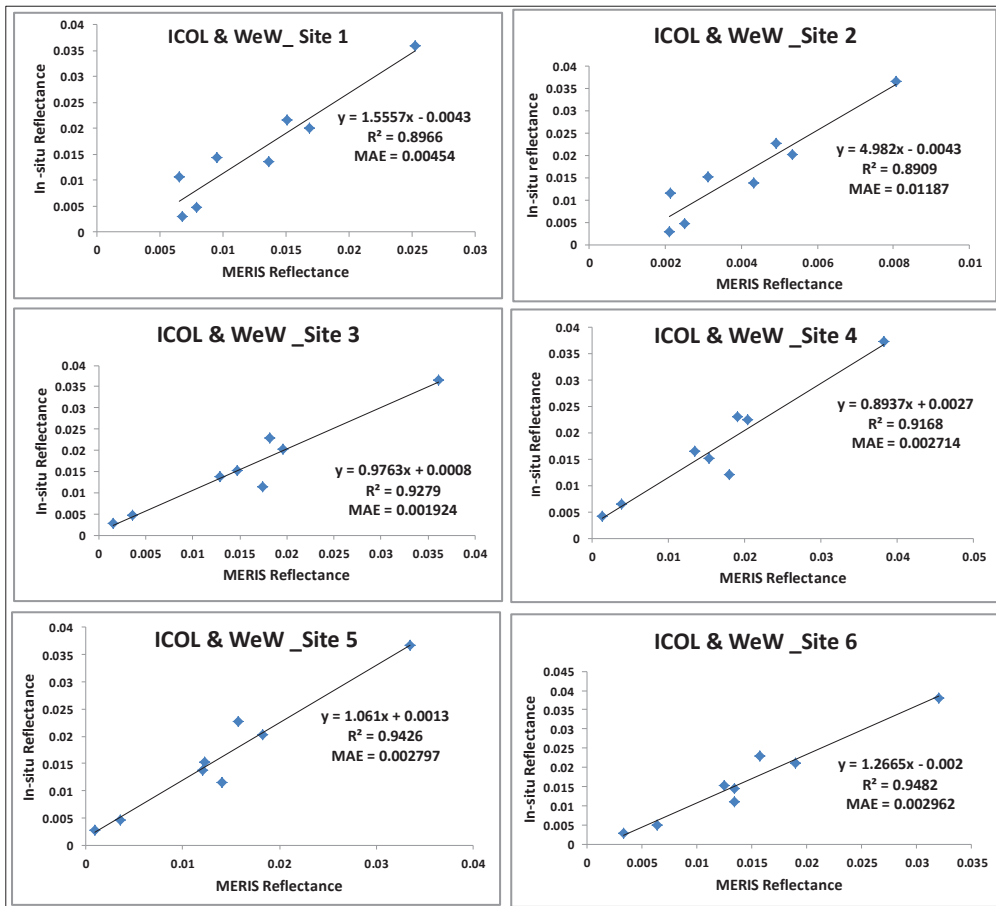


Figure 5.9: Correlation of the Spectral match-ups of WeW – ICOL and In-situ Reflectance Spectra

The statistical analysis of the WeW - ICOL and In-situ reflectance spectra validation showed a good correlation with R^2 range between 0.9 and 0.95 as presented on figure 5.9. The finest match was observed in the visible range notably between 412.5 nm to 510 nm. The MAE was lower with the lowest 0.0019 on point 3 whilst on the same point on ICOL – C2R it was relatively high 0.0036. However, at all matched points ICOL-WeW had low MAE as compared to ICOL- C2R. On the other hand C2R processor alone gave the strongest deviation and this problem was also observed by Kratzer et al. (2008); (Kratzer and Vinterhav, 2010).

5.4 Phycocyanin Concentration from MERIS image

Field data was categorised into two datasets, one from Wisp-3 measurements and the other from real-time fluorescence in-situ measurements to be discussed later in this chapter. Both datasets were used to substantiate the model outcome. The results and discussion on this part focuses mainly on retrieval and validation of MERIS image of 28 September 2011 with WISP-3 Spectroradiometric measurements. The second part on validation deals with MERIS 13 images and real-time fluorescence measurements.

After atmospheric correction, semi empirical band ratio model was implemented for the derivation of PC concentrations and PC absorption coefficients on the entire image. The detailed steps on the procedure are explained in section 4.6 of chapter 4. PC pigment concentrations measured in Lake IJsselmeer simultaneously with satellite overpass are presented in table 5.2 together with a_{pc} . The results demonstrate that semi-empirical band ratio model performed well in deriving PC pigment as a proxy for cyanobacteria concentration and distribution in IJsselmeer. Six sampled sites MERIS image gave PC concentrations which ranged between 68.1 and 72.3 mg/m³ and this is illustrated on figure 5.10. The best match was at point 1, 2, 3, and 4 with a difference of between 0.38 mg/m³ and 4.54 mg/m³. However, the distribution pattern of cyanobacteria concentrations varied from less than 27 mg/m³ in south western parts of Lake IJsselmeer up to 120 mg/m³ in North eastern and western parts. This range of concentrations was almost in agreement with literature values from (Simis et al., 2005b) who carried out a related research in the same study area on 9 September 2003 and their values ranged between 25mg/m³ and 80 mg/m³. A very steep gradient of concentrations was mapped in the South eastern part where the shoreline areas recorded a biomass exceeding 100 mg/m³ whilst the south western part it was as low as 30 mg/m³. A good positive correlation of ($R^2 = 0.7257$; $MAE = 4.67$ mg/m³ (7.53%)) between measured and modelled PC concentration was obtained. In addition, the lowest relative error was observed on site 2 with 0.5% (table 5.2) and the largest were observed on site 5 and 6 with 13.8% and 17.8% respectively. The percentage error was obtained by dividing the MAE with the average of the measured (actual) PC concentrations and finally by multiplying with 100. The estimated PC concentrations were obtained using the mean specific absorption coefficient obtained at 620 nm ($a_{pc} = 0.007$) previously applied for various lakes in Spain and Netherlands in work of (Ruiz-Verdú Simis et al., 2008; Simis et al., 2005b). Generally, application of a fixed specific absorption coefficient was successful in estimating PC concentrations. There are two possibilities which resulted in MERIS derived concentrations to be higher than measured ones. The ratio of 709 nm to 620 for MERIS is greater than that of WISP-3 or ICOL – C2R overestimated the PC concentrations.

The spatial patterns of MERIS imagery on September 28 were consistent with in-situ WISP-3 measurements for the same day. Whilst some consistence was noticed, some variations in cyanobacteria within a pixel of MERIS were observed. For instance, in-situ measurements from site/point 2 and 3 were slightly different whereas those from the model were similar. This suggests that there exist some concentration variations within one pixel (300m x 300m) of MERIS sensor. This same scenario was observed on WISP-3 measured reflectance in same pixel with different reflectance, 20% and 17% respectively. Presumably, the model calculates by averaging the values of concentrations in a pixel or the

resolution of the satellite applied. Nearly at all measured points, MERIS tended to overestimate PC concentrations. The discrepancy in matching between in-situ and MERIS derived PC concentration values could have resulted from what Salama et al. (2011) referred to as “subscale variation”. This variation originates from the difference between in-situ point measurements and satellite pixel based observation.

Table 5-2 Retrieved PC Concentrations and absorption coefficients from MERIS and measured PC concentrations

Site/point measured/observed	Wisp-3 PC Concentration (mg/m ³)	MERIS PC Concentration (mg/m ³)	Relative error	PC absorption coefficient (m ⁻¹)
1	65.56	70.1	0.0693	0.05329
2	71.88	71.52	0.0050	0.05705
3	70.36	71.52	0.0165	0.05705
4	69.17	72.31	0.0454	0.05909
5	62.37	70.96	0.1377	0.05568
6	57.81	68.09	0.1778	0.05016

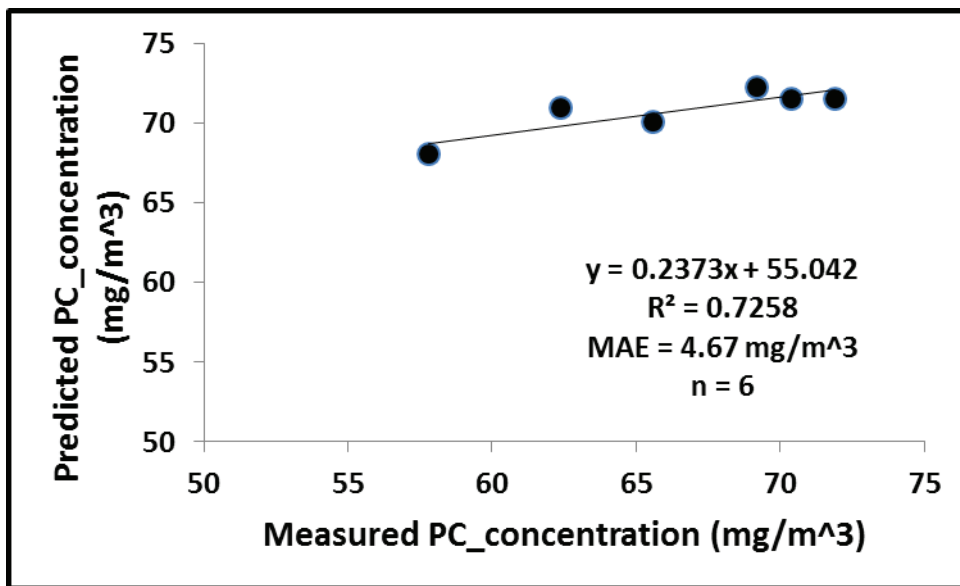


Figure 5.10: Correlation between WISP-3 measured and MERIS predicted PC concentrations.

5.4.1 Phycocyanin Absorption

Good correlations were observed between PC absorption coefficients at 620 nm and predicted PC concentrations with 0.983 R² value, figure 5.11 (a).

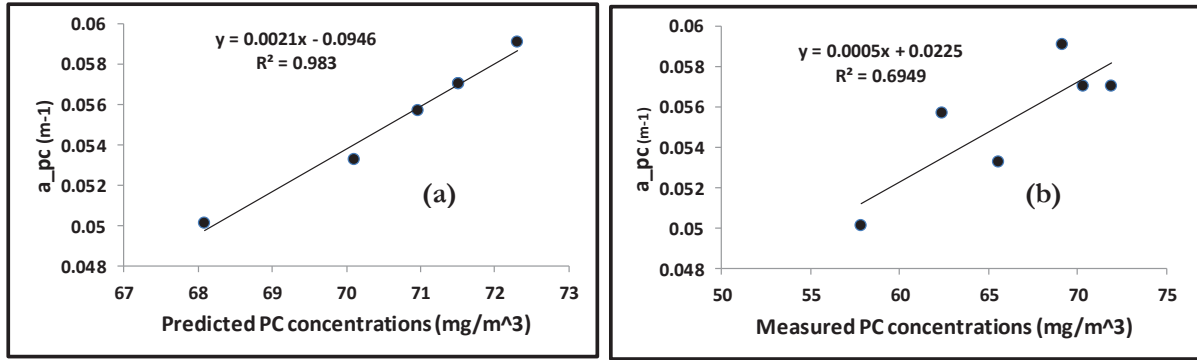


Figure 5.11: a, b: Scatter plots showing relationship between predicted PC concentration versus PC absorption and (b) Observed PC concentration versus PC absorption.

These findings were similar to (Dingtian and Pan, 2006; Randolph et al., 2008; Simis et al., 2007). The in-situ measured PC concentrations derived also demonstrated a good correlation with $R^2 = 0.697$, figure 5.8 (b). Thus, remote sensing estimates were in strong agreement with the in situ measurements. Hunter et al. (2010), got similar findings in his study which he carried out in eutrophic lakes of United Kingdom using the same model. The values of $a_{pc}(620)$ estimated by the semi empirical algorithm were strongly correlated with the measured concentration of PC concentration ($R^2 = 0.984$) and the resulting concentrations of PC derived from these coefficients also demonstrated a near 1:1 relationship with measured PC values (RMSE=3.98 mg/ m³ (13.7%)).

Greater performance of (Simis et al., 2005b) algorithm is certainly attributable to fact that it corrects for the contribution chl_a to absorption at 620 nm (Hunter et al., 2010; Seppälä et al., 2007). In addition to the aforementioned point, Hunter et al. (2010) also asserted that relative contribution of chl_a at 620 nm is highly dependent on the floristic composition of phytoplankton species. From this point of view, relative contribution of chl_a to PC pigment absorption at wave band 620 nm can thus be expected to decrease PC: chl_a ratios. This implies that an increase in bio-volume of chl_a at 620 nm is expected to result in error on estimating PC concentrations. These results concurs with Becker et al. (2009) who envisaged that optical absorption component is directly related to the concentration where the higher the absorption a_{pc} than a_{chl_a} , the more cyanobacteria concentrations. Generally on many parts of the Lake PC values were > 50 mg/ m³.

5.5 Phycocyanin Intensity Index

This section provides results and discussion of PC.I.I for the fourteen images which were all corrected for the effect of the atmosphere. The index was calculated according to the algorithm given in equation (16) chapter 4 and the index values were log transformed before they were plotted. The results of this study indicated that PC.I.I is well characterized by the pigment concentration of cyanobacteria. September were Figure 5.12 a, and b illustrates correlation between PC.I.I and PC MERIS derived concentrations with ($R^2 = 0.903$ and 0.964) for 1st of and 28 September respectively. We also found that on 18 April chl_a dominated and as a result the index gave a weak correlation with ($R^2 = 0.4803$) as illustrated on (fig 5.12, c).

We implemented index algorithm on fourteen images and yielded moderate correlation with PC concentrations ($R^2 = 0.55$ and RMSE 7.614) and this is illustrated on figure 5.13. It is important to note that semi-empirical band ratio gave a linear trend where decrease in chl_a resulted in an increase in PC concentrations. It was deduced that chl_a in the southern area and other parts of the lake reduced the sensitivity of semi empirical band ratio model and consequently weaker relationships of PC to index in

these areas described above. The scatter plot on figure 5.14 shows a poor correlation between chl_a and the index.

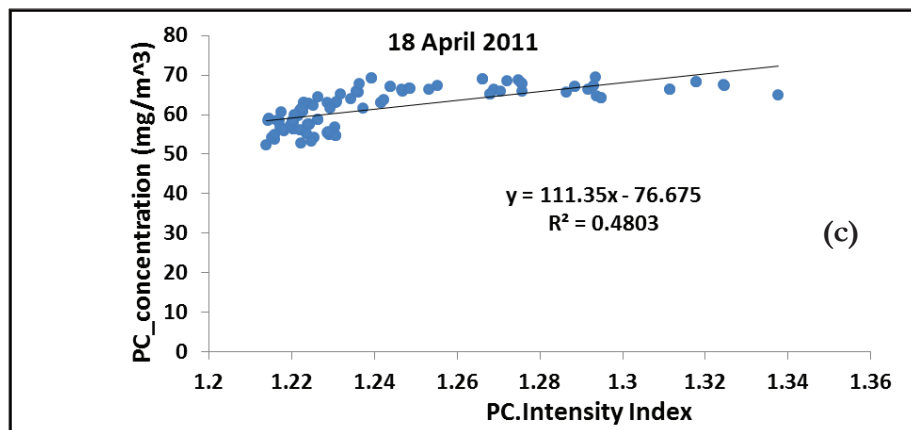
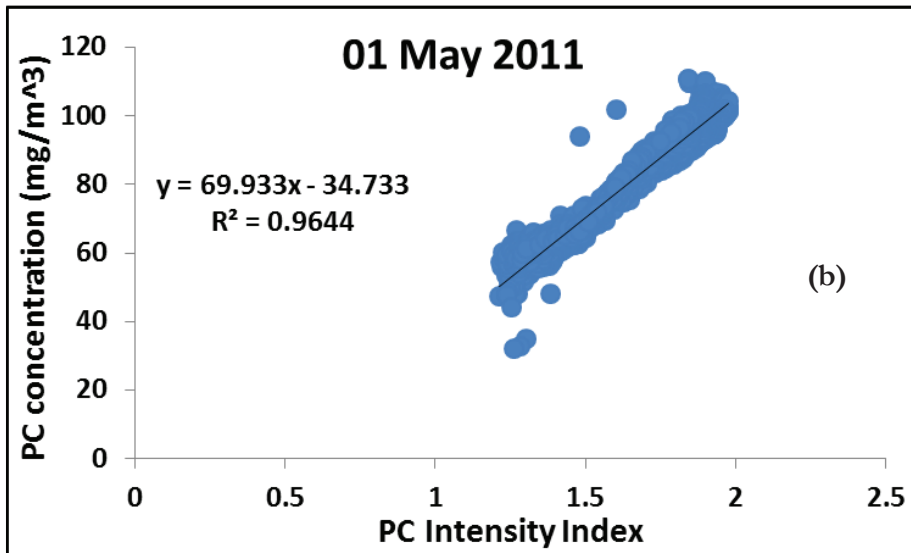
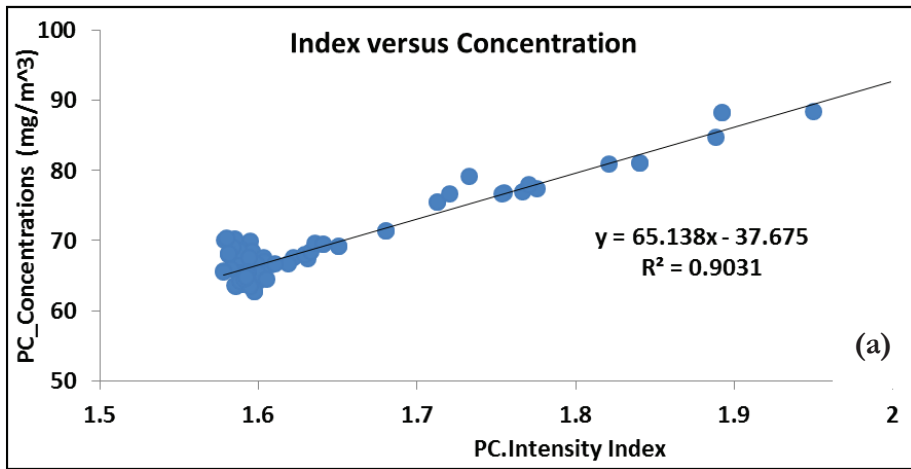


Figure 5.12: a, b, c: Relationship between PC.I.I and PC concentration for 28 September 2011, 10 May and 18 April. The PC.I.I plotted values were log transformed before they were plotted.

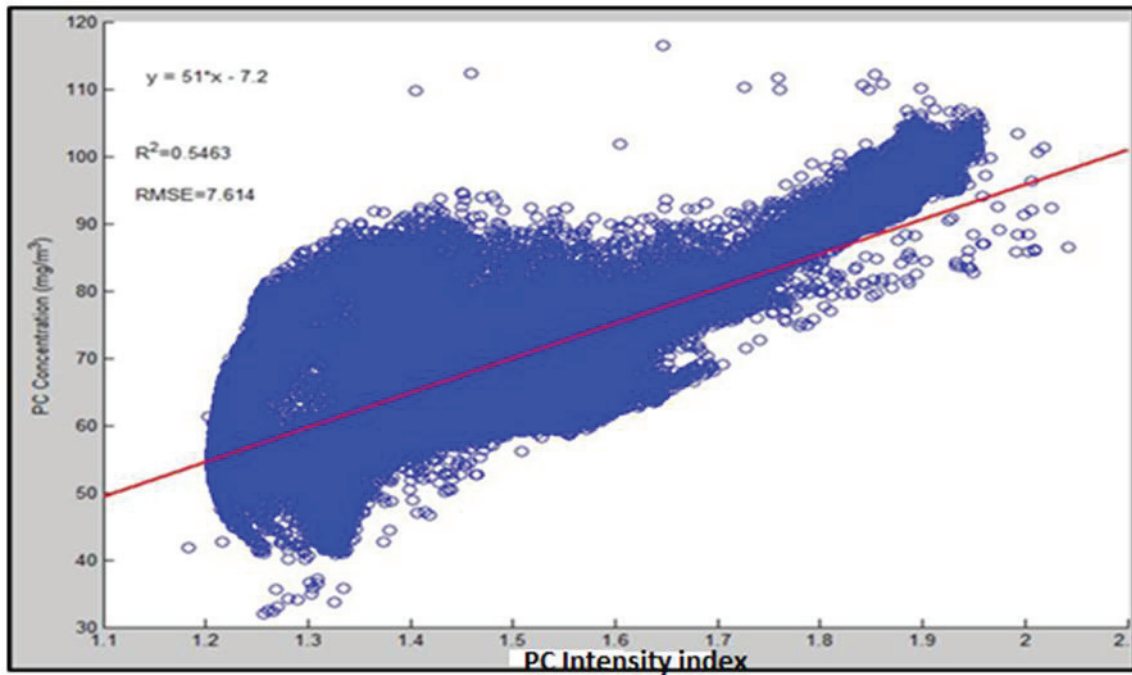


Figure 5.13: Scatter plot of PC.I.I versus PC concentrations for 14 maps. The PC.I.I plotted values are log transformed

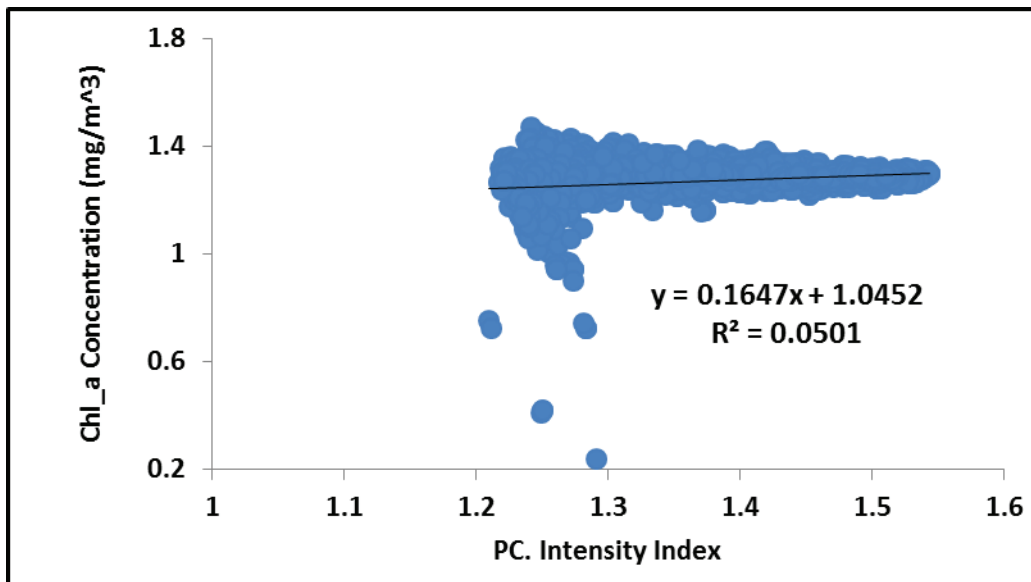
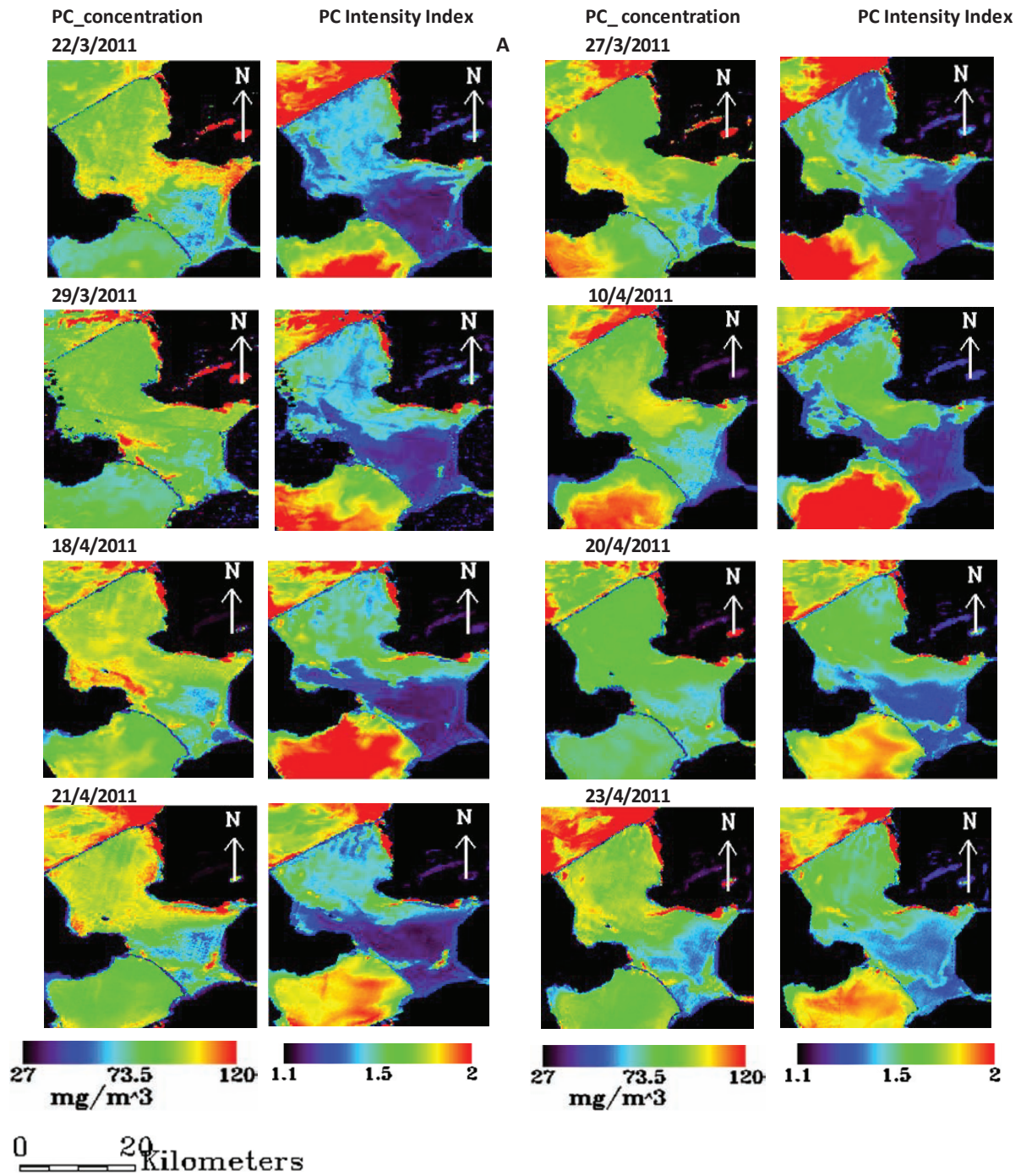


Figure 5.14: Scatter plot of PC.I.I versus chl_a concentrations for 14 maps

One intriguing point on the findings from this study was that, the index increased with PC concentrations. However, there was an abrupt change in some parts of the lake in case where chl_a increased sharply resulting in lower PC and index correlation. This changed the performance of the index significantly for PC concentrations. Thus, a conclusion can be drawn from the scatter plots on figure 5.12 (c) and 5.13.



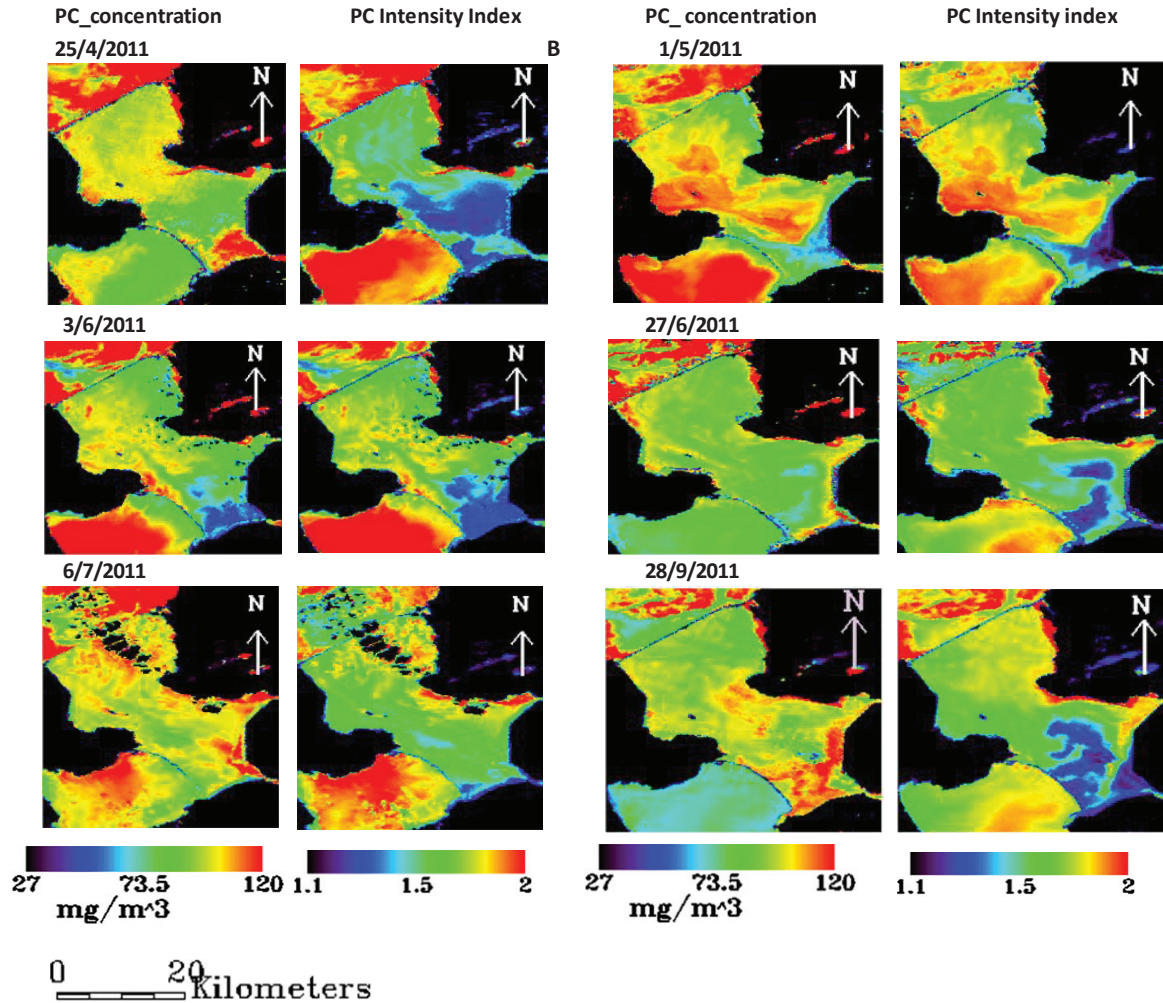


Figure 5.15: A and B: Distribution maps of PC concentration and PC Intensity Index.

5.5.1 Cyanobacteria Distribution

The distribution patterns of cyanobacterial biomass of phycocyanin showed varying concentrations from 27 mg/m³ to 120 mg/m³ as illustrated on maps on figure 5.15 A and B. The PC concentrations from in-situ measurements were above 50 mg/m³ and is reliable for lake IJsselmeer based on Simis et al. (2005b)'s findings. The PC: chl_a ratios were higher and this contributed to superiority PC concentration retrieval from the model. A close investigation on the results from the comparison of each dated map, PC concentration against PC intensity index was made. Maps of 22, 27, 29 March and 18 April were observed to be dominated by chl_a especially in the Southern part of the lake. We noted that in the southern part of the lake concentrations of PC pigment were low and it may be assumed that the decrease was due to the presence of other accessory photosynthetic pigments. Simis et al. (2005b) strongly attributed this effect to chl_b. Other literature also supported these findings for example, Gons et al. (2005a) mapped high chl_a concentrations in the southern lake IJsselmeer. There was a huge gradient of PC concentration variation from Southern part of the lake to Northern part especially on 23rd of April and 3rd of June. The profile plots on appendix C (fig 4) show the variations of PC concentrations from S to N direction across the middle of the lake on the six selected maps with a distance approximately 54 km. Another striking feature on this study was a huge cyanobacteria surface bloom mapped on 1st of May notably on the central and western part of the lake with concentrations above 70 mg/m³ and in some cases almost double. Perhaps, this was a “spring bloom” prompted by nutrient upwelling and rise in temperature. Wind could also have

played part in the distribution pattern of this bloom, from south-east towards north-west. The eastern shoreline was also characterized by high PC concentrations, above 100mg/m³.

Indeed, the P.C.I.I worked well especially where PC: chl_a ratio was high. The occurrence of both PC and chl_a concentrations reduced the accuracy of the index. Nevertheless, in places where chl_a existed in concentrations higher than 17mg/m³ and PC pigment occurring below 50mg/m³ the index performed weakly, not greater than 1.5. Concentrations between 50 mg/m³ and 120 mg/m³ were observed to correlate with index the range between 1.6 and 2. The shoreline in the north eastern part recorded had highest PC pigment concentration patches and this could be attributed to predominant wind effects from south- western direction. In general, maps on figure 5.15 of PC intensity index PC concentration showed a linear correlation in most parts of the lake with the exception of 22, 27, 29 March, 10, 18, 21, and 25 April maps with high chl_a concentrations notably in the southern region of the lake. In overall, the index performed well as it conformed to the PC concentrations in most parts of the lake.

From the findings of this research we assumed that cyanobacteria could be sensitive to stress conditions induced by sediment loads at the mouth of river IJssel resulting from rainfall runoff flowing into the lake. Nevertheless, cyanobacteria abundance in the southern part of the lake has been reported in some cases to be high regardless to dominance also exhibited by chl_a. Although wind data was not analysed in this study we found from literature that it wind speed and direction was critical in the horizontal distribution of cyanobacteria blooms (Graham et al., 2008; P. W. Lehman et al., 2005; Nöges et al., 2010). On the other hand, vertical distribution was affected by wind velocity. We found that on 28 September the wind speed was 4 m/s, (see appendix A under ancillary data) and this was in agreement with 3 m/s postulated by (Wu et al., 2010) in Taihu lake China where they focused horizontal distribution and transport processes of cyanobacteria bloom forming.

5.5.2 Three-tier Alert System

Accumulation of algal colonies at the surface represents the concentration and toxicity of cyanobacteria blooms and these are usually not homogeneously distributed over the water column. Thus, the main objective of this study was to develop a P.C.I.I from remote sensing techniques and utilize it as a recreational water quality monitoring tool. Based on the findings of this study, recreational exposure to cyanobacteria toxins was addressed by adopting guidance/warning levels that were developed with thresholds set according to WHO recreational water standards (Ibelings, 2005; WHO, 2003).

Table 5-3: PC Intensity Index Guidance levels for Lake IJsselmeer

Alert level	Index	Risk	Action
< 10 mg/m³	–	low	Safe
10 - 20 mg/m³	–	Moderate	Caution
>20 mg/m³	>1	High	Dangerous

Our developed index is based on three-tier alert levels which can be adopted for monitoring recreational waters. Table 5.3 shows the developed index and as can be noted from the index the whole of IJsselmeer has cyanobacteria concentrations exceeding the lower limit of high risk greater than 1 (equivalent to 20 mg/ m³). A concentration of 27mg/m³ was found to be the lowest in our case, and this is a clear translation that human life is susceptible to adverse health effects of cytotoxins, hepatoxins and

neurotoxins. The concentrations of cyanobacteria in the entire Lake between March and September were found to be well above the recommended recreational water quality standards. Related provisional guidelines for recreational waters were developed in USA by (Graham et al., 2008) according to Chorus and Bartram (1999) and the levels were set as follows;

- Low risk: less than 10 micrograms per liter ($\mu\text{g/L}$) equivalent to 10 mg/m^3
- Moderate risk: 10–20 $\mu\text{g/L}$
- High risk: 20–2,000 $\mu\text{g/L}$
- Very high risk: greater than 2,000 $\mu\text{g/L}$

We found out that, the index can provides a convenient means of summarizing complex cyanobacteria distribution and facilitate its communication to the general public. It can be utilized as an effective tool for summarizing the cyanobacteria concentrations for monitoring for recreational water bodies and alerting the public accordingly.

5.6 Phycocyanin Fluorescence

PC pigment has a specific fluorescence characteristic at 620 nm and if excited at this wavelength it will emit light at a longer wavelength around 665 nm as reported by (Brient et al., 2007). The PC concentration at any given time and point is proportional to the amount of PC fluorescence emitted. Thus, fluorescence provides a continuous of measure of cyanobacteria concentration. Based on this relationship, real-time phycocyanin fluorescence in-situ measurements were used to validate MERIS derived PC concentrations. Daily, monthly and seasonal variability of cyanobacteria in IJsselmeer was investigated based on turbidity, temperature, and oxygen. The results of the analysis showed that PC fluorescence was in agreement with MERIS PC derived concentrations for data collected at two locations (Pole 46 and 47). Log transformations for real-time in-situ PC fluorescence were performed on the results to make comparisons easier with MERIS data and with other variables.

5.6.1 Diurnal and Monthly Variations of Cyanobacteria

PC fluorescence was first assessed in terms of diurnal variations from average values taken between 8:00 am and 15:00 pm and a demonstration of its variability is presented on figure 5.16 (a) and (b) for the July and September 2011. The diurnal variation of PC fluorescence was found to be low in the morning on 6 July and around 9 am the fluorescence steadily increased probably due to solar radiation. As the intensity of the sunlight increased in the day it depressed the cyanobacteria algae a condition referred to as photo inhibition of photosynthesis by (Kurzbaum et al., 2007) resulting from extreme excitation. Later in the day, it can be deduced that maximum emission was reached at 15:00 hours.

On the other hand, on 28 September it seemed there was alternating light conditions which resulted in fluctuating diurnal cyanobacteria blooms at the surface of the water. Literature also reveals that photosynthetic activity diurnal pattern in afternoons are characterised by low levels of fluorescence in the mid-day provided intensity of light is high. Thus, PC pigment exposed to low light levels does not unveil a significant decrease (Figuroa et al., 1997). It can be concluded that on 28 September there was a lot of sunlight which resulted in high fluctuations in the morning hours as illustrated on figure 5.17 b.

In this study, we found that it was important have two samples as a single day could not be sufficient to evaluate the importance of PC fluorescence as also argued by (Nõges et al., 2010) because of the likelihood of a single day characterized by same light intensity conditions hence not enough to show significant variations.

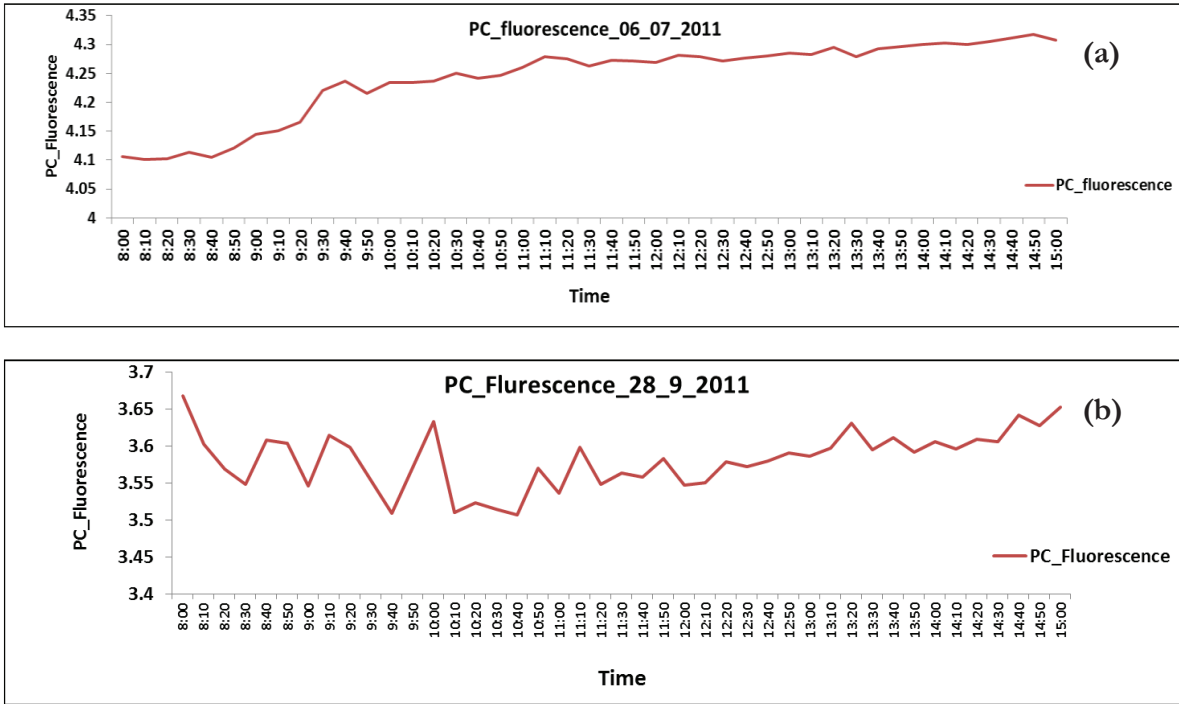


Figure 5.16 a, b: Daily averages of PC Fluorescence variation between 8:00 am and 15:00 pm for 6 July and 28 September. PC Fluorescence values were log transformed before they were plotted.

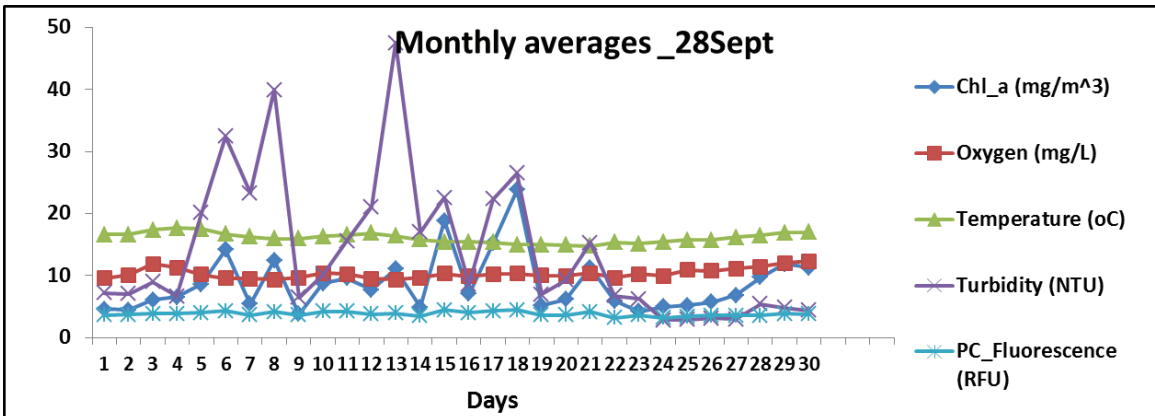


Figure 5.17: Monthly Variations of Oxygen, Temperature, Turbidity, chl_a and PC

The parameters shown on figure 5.18 are diurnal averaged values for each respective day between 8:00 and 15:00 hours. From this figure it can be deduced that fluorescence, oxygen and temperature did not vary much for the entire month. Temperature steadily fluctuated between 15°C and 18 °C. However, turbidity showed a marked increase between 4 and 8 and 11 and 13 September. Increase in turbidity resulted in an increase in chl_a at most given days with the exception from 22 to 28. Another possibility of high turbidity could be attributed to TSM loaded in the lake. It was not clearly understood what caused the fluctuation when chl_a was increasing at the end of the month. This scenario was also noticed from most MERIS images on figure 5.15 on the southern part areas of the lake because increase in algal biomass is expected to make the water more turbid. Nöges et al. (2010) posited that cyanobacteria booms increases the turbidity of the water bodies and this has an adverse effects notably toxin production as well as pungent smell.

5.6.2 Seasonal Variability of Cyanobacteria blooms

Usually rising temperatures, high nutrient loading favor cyanobacterial blooms dominance which in turn increase the turbidity of lake leading to depletion of oxygen levels (Nõges et al., 2010). The time series on figure 5.19 indicates the variability of five parameters (on the legend) in IJsselmeer. PC fluorescence and Oxygen are displayed on secondary a-axis. These variables are monthly averaged resulting from daily means calculated between 8:00 am and 15:00 pm. Thus, each month is represented by a single average value. It was observed that during the month of March oxygen levels were high because oxygen is saturated in winter and less biomass of phytoplankton species thrive because of inhibiting low temperatures.

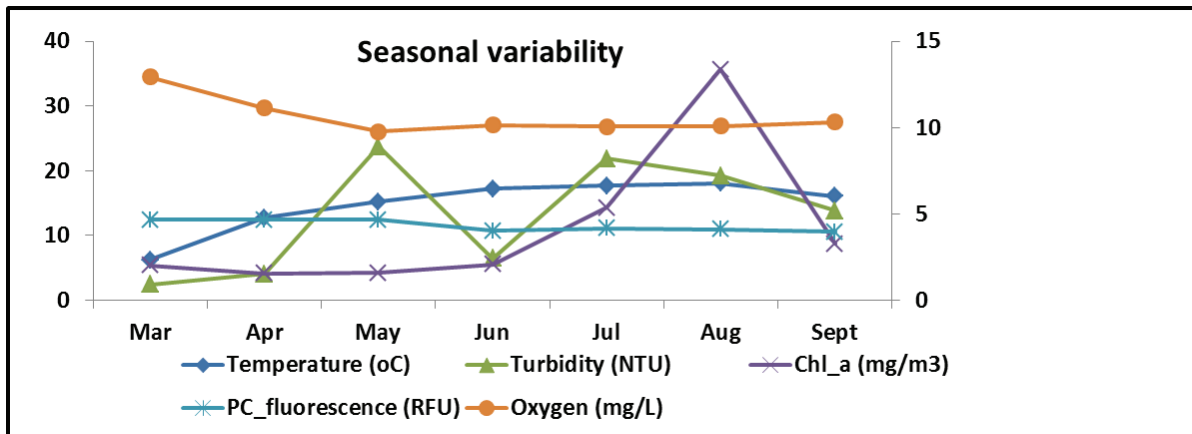


Figure 5.18: Seasonal variations of turbidity, temperature, Oxygen, PC fluorescence and chl_a. Log transformed PC fluorescence and Oxygen are displayed on secondary axis.

The PC fluorescence, plotted on the secondary axis showed an increase in May and also temperature increased from around 5°C in March to about 16°C in May. Turbidity recorded high most probably from the blooms which were close to the water surface however, it dropped in June. Temperature steadily increased between March and April and September. Chl_a was the dominating algal pigment on August whilst PC fluorescence did not show any increase. The reason for this trend could not be well established but we attribute it to the instrument that could have failed to record well PC fluorescence. The increase in PC was expected to be high around summer period because of maximum stability attained the water column with high vertical nutrient and algal concentration gradients (Salmaso, 2000).

Spring and summer time are associated with abundance of cyanobacteria blooms and this is because of high nutrients received by the water body from rainfall intensity events rather than duration for example convection rain fall during summer months. High pulse runoff into the lake brings loads of nitrates and phosphorus although these are out of the scope of this study. Autumn and winter are characterized by a decrease in cyanobacteria blooms whilst during spring and summer times the trend is the opposite. Mihaljević and Stević (2011) as well as Ibelings et al. (1998) carried out a similar study in Croatia and Netherlands respectively and had similar findings.

5.6.3 Comparisons of PC Concentrations and Chl_a from MERIS and Real-time Measurements

This study found linear relationship between the averaged values of real-time PC fluorescence measurements and MERIS derived cyanobacterial concentrations. The general agreement between the MREIS derived cyanobacterial concentrations and the fluorimeter concentrations for the September 22, 27, 29 March, 10, 18, 20, 21, 25 April, 01 May, 03, 27 June, 06 July and 28 September bloom events was good. Figure 5.15 presents the outcome of the validation. The values used in the scatter plots are available

on table 6 appendix D. The positive correlation between PC fluorescence and cyanobacterial concentrations was also reported by (Izydorczyk et al., 2005) in their study which they carried out in the Sulejow Reservoir, Poland. The plot on pole 46 showed a negative slope because on 1st of May were huge 103 mg/m³ corresponding to 8619.86 relative fluorescence units (RFU) and 6th of July with 82.12 mg/m³ corresponding to 17626.05 RFU whereas on other months fluorescence units were greater than 64000 RFU. This data is provided in appendix D as aforementioned.

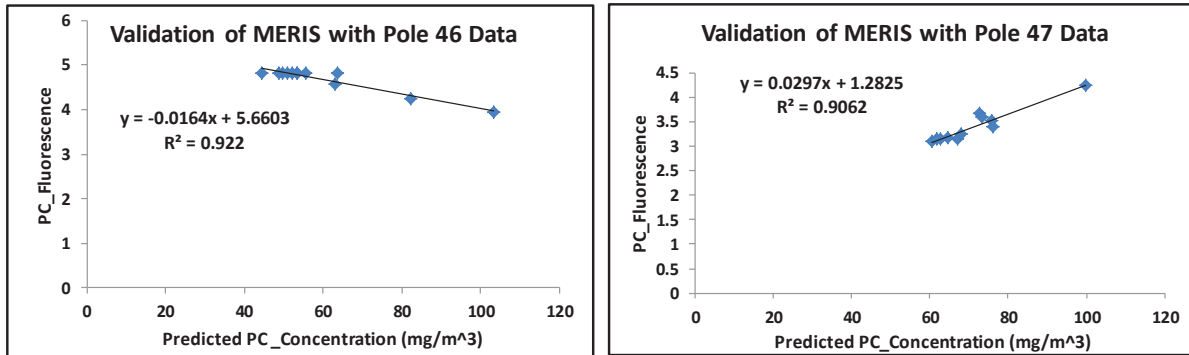


Figure 5.19: Scatter plots of PC fluorescence and MERIS PC concentrations. PC Fluoresce is given in (RFU) units

Real-time measurements on pole 46 and 47 revealed a stronger correlation for each MERIS scene in all cases with $R^2 = 0.922$ and 0.906 respectively as shown of figure 5.19. However, a negative slope on pole 46 was attributed to lower units recorded by the sensor but corresponding well to high concentrations in the months of July and May. These results demonstrate that, this methodology can be used to develop a cost-effective practical screening method for rapid detection and warning of potentially toxic cyanobacterial blooms in the IJsselmeer as envisaged by (Becker et al., 2009). In a study carried in the Mediterranean European lakes by (Gómez et al., 2011) showed that PC fluorescence was in strong agreement with MERIS derived concentrations where $R^2 = 0.9764$.

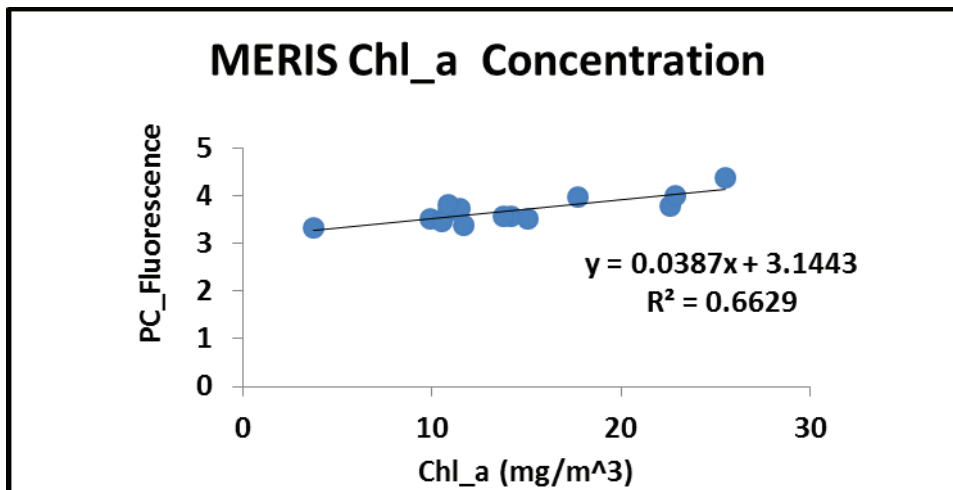


Figure 5.20: Comparisons between PC fluorescence and MERIS chl_a concentrations

In this study we also compared the PC fluorescence to chl_a concentrations derived from 14 MERIS images and the comparisons were based on the fluorescence data extracted from pole 46 as shown on figure 5.21. The findings of our study indicated that there was a good correlation between the two with R^2 value 0.663.

5.7 Seasonal Succession of Cyanobacteria and chl_a

The results of plots on figure 5.21 illustrates that MERIS derived Index, PC and Chl_a concentrations had similar distribution pattern with real-time PC fluorescence and chl_a. There was an increase in concentrations between 22 and 29 March. The lake seemed to have been dominated by chl_a in the south and fairly in the northern areas by cyanobacteria. This fact is well backed by the index which is lower during this period. This was probably due to sunny conditions which might have prevailed and resulted in the temperature increase. However, at pole 47 a slight different trend was observed where concentrations were low and only increased on 10 April. In May large value of PC concentration and chl_a at pole 46 was measured; 103 mg/m³ and chl_a 29 mg/ m³ respectively. The same pattern was also observed on pole 47 in May. This period coincided with spring when there was a lot of nutrient mixing. This pronounced bloom can be attributed to thermal stratification which (Nöges et al., 2010) associated it with interplay between temperature and wind.

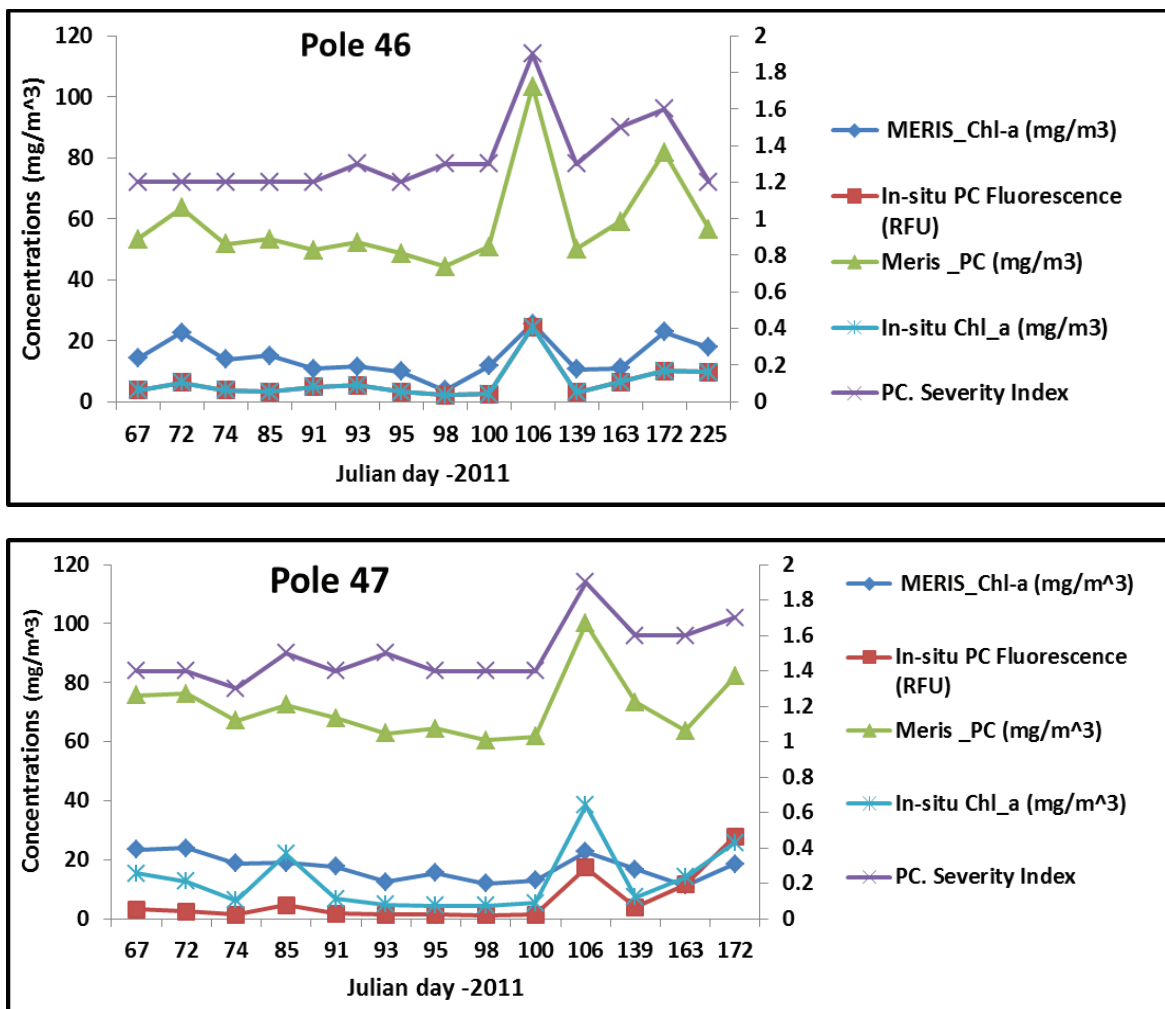


Figure 5.21a, b: Time series of PC and chl_a from in-situ measurements and MERIS image for pole 46 and 47. PC fluorescence is displayed on the secondary axis and its values were log transformed before they were plotted.

Peeters et al. (2007) concurred that spring bloom by phytoplankton growth from vertical mixing seems to be a “rule rather than an exception”. The PC.I.I agreed well with concentrations suggesting that PC was the dominating pigment. On 6 July the concentrations declined at both locations and only started to

increase steadily in September. These findings concur with those of (Kanoshina et al., 2003; Salmaso, 2000) in which they studied cyanobacteria events and deduced that there was seasonal succession where the intensity and magnitude varied substantially.

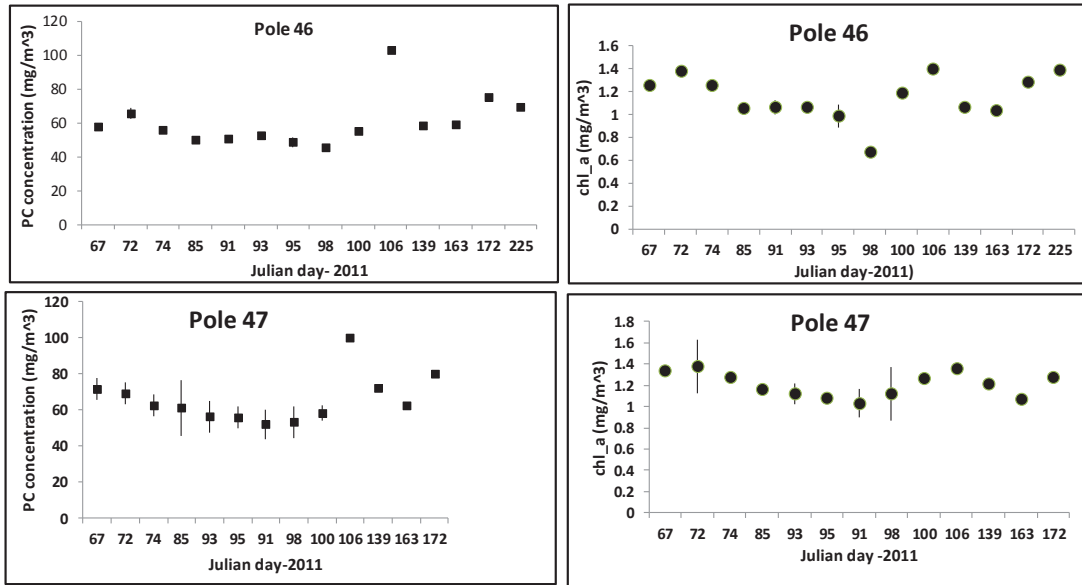


Figure 5.22: Mean and Standard deviation (vertical bar) of chl_a and PC concentration

The results of mean and standard deviation for MERIS derived chl_a and PC concentrations indicate that at most sampled sites neither PC nor chl_a deviated much from the mean notably on pole 46. However, seasonal variation in PC concentration between March and April was noted on pole 47 this scenario is shown on figure 5.22. Likewise, chl_a showed some variation in the same period on pole 47. This could be attributed to environmental factors and weather conditions which prevailed during that period such as wind and temperature. The results agree with Lehman et al., (2008) who found that concentration of PC and chl_a varied seasonally from one month to another due to environmental factors as well as wind and water temperature. However their study was carried in a river system in Sa Francisco.

From this study, we deduced that there was variability in cyanobacteria distribution from all the months investigated. Intense blooms were mostly concentrated on the North eastern part of the lake along the shoreline where the surface water was transported by the wind-induced currents as argued by (Kanoshina et al., 2003). The findings of our study also indicated that the concentration of cyanobacteria in L. IJsselmeer from March to September on average were above 50 mg/m³. This is well above WHO thresholds for low risk exposure and it implies that human life aquatic life forms are exposed to cytotoxins, Hepatotoxins and neurotoxins. We therefore recommend the responsible authorities to adopt and consider seriously the developed index as an effective, efficient and fast monitoring tool.

5.8 Limitations

- Netherlands experiences overcast conditions as such challenges were encountered to obtain cloud free images for match-up with in situ measurements during the field campaign period.
- Another constraint was limited flexibility of ferry boats to take many sample point measurements which covers several parts of the lake as it was important to investigate spatial variability from in-situ measurements and make our validation solid.

6 CONCLUSIONS AND RECOMMENDATIONS

6.1 Conclusions

Based on the objectives and research questions of this study the following conclusions were made;

- This study has shown that MERIS band 620 nm is suitable for detecting PC pigment as a proxy for cyanobacteria concentrations. The 300 m pixel resolution coupled with narrow position of spectral bands, have proved MERIS a suitable satellite for real-time monitoring applications observing changes happening over short time scales.
- The semi empirical band ratio based model 709:620 nm proved to be a crucial utility in detecting PC pigment concentrations and its spatial distribution in Lake IJsselmeer. The absorption coefficient of PC returned by model gave a strong linear relationship with MERIS derived and WISP-3 PC concentrations with almost 1:1 relationship and this indicated the reliability of the model.
- Real-time PC fluorescence was very indicative of cyanobacteria concentrations and it demonstrated a stronger correlation with MERIS predicted PC concentrations thus; the correlation was near 1:1. MERIS predicted PC concentrations correlated well with WISP-3 in-situ measured PC concentrations. Simis PC values were used in this study as reference values.
- WISP-3 spectrometer was first tested in this study in the IJsselmeer as ground truth for validating MERIS satellite and our results have proved that it is a reliable accurate instrument. It acquired all the water quality parameters needed.
- The developed phycocyanin intensity index presented a stronger linear relationship with PC concentrations and has also proved to be a convenient means for summarizing variable cyanobacterial concentrations in Lake IJsselmeer.
- Based on linear relationship between PC.I.I and PC concentrations a three-tier alert system for recreational water warning levels was developed by adopting WHO recreational water guidance threshold alert levels. Thus, this study found that PC.I.I forms a good framework for monitoring potentially toxic cyanobacteria blooms in the IJsselmeer.
- The distribution and concentration of cyanobacteria was not homogeneous in Lake IJsselmeer as depicted on the maps, it varied spatially and in temporal scale. This study also deduced that PC pigment concentration was in the higher risk category (>20 mg/m³) in the whole lake and therefore the index represented the dangerous tier level of cyanobacteria in Lake IJsselmeer. Thus the contribution of remote sensing techniques in deriving indicators of cyanobacteria has provided a robust and versatile monitoring tool for recreational waters.
- The application of adjacency effects correction significantly reduced radiances from land pixels which if not removed would be recorded by the satellite sensor and consequently interferes with atmospheric correction processes. The reflectances improved considerably the implementation of the ICOL and C2R processor.

- The atmospheric correction algorithms/models for case 2 waters, WeW and C2R processors showed no significant difference after they were matched with WISP-3 reflectances except that WeW could not process the NIR bands 708.75 and 778.75 need for derivation of backscattering as well as 708.75 for semi-empirical band ratio for deriving PC concentrations.
- The implementation of ICOL-C2R for atmospheric correction enabled the retrieval of PC concentrations which correlated well with WISP-3 in-situ measurements as compared to C2R alone.
- Higher temperatures greater than 15°C and high nutrient levels favored cyanobacteria bloom formation whilst wind influenced strongly algal colony formations and surface scums distribution. From the time series analysis of seasonal variability of PC concentrations it was established that, PC concentrations varied from one season to another with peak on the onset of spring and summer months.

6.2 Recommendations

- A more accurate algorithm which does not under estimate PC concentrations should be developed in situations where ratio of PC: chl_a is lower. An investigation on the likelihood of other photosynthetic pigments having an influence at band 620 nm should be investigated
- Future researchers who propose to derive water quality parameters using remote sensing techniques should make ICOL a priority for correcting adjacency effects for inland water bodies. The adjacency effects processor for case 2 inland waters worked well in Lake IJsselmeer as there was a considerable improvement in reflectance that was expected to lower significantly PC absorption at 620 nm leading to unrepresentative PC concentrations.
- Wind influence on horizontal and vertical distribution of cyanobacteria in Lake IJsselmeer should be critically investigated as this study explored this parameter in a more rudimentary approach.
- Since a few points were sampled due to the already mentioned reasons, it is imperative to have evenly distributed fixed real-time in vivo PC fluorescence measuring sensors in the future so that validation of variable PC concentrations can be more concrete with satellite data.
- In essence PC fluorescence does not give the real value of PC concentration although there was a significant linear relationship between the two. In other words the relationship is more qualitative rather than quantitative as such it is imperative to find a way to quantify PC fluorescence.

LIST OF REFERENCES

- Andre, M., and Bernard, B. G. (1991). Diffuse Reflectance of Ocean Water: Its dependence on sun angle as influenced by the molecular scattering contribution. [Journal]. *APPLIED OPTICS*, 30(30), 4424 - 4438.
- Backer, L. C. (2002). Cynobacterial Harmful Algal Blooms : Developing a Public Health Response. *Lake and Reservoir Management*, 1(18), 20 - 21.
- Bartram, J., and Ballance, R. (1999). Water quality monitoring: A practical guide to the design and implementation of freshwater quality studies and monitoring programmes Retrieved from info@routledge.com
- Becker, R. H., Sultan, M. I., et al. (2009). Mapping cyanobacterial blooms in the Great Lakes using MODIS. *Journal of Great Lakes Research*, 35(3), 447-453. doi: 10.1016/j.jglr.2009.05.007
- Brient, L., Lengronne, M., et al. (2007). A phycocyanin probe as a tool for monitoring cyanobacteria in freshwater bodies. *Journal of Environmental Monitoring*, 248–255. doi: doi:10.1039/B714238B
- Buiteveld, H. (1995). A model for calculation of diffuse light attenuation (PAR) and Secchi depth. *Aquatic Ecology*, 29(1), 55-65. doi: 10.1007/bf02061789
- Campbell, G., Phinn, S. R., et al. (2011). Remote sensing of water quality in an Australian tropical freshwater impoundment using matrix inversion and MERIS images. *Remote Sensing of Environment*, 115(9), 2402-2414. doi: 10.1016/j.rse.2011.05.003
- CEARAC, N. (2007). Eutrophication Monitoring Guidelines by Remote Sensing for the NOWPAP Region NOWPAP Special Monitoring & Coastal Environmental Assessment Regional Centre (NOWPAP CEARAC), *Special Monitoring and Coastal Environmental Assessment* Retrieved from <http://cearac.nowpap.org/>
- Chorus, I., and Bartram, J. (Eds.). (1999). *Toxic Cyanobacteria in Water: A guide to their public health consequences, monitoring and management*. London EC4) 4EE: F & FN Spon, 11 New Fetter Lane.
- Codd, G. A., Morrison, L. F., et al. (2005). Cyanobacterial toxins: risk management for health protection. *Toxicology and Applied Pharmacology*, 203(3), 264-272. doi: 10.1016/j.taap.2004.02.016
- Dekker, A. G. (1993). *Detection of optical water quality parameters for eutrophic waters by high resolution remote sensing*.
- Dekker, A. G., Vos, R. J., et al. (2002). Analytical algorithms for lake water TSM estimation for retrospective analyses of TM and SPOT sensor data. *International Journal of Remote Sensing*, 23(1), 15-35. doi: 10.1080/01431160010006917
- Dekker, W. (2004). What caused the decline of the Lake IJsselmeer eel nstock after 1960? I. *ICES Journal of Marine science*, 394 - 404.
- Dingtian, Y., and Pan, D. (2006). Hyperspectral retrieval model of phycocyanin in case II waters. *Chinese Science Bulletin*, 51(0), 149-153. doi: 10.1007/s11434-006-9149-4
- Dingtian., Y., Delu, P., et al. (2006). Retrieval of chlorophyll<i>a</i> and suspended solid concentrations by hyperspectral remote sensing in Taihu Lake, China. *Chinese Journal of Oceanology and Limnology*, 24(4), 428-434. doi: 10.1007/bf02842860
- Doerffer, R., and Schiller, H. (2007). The MEdium Resolution Imaging Spectrometer. [Journal]. *International Journal of Remote Sensing*, 28(3 - 4), 517–535. doi: 10.1080/01431160600821127
- Doron, M., Bélanger, S., et al. (2011). Spectral variations in the near-infrared ocean reflectance. *Remote Sensing of Environment*, 115(7), 1617-1631. doi: 10.1016/j.rse.2011.01.015
- Duan, H., Ma, R., et al. (2010). Comparison of different semi-empirical algorithms to estimate chlorophyll-a concentration in inland lake water. *Environmental Monitoring and Assessment*, 170(1), 231-244. doi: 10.1007/s10661-009-1228-7
- Ernst, B., Nesor, S., et al. (2006). Determination of the filamentous cyanobacteria *Planktothrix rubescens* in environmental water samples using an image processing system. *Harmful Algae*, 5(3), 281-289. doi: 10.1016/j.hal.2005.08.003
- ESA. (2006). *MERIS Product Handbook* (Vol. 2.1).
- ESA. (2008). OBSERVATIONS OF THE LARGEST ITALIAN LAKES FROM MERIS, from <http://earth.esa.int/EOLi/EOLi.html>http://earth.esa.int/workshops/meris_aatsr2008/participants/539/pres_539_Giardino.pdf

- Figueroa, F. L., Salles, S., et al. (1997). Effects of solar radiation on photoinhibition and pigmentation in the red alga *Porphyra leucosticta*. *MARINE ECOLOGY PROGRESS SERIES*, 151 81-90.
- Gao, B.-C., Montes, M. J., et al. (2009). Atmospheric correction algorithms for hyperspectral remote sensing data of land and ocean. *Remote Sensing of Environment*, 113, Supplement 1(0), S17-S24. doi: 10.1016/j.rse.2007.12.015
- Giardino, C., Bresciani, M., et al. (2010). Application of Remote Sensing in Water Resource Management: The Case Study of Lake Trasimeno, Italy. *Water Resources Management*, 24(14), 3885-3899. doi: 10.1007/s11269-010-9639-3
- Gómez, J., Alonso, C., et al. (2011). Remote sensing as a tool for monitoring water quality parameters for Mediterranean Lakes of European Union water framework directive (WFD) and as a system of surveillance of cyanobacterial harmful algae blooms (SCyanoHABs). *Environmental Monitoring and Assessment*, 1-18. doi: 10.1007/s10661-010-1831-7
- Gons, H., Hakvoort, H., et al. (2005a). Optical Detection of Cyanobacterial Blooms. In J. Huisman, H. Matthijs & P. Visser (Eds.), *Harmful Cyanobacteria* (Vol. 3, pp. 177-199): Springer Netherlands.
- Gons, H., Hakvoort, H., et al. (2005b). Optical Detection of Cyanobacterial Blooms Harmful Cyanobacteria. In J. Huisman, H. Matthijs & P. Visser (Eds.), (Vol. 3, pp. 177-199): Springer Netherlands.
- Gordon, H. R., Brown, O. B., et al. (1975). Computed Relationships Between the Inherent and Apparent Optical Properties of a Flat Homogeneous Ocean. *Applied Optics*, 14(2), 417 - 427. doi: 10.1364/AO.14.000417
- Graham, J. L., Loftin, K. A., et al. (2008). *Cyanobacteria in lakes and reservoirs* (9 ed. Vol. 1.0): U.S. Geological Survey Techniques of Water-Resources Investigations.
- Guanter, L., Ruiz-Verdú, A., et al. (2010). Atmospheric correction of ENVISAT/MERIS data over inland waters: Validation for European lakes. *Remote Sensing of Environment*, 114(3), 467-480. doi: 10.1016/j.rse.2009.10.004
- Gulati, R. D., and van Donk, E. (2002). Lakes in the Netherlands, their origin, eutrophication and restoration: state-of-the-art review. *Hydrobiologia*, 478(1), 73-106. doi: 10.1023/a:1021092427559
- Harff, J., Björck, K., et al. (2011). *the Baltic sea Basin*. Springer.
- Herrera-Silveira, J. A., and Morales-Ojeda, S. M. (2009). Evaluation of the health status of a coastal ecosystem in southeast Mexico: Assessment of water quality, phytoplankton and submerged aquatic vegetation. *Marine Pollution Bulletin*, 59(1-3), 72-86. doi: 10.1016/j.marpolbul.2008.11.017
- Hoyer, M. V. (2010). North American Lake Management Society (NAMLS). *Thesis NAMLS*.
- Huitema, D. (2002). IJsselmeer Basin (C. f. C. T. a. E. P. (CSTM), Trans.) (pp. 1 - 72): University of Twente (UT).
- Hunter, P. D., Tyler, A. N., et al. (2010). Hyperspectral remote sensing of cyanobacterial pigments as indicators for cell populations and toxins in eutrophic lakes. *Remote Sensing of Environment*, 114(11), 2705-2718. doi: 10.1016/j.rse.2010.06.006
- Hunter, P. D., Tyler, A. N., et al. (2008). Spectral discrimination of phytoplankton colour groups: The effect of suspended particulate matter and sensor spectral resolution. *Remote Sensing of Environment*, 112(4), 1527-1544. doi: 10.1016/j.rse.2007.08.003
- Ibelings. (2005). Risks of toxic cyanobacterial blooms in recreational waters: guidelines. In I. Chorus (Ed.), *Current approaches to cyanotoxin risk assessment, risk management and regulations in different countries* (pp. 1 - 122). Berlin: Federal Environmental Agency.
- Ibelings, B. W., Admiraal, W., et al. (1998). Monitoring of algae in Dutch rivers: does it meet its goals? *Journal of Applied Phycology*, 10(2), 171-181. doi: 10.1023/a:1008049000764
- Ibelings, B. W., and Chorus, I. (2007). Accumulation of cyanobacterial toxins in freshwater “seafood” and its consequences for public health: A review. *Environmental Pollution*, 150(1), 177-192. doi: 10.1016/j.envpol.2007.04.012
- Ibelings, B. W., and Havens, K. E. (2008). Cyanobacterial toxins: a qualitative meta-analysis of concentrations, dosage and effects in freshwater, estuarine and marine biota Cyanobacterial Harmful Algal Blooms: State of the Science and Research Needs. In H. K. Hudnell (Ed.), (Vol. 619, pp. 675-732): Springer New York.
- Izydorczyk, K., Tarczynska, M., et al. (2005). Measurement of phycocyanin fluorescence as an online early warning system for cyanobacteria in reservoir intake water. [Research Support, Non-U.S. Gov't]. *Environ Toxicol*, 20(4), 425-430. doi: 10.1002/tox.20128

- Jiang, T., Zhang, J.-p., et al. (2001). Crystal Structure of R-Phycocyanin and Possible Energy Transfer Pathways in the Phycobilisome. *Biophysical Journal*, 81(2), 1171-1179. doi: 10.1016/s0006-3495(01)75774-8
- Kanoshina, I., Lips, U., et al. (2003). The influence of weather conditions (temperature and wind) on cyanobacterial bloom development in the Gulf of Finland (Baltic Sea). *Harmful Algae*, 2(1), 29-41. doi: 10.1016/s1568-9883(02)00085-9
- Kirk, J. T. O. (1994). Characteristics of the light field in highly turbid waters *Current Approaches in Remote Sensing* (pp. 702 -706).
- Koponen, S. (2006). Remote sensing of water quality: The development and use of water processors available in BEAM (pp. 1 - 58). Finland, Helsinki: Helsinki University of Technology TKK, Department of Radio Science and Engineering
- Kratzer, S., Brockmann, C., et al. (2008). Using MERIS full resolution data to monitor coastal waters — A case study from Himmerfjärden, a fjord-like bay in the northwestern Baltic Sea. *Remote Sensing of Environment*, 112(5), 2284-2300. doi: 10.1016/j.rse.2007.10.006
- Kratzer, S., and Vinterhav, C. (2010). Improvement of MERIS level 2 products in Baltic Sea coastal areas by applying the Improved Contrast between Ocean and Land processor (ICOL) – data analysis and validation. [Remote Sensing and Water Optics, paper]. *JOURNAL OF BASIC RESEARCH IN MARINE SCIENCES WITH EMPHASIS ON EUROPEAN SEAS.*, 52, 211-236.
- Kurzbaum, E., Eckert, W., et al. (2007). Delayed fluorescence as a direct indicator of diurnal variation in quantum and radiant energy utilization efficiencies of phytoplankton. *Photosynthetica*, 45(4), 562-567. doi: 10.1007/s11099-007-0096-z
- Kutser, T., Metsamaa, L., et al. (2006). Monitoring cyanobacterial blooms by satellite remote sensing. *Estuarine, Coastal and Shelf Science*, 67(1-2), 303-312. doi: 10.1016/j.ecss.2005.11.024
- Laane, W. E. M., and Peters, J. S. (1993). Ecological objectives for management purposes: applying the Amoeba approach. *Journal of Aquatic Ecosystem Stress and Recovery (Formerly Journal of Aquatic Ecosystem Health)*, 2(4), 277-286. doi: 10.1007/bf00044031
- Lehman, P. W., Boyer, G., et al. (2005). Distribution and toxicity of a new colonial *Microcystis aeruginosa* bloom in the San Francisco Bay Estuary, California. *Hydrobiologia*, 541(1), 87-99. doi: 10.1007/s10750-004-4670-0
- Lehman, P. W., Boyer, G., et al. (2008). The influence of environmental conditions on the seasonal variation of &Microcystis cell density and microcystins concentration in San Francisco Estuary. *Hydrobiologia*, 600(1), 187-204. doi: 10.1007/s10750-007-9231-x
- Lürling, M., and Faassen, E. J. (2011). Controlling toxic cyanobacteria: Effects of dredging and phosphorus-binding clay on cyanobacteria and microcystins. *Water Research*(0), 1 - 13. doi: 10.1016/j.watres.2011.11.008
- Marnix, L. (2007). *Improving the remote sensing of coloured dissolved organic matter in inland freshwaters*. (Ph.D Dissertation), Universiteit Amsterdam, Sense Research School. Retrieved from <http://dare.uvu.vu.nl/bitstream/1871/10799/5/8066.pdf>
- Mihaljević, M., and Stević, F. (2011). Cyanobacterial blooms in a temperate river-floodplain ecosystem: the importance of hydrological extremes. *Aquatic Ecology*, 45(3), 335-349. doi: 10.1007/s10452-011-9357-9
- Mishra, S., Mishra, D. R., et al. (2009). A Novel Algorithm for Predicting Phycocyanin Concentrations in Cyanobacteria: A Proximal Hyperspectral Remote Sensing Approach. *Remote Sensing of Environment*, 758 - 775. doi: 10.3390/rs1040758
- Mittenzwey, K. H., Ullrich, S., et al. (1992). Determination of chlorophyll a of inland waters on the basis of spectral reflectance. *Limnology and Oceanography*, 37, 147-149.
- Morel, A. (2006). Meeting the Challenge of Monitoring Chlorophyll in the Ocean from Outer Space. In B. Grimm, R. J. Porra, W. Rüdiger & H. Scheer (Eds.), *Chlorophylls and Bacteriochlorophylls* (Vol. 25, pp. 521-534): Springer Netherlands.
- Mueller, J. L., F., G. S., et al. (2003). *Ocean Optics Protocols For Satellite Ocean Color Sensor Validation*, Goddard Space Flight Space Center Greenbelt, Maryland 20771.
- Newcombe, G., House, J., et al. (2010). Management Strategies for Cyanobacteria (blue-green algae): a Guide for Water Utilities (pp. 1 - 112). WQRA Head Office: CRC for Water Quality and Treatment.

- Nõges, P., Adrian, R., et al. (2010). The Impact of Variations in the Climate on Seasonal Dynamics of Phytoplankton In G. George (Ed.), *The Impact of Climate Change on European Lakes* (Vol. 4, pp. 253-274): Springer Netherlands.
- Odermatt, D., Giardino, C., et al. (2010). Chlorophyll retrieval with MERIS Case-2-Regional in perialpine lakes. *Remote Sensing of Environment*, 114(3), 607-617. doi: 10.1016/j.rse.2009.10.016
- Odermatt, D., Kiselev, S., et al. (2008). ADJACENCY EFFECT CONSIDERATIONS AND AIR/WATER CONSTITUENT RETRIEVAL FOR LAKE CONSTANCA (pp. 8). Frascati, Italy: ESA.
- Otsuki, A., Omi, T., et al. (1994). HPLC fluorometric determination of natural phytoplankton phycocyanin and its usefulness as cyanobacterial biomass in highly eutrophic shallow lake. *Water, Air, & Soil Pollution*, 76(3), 383-396. doi: 10.1007/bf00482714
- Paerl, H. W., and Paul, V. J. (2011). Climate Change: Links to Global Expansion of Harmful Cyanobacteria. *Water Research, In Press, Accepted Manuscript*. doi: 10.1016/j.watres.2011.08.002
- Peeters, F., Straile, D., et al. (2007). Turbulent mixing and phytoplankton spring bloom development in a deep lake. *Limnology and Oceanography*, 52 (1), 286-298.
- Peters, S., and Laanen, M. (2005). WISP-3 Manual (pp. 1 - 19): Water Insight.
- Raat, A. J. P. (2001). ECOLOGICAL REHABILITATION OF THE DUTCH PART OF THE RIVER RHINE WITH SPECIAL ATTENTION TO THE FISH. *REGULATED RIVERS: RESEARCH & MANAGEMENT*, 17(2), 131-144. doi: 0.1002:rrr.608
- Randolph, K., Wilson, J., et al. (2008). Hyperspectral remote sensing of cyanobacteria in turbid productive water using optically active pigments, chlorophyll a and phycocyanin. *Remote Sensing of Environment*, 112(11), 4009-4019. doi: 10.1016/j.rse.2008.06.002
- Rijkeboer, M., Dekker, A., et al. (1997). Subsurface irradiance reflectance spectra of inland waters differing in morphometry and hydrology. *Aquatic Ecology*, 31(3), 313-323. doi: 10.1023/a:1009916501492
- Rijkswaterstaat. (2011). *Water Management in the Netherlands*: Ministry of Infrastructure and Environment.
- Romay, C., Armesto, J., et al. (1998). Antioxidant and anti-inflammatory properties of C-phycocyanin from blue-green algae. *Inflammation Research*, 47(1), 36-41. doi: 10.1007/s000110050256
- Ruiz-Verdú, A., Koponen, S., et al. (2008). DEVELOPMENT OF MERIS LAKE WATER ALGORITHMS: VALIDATION RESULTS FROM EUROPE. In C. Brockmann (Ed.), *MERIS LAKES* (pp. 65). Germany: esaBEAM.
- Ruiz-Verdú, A., Simis, S. G. H., et al. (2008). An evaluation of algorithms for the remote sensing of cyanobacterial biomass. *Remote Sensing of Environment*, 112(11), 3996-4008. doi: 10.1016/j.rse.2007.11.019
- Salama, M. S., and Su, Z. (2011). Resolving the Subscale Spatial Variability of Apparent and Inherent Optical Properties in Ocean Color Match-Up Sites *IEEE TRANSACTIONS ON GEOSCIENCE AND REMOTE SENSING*, 49(7), 2612-2622. doi: 10.1109/TGRS.2011.2104966
- Salmaso, N. (2000). Factors affecting the seasonality and distribution of cyanobacteria and chlorophytes: a case study from the large lakes south of the Alps, with special reference to Lake Garda. *Hydrobiologia*, 438(1), 43-63. doi: 10.1023/a:1004157828049
- Sante, R. (2007). ICOL. In C. M. Brockman & B. Zuhle (Eds.), *D11: Demonstration Products and Qualification Report (DPQR)* (Vol. 0.1, pp. 26). BC premise.: Université du Littoral, France.
- Schalles, J. F., and Yakobi, Y. (2000). Remote detection and seasonal patterns of phycocyanin, carotenoid, and chlorophyll pigments in eutrophic water. *Limnology and Oceanography*, 55, 153 - 168.
- Seppälä, J., Ylöstalo, P., et al. (2007). Ship-of-opportunity based phycocyanin fluorescence monitoring of the filamentous cyanobacteria bloom dynamics in the Baltic Sea. *Estuarine, Coastal and Shelf Science*, 73(3-4), 489-500. doi: 10.1016/j.ecss.2007.02.015
- Simis, S. G. H., Peters, S. W. M., et al. (2005a). Remote sensing of the cyanobacterial pigment phycocyanin in turbid inland water. 237-245.
- Simis, S. G. H., Peters, S. W. M., et al. (2005b). Remote Sensing of the Cyanobacterial Pigment Phycocyanin in Turbid Inland Water. *Limnology and Oceanography*, 50(1), 237-245.
- Simis, S. G. H., Ruiz-Verdú, A., et al. (2007). Influence of phytoplankton pigment composition on remote sensing of cyanobacterial biomass. *Remote Sensing of Environment*, 106(4), 414-427. doi: 10.1016/j.rse.2006.09.008
- StatLine, C. (2011). Climate data weather station De Bilt; temperature, precipitation and sunshine, from <http://statline.cbs.nl/StatWeb/publication/?VW=T&DM=SLN&PA=80370ENG&LA=EN>

- Topçu, D., and Brockmann, U. (2004). Nutrients and organic compounds in the North Sea (Concentrations, Dynamics and Methods): a review. *Marine Biodiversity*, 34(1), 89-172. doi: 10.1007/bf03043230
- Vardaka, E., Moustaka-Gouni, M., et al. (2005). Cyanobacterial blooms and water quality in Greek waterbodies. *Journal of Applied Phycology*, 17(5), 391-401. doi: 10.1007/s10811-005-8700-8
- Vincent, R. K., Qin, X., et al. (2004). Phycocyanin detection from LANDSAT TM data for mapping cyanobacterial blooms in Lake Erie. *Remote Sensing of Environment*, 89(3), 381-392. doi: 10.1016/j.rse.2003.10.014
- WHO. (2003). *Guidelines for safe recreational water environments* (Vol. 1). Geneva: WHO.
- Wikipedia. (2012). Climate - Netherlands Retrieved 26 January 2012, from <http://en.wikipedia.org/wiki/Netherlands#Climate>
- Willmott, C. J., and Matsuura, K. (2005). Advantages of the mean absolute error (MAE) over the root mean square error (RMSE) in assessing average model performance. *Climate Research*, 30(1), 79-82. doi: 10.3354/cr030079
- Wu, X., Kong, F., et al. (2010). Horizontal distribution and transport processes of bloom-forming *Microcystis* in a large shallow lake (Taihu, China). *Limnologia - Ecology and Management of Inland Waters*, 40(1), 8-15. doi: 10.1016/j.limno.2009.02.001
- Wynne, T. T., Stumpf, R. P., et al. (2010). Characterizing a cyanobacterial bloom in western Lake Erie using satellite imagery and meteorological data. *Limnology and Oceanography*, 55(5), 2025–2036. doi: 10.4319/lo.2010.55.5.2025
- Xie, L., Hagar, J., et al. (2011). The influence of environmental conditions and hydrologic connectivity on cyanobacteria assemblages in two drowned river mouth lakes. *Journal of Great Lakes Research*, 37(3), 470-479. doi: 10.1016/j.jglr.2011.05.002

APPENDICES

Appendix A: MERIS Overpass Schedule, Mean and Standard Deviation of PC and Chl_a concentrations and Ancillary Data

Table 1: MERIS Overpass Schedule.

Date	Time	Orbit	Track	Date	Time	Orbit	Track
09-09-2011	10:33:11	49821	238	28-09-2011	10:36:40	50094	80
11-09-2011	10:59:31	49850	267	29-09-2011	10:00:20	50108	94
12-09-2011	10:23:19	49864	281	01-10-2011	10:26:48	50137	123
14-09-2011	10:49:42	49893	310	03-10-2011	10:53:10	50166	152
15-09-2011	10:13:26	49907	324	04-10-2011	10:16:55	50180	166
17-09-2011	10:39:51	49936	353	06-10-2011	10:43:19	209	195
18-09-2011	10:03:32	49950	367	07-10-2011	10:07:01	50223	209
20-09-2011	10:30:00	49979	396	09-10-2011	10:33:28	50252	238
22-09-2011	10:56:20	50008	425	11-10-2011	10:59:47	50281	267
23-09-2011	10:20:07	50022	8	12-10-2011	10:23:35	50295	281
25-09-2011	10:46:31	50051	37	14-10-2011	10:49:58	50324	310
26-09-2011	10:10:14	50065	51	15-10-2011	10:13:42	50338	

Source: <http://earth.esa.int/EOLi/EOLi.html>

The table above shows the dates on which MERIS Satellite passed over the IJsselmeer.

Table 2 Mean and Standard Deviation Chl_a concentrations and PC fluorescence from Data at Pole 46

Chl _a (mg/m ³) Pole 46			PC Fluorescence (RFU)	Pole 46
Date	Mean	Standard deviation	Mean	Standard deviation
22/03/2011	3.768	0.717	65089.3	147.9
27/03/2011	6.272	0.503	65483.7	32.9
29/03/2011	3.820	0.316	65195.	79
10/04/2011	3.327	0.469	65233.7	92.5
18/04/2011	4.888	0.718	65406.2	81.8
20/04/2011	5.329	0.567	65376.5	92.9
21/04/2011	3.276	1.027	65133.2	221.1
23/04/2011	2.158	0.2	64849.3	73.7
25/04/2011	2.483	0.264	64841.8	69.6
01/05/2011	24.495	1.171	8619.9	294.7
03/06/2011	2.957	0.237	325.5	145.9
27/06/2011	6.462	0.772	7152.2	669.9
06/07/2011	9.971	1.767	17626.1	2493.4
28/09/2011	9.71	2.774	3830.1	343.3

Table 3 Mean and Standard Deviation Chl_a concentrations and PC fluorescence from Data at Pole 46

Chl_a (mg/m ³) Pole 47			PC Fluorescence (RFU)	Pole 47
Date	Mean	Standard deviation	Mean	Standard deviation
22/03/2011	1.34	0.036	3257.3	500.9
27/03/2011	1.38	0.252	2554.3	610.7
29/03/2011	1.28	0.017	1401.9	257.6
10/04/2011	1.16	0.015	4561.3	620.1
18/04/2011	1.12	0.095	1746.3	317.1
20/04/2011	1.08	0.018	1396.8	196.
21/04/2011	1.03	0.134	1473.5	183.7
23/04/2011	1.12	0.256	1237	206.1
25/04/2011	1.27	0.041	1445.7	306.4
01/05/2011	1.34	0.0001	17333.4	385.1
03/06/2011	1.21	0.003	3975	1036.9
27/06/2011	1.07	0.023	11664	3057.8
06/07/2011	1.28	0.0003	27902.	3082.5
28/09/2011	No data available	-	-	-

Table 4 Ancillary Data measured for 28 September 2011

Date	Parameter	Units
28/09/2011	Secchi depth	1.5m
	Wind speed	4m/s
	Water temperature	15.8°C
	Sea level pressure	1033hPa

Appendix B: Atmospheric Correction Processor Algorithms

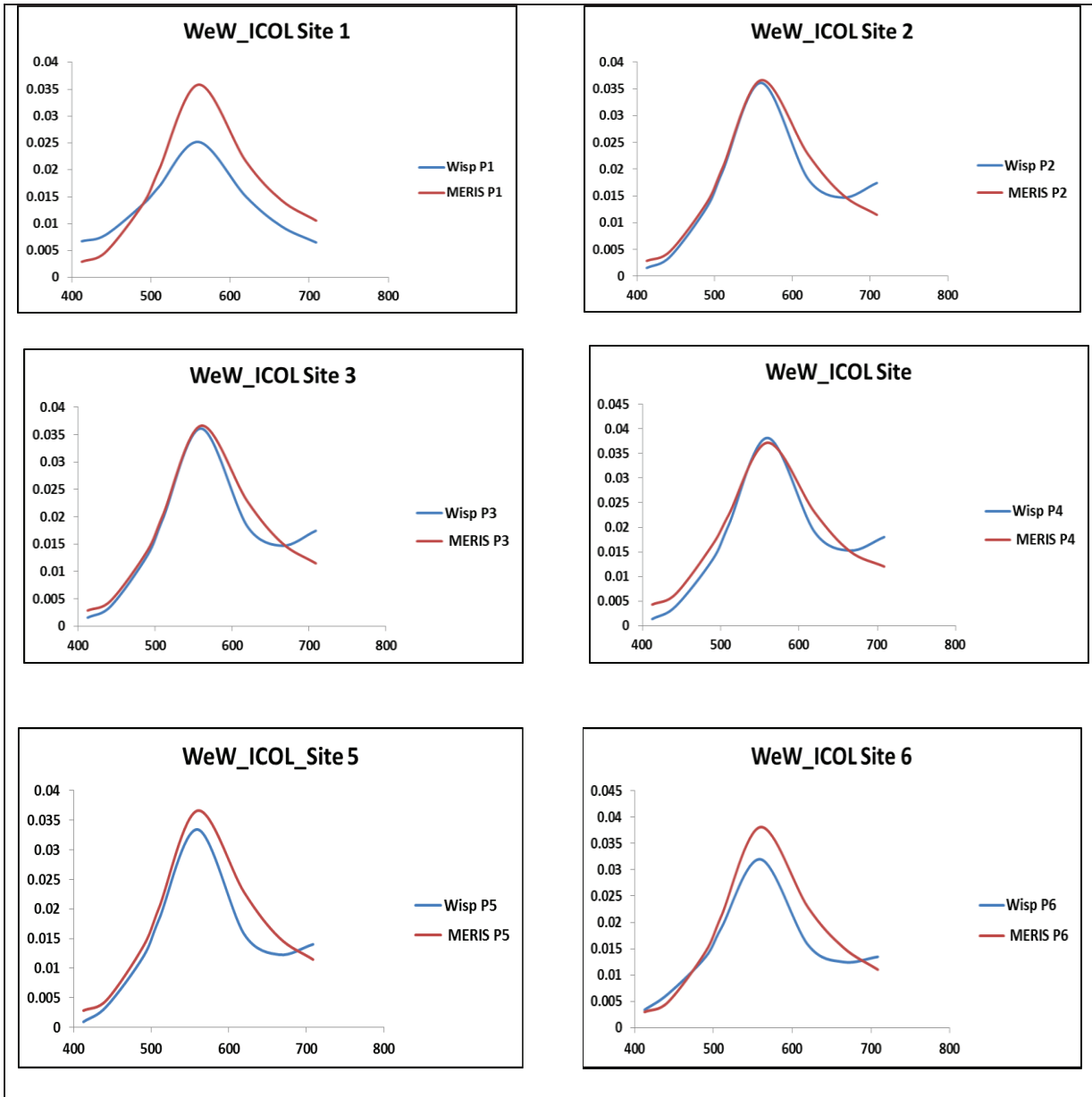


Figure 1 WeW - ICOL and WISP-3 Accuracy assessment of Atmospheric Correction for the 6 sampled geographical locations in Lake IJsselmeer. Detailed information on the results is provided under section 5.2.3

In this study MERIS FR level 1b which are resampled on a path oriented grid also with pixel values that were calibrated in order to match TOA radiances were used in this study in BEAM VISAT version 4.9.

WeW version 1.2.8, C2R version 1.5.1 and ICOL version 2.7.4 algorithms were used in BEAM VISAT 4.9 software as plugins. The processors are indicated on figure 2 and 3.

Case 2 Water Processor

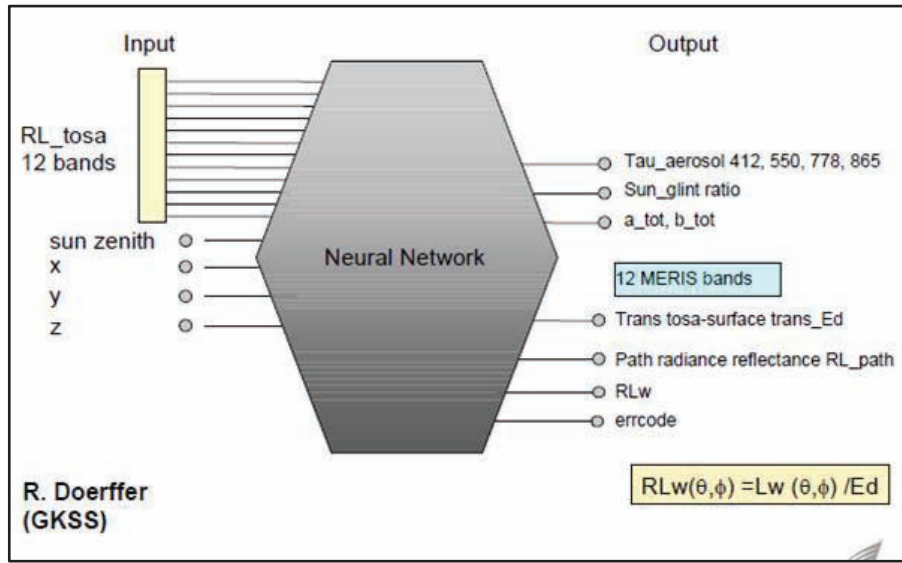


Figure 2 Case 2 Regional Processor Atmospheric Correction algorithm based on neural network for deriving water leaving radiance reflectance (R_{Lw}). This processor was developed using data from coastal waters which has the same optical properties with inland turbid waters. It was developed by Roland Doerffer (GKSS, Germany), Brockmann Consulting in Germany. Its outputs include; water leaving radiance reflectance for the first 12 MERIS bands, water quality parameters, IOPs and atmospheric parameters.

WeW Processor

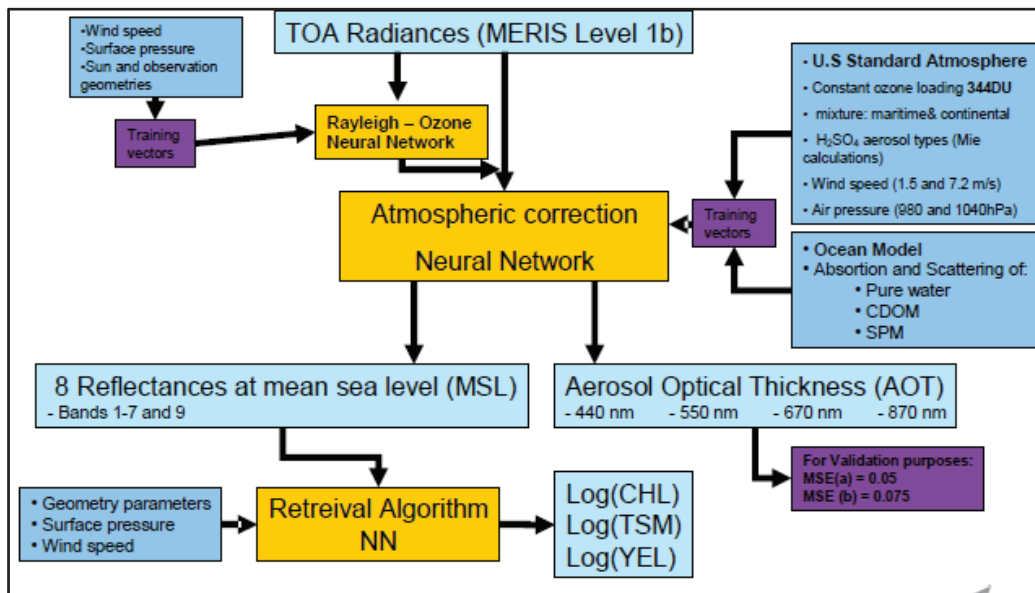


Figure 3 WeW Processor atmospheric correction processing steps in BEAM VISAT software. The processor was developed by the Freie Universitaet Berlin (FUB) for Case 2 waters. Its outputs include; water quality parameters AOT for band 440, 550, 670 and 870 as well as water leaving (RS) band 1 to 7 and band 9 (Koponen, 2006)

Appendix C: IJsselmeer PC Concentration Profile Plots

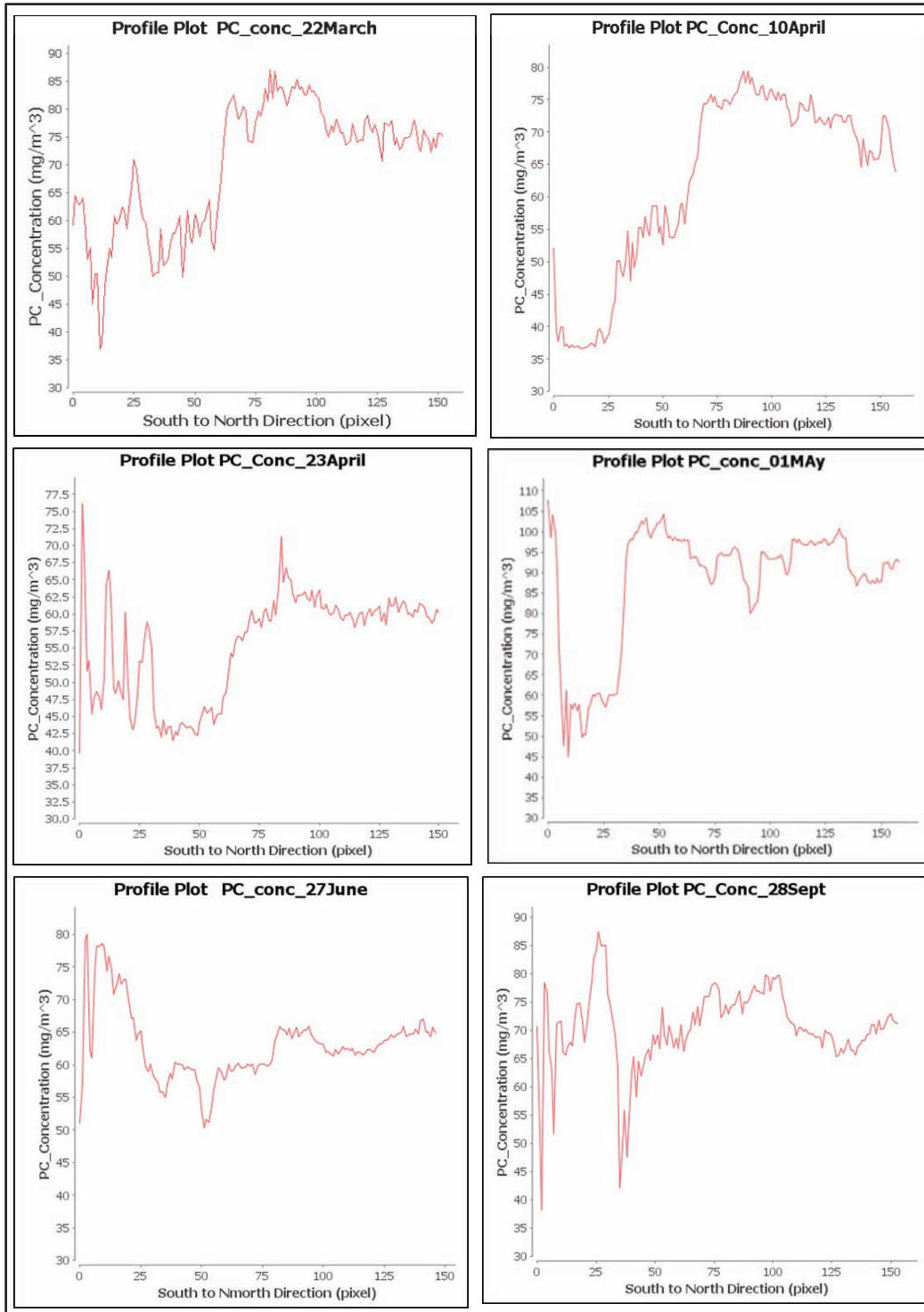


Figure 4 Profile Plots of PC Concentrations from South and North Direction in IJsselmeer

The profile plots on figure 4 illustrates the spatial variation of cyanobacteria concentrations in the lake on 22 March, 10 April, 23 April, 01 May, 27 June and 28 September. The distance was approximately 54 kilometres cutting across the middle of the lake.

Appendix D: PC Fluorescence and MERIS Retrieved PC Concentrations

Table 6 PC Concentrations data extracted from 14 MERIS images and PC fluorescence measured two sites in the IJsselmeer

Date	PC MERIS site 46 (mg/m³)	PC Fluorescence site 46 (RFU)	PC MERIS Site 47 (mg/m³)	PC Fluorescence site 47 (RFU)
22 March 2011	53.24	65089.3	75.72	3257.25
27 March 2011	63.62	65483.7	76.20	2554.3
29 March 2011	55.69	65195.05	67.08	1401.93
10 April 2011	53.32	65233.7	72.53	4561.3
18 April 2011	49.70	65406.2	68.09	1746.3
20 April 2011	52.25	65376.5	62.81	1396.81
21 April 2011	48.65	65133.2	64.51	1473.51
23 April 2011	44.30	64849.3	60.49	1237
25 April 2011	50.3	64841.8	61.68	1445.72
01 May 2011	103.33	8619.86	99.72	1733.44
03 June 2011	49.98	325.45	73.42	3975
27 June 2011	59.1	7152.23	63.73	11664
06 July 2011	82.12	17626.05	81.84	27902.02
28 September	63.07	3830	68.24	No data